SYNTHESIS AND CHARACTERIZATIONS OF SILVER/POLYMETHYLMETHACRYLATE NANOCOMPOSITES VIA *IN-SITU* TECHNIQUE

NOORSAIYYIDAH DARMAN SINGHO

DISSERTATION SUBMITTED IN FULFILLMENT OF THE REQUIREMENTS FOR THE DEGREE OF MASTER OF ENGINEERING SCIENCE

FACULTY OF ENGINEERING
UNIVERSITY OF MALAYA
KUALA LUMPUR
2013

UNIVERSITY OF MALAYA

ORIGINAL LITERARY WORK DECLARATION

Name of Candidate: NOORSAIYYIDAH DARMAN SINGHO

Registration/Matric No: KGA 090059

Name of Degree: Master of Engineering Science

Title of Dissertation ("this Work"):

Synthesis and Characterization of Silver/Polymetylmethacrylate Nanocomposites Via *In-situ* Technique.

Field of Study: Nanotechnology

I do solemnly and sincerely declare that:
(1) I am the sole author/writer of this Work;
(2) This Work is original;
(3) Any use of any work in which copyright exists was done by way of fair dealing and for permitted purposes and any excerpt or extract from, or reference to or reproduction of any copyright work has been disclosed expressly and sufficiently and the title of the Work and its authorship have been acknowledged in this Work;
(4) I do not have any actual knowledge nor ought I reasonably to know that the making of this work constitutes an infringement of any copyright work;
(5) I hereby assign all and every rights in the copyright to this Work to the University of Malaya ("UM"), who henceforth shall be owner of the copyright in this Work and that any reproduction or use in any form or by any means whatsoever is prohibited without the written consent of UM having been first had and obtained;
(6) I am fully aware that if in the course of making this Work I have infringed any copyright whether intentionally or otherwise, I may be subject to legal action or any other action as may be determined by UM.

Candidate's Signature: **Date:**

Subscribed and solemnly declared before,

Witness's Signature: **Date:**

Name:

Designation:

ABSTRACT

In the present study, the synthesis of Ag/PMMA nanocomposites is addressed. $AgNO_3$ was used as a source of silver ions, polyethylene glycol (PEG) as a reducing agent and Daxad 19 as a stabilizer and reducing agent. Silver nanoparticles were synthesized by chemical reduction method in various concentration of silver nitrate ($AgNO_3$) and Daxad 19 at different reactant temperature. The as-synthesized silver nanoparticles were used as primary source to produce Ag/PMMA nanocomposites via *in-situ* technique. The effect of reactant temperatures, PMMA weight ratio and the percentage loading of silver nanoparticles in the Ag/PMMA nanocomposites were studied. UV-vis studies indicate that the maximum surface plasmon resonance (SPR) peak occurred at 419 nm with refractive index, 1.8. The smallest particle size is 24 nm as shown from the TEM image. FESEM studies show that Ag/PMMA nanocomposites start to agglomerates at higher temperature, 120 °C. TGA studies indicate that the stability of Ag/PMMA nanocomposites increases when the percentage loading of silver nanoparticles in PMMA increases. FTIR studies show that the chemical bonding are dominated by $AgNO_3$, PMMA and DMF solution. The Raman spectra of Ag/PMMA nanocomposites for 10 percent loading of silver nanoparticles get enhanced with increasing of reactant temperature. The dielectric studies indicate that the dielectric constant, ε' and dielectric loss, ε'' increase with the increase of percentage loading of silver nanoparticles in PMMA. The optimum result of the synthesis Ag/PMMA nanocomposites is at 80 °C with 10 percent loading of silver nanoparticles.

ABSTRAK

Dalam kajian ini, bahan komposit nano Perak/PMMA telah ditangani. $AgNO_3$ telah digunakan sebagai sumber ion perak, polietilena glikol (PEG) sebagai agen penurunan dan *Daxad* 19 sebagai penstabil dan ajen penurunan. Zarah nano perak disentesiskan dengan cara penurunan kimia di dalam pelbagai kepekatan nitrat perak ($AgNO_3$) dan *Daxad* 19 pada suhu tindak balas yang berbeza. Nano perak yang telah disintesis akan digunakan sebagai sumber utama untuk menghasilkan bahan komposit nano Perak/PMMA secara teknik *in-situ*. Kesan terhadap suhu tindak balas, nisbah berat PMMA dan pemuatan peratusan zarah nano perak dalam bahan komposit nano Perak /PMMA telah dikaji. Kajian *UV-vis* menunjukkan bahawa maksimum *resonance plasmon* permukaan (SPR) spectrum berlaku pada panjang gelombang 419 nm dengan indeks biasan, 1.8. Saiz zarah terkecil ialah 24 nm seperti ditunjukkan dari gambarajah TEM. Kajian FESEM menunjukkan bahawa komposit nano Perak / PMMA mula bercantum antara satu sama lain pada suhu tinggi iaitu 120 °C. Kajian TGA menunjukkan bahawa kestabilan bahan komposit nano Perak / PMMA meningkat apabila peratusan pemuatan zarah nano Perak bertambah. Kajian FTIR menunjukkan bahawa ikatan-ikatan kimia antara partikal di dominan oleh $AgNO_3$, PMMA dan larutan DMF. Raman spektrum bagi bahan komposit nano Perak / PMMA dengan pemuatan 10 peratus zarah nano perak menunjukkan peningkatan spektrum apabila terdapat peningkatan suhu. Kajian dielektrik menunjukkan bahawa pemalar dielektrik, ε' dan kehilangan dielektrik, ε'' meningkat dengan peningkatan pemuatan peratusan zarah nano Perak di dalam PMMA. Hasil optimum sintesis bahan komposit nano Perak/ PMMA adalah pada suhu 80 ° C dengan muatan 10 peratus zarah nano perak.

ACKNOWLEDGEMENTS

I wish to express my sincere gratitude and appreciation to the following people who have contributed in one way or another to make this study possible.

First, I express my sincere gratitude to Associate Professor Dr. Hj. Mohd Rafie Johan for allowing me to conduct this research under his auspice. I am especially grateful for the freedom he gave me during the course of this work. As the thesis supervisor, he supported me in all stages of this work. He is the initiator of this project and he always gave me constant encouragement and advice in spite of his tight schedule. Without his coherent and illuminating instruction, this thesis would not have reached its present form. I would like also to thank to my co-supervisor Dr. Roslina Ahmad.

I extend my sincere thanks to all members of the Department of Mechanical Engineering especially to all lab technician and all those who contributed directly or indirectly. Their supports are very helpful to me for the success of this research.

Without the support of all members of my family, I would never have finished this thesis and I would never have found the courage to overcome all these difficulties during this work. My thanks go to my parents (Abah and Mak) and my parent in law (Mamah) for their confidence and their love during all these years.

The most special thanks go to my soulmate, my husband Dr. Andri Andriyana who always supports me and helps me to overcome the difficulties without complaining. You gave me your unconditional support and love through all this long process.

Gracious thanks to University Malaya for their financial support (Fund No: PS113/2010A) which enable me to conduct this research.

Above all, I owe it all to Almighty God for granting me the wisdom, health and strength to undertake this research task and enabling me to its completion.

TABLE OF CONTENTS

CHAPTER 3 METHODOLOGY

CHAPTER 4 RESULTS AND DISCUSSION

CHAPTER 5 CONCLUSIONS AND FUTURE WORK RECOMMENDATIONS

LIST OF FIGURES

LIST OF TABLES

LIST OF SYMBOLS

A	Absorbance
A	Cross section area
C	Concentration of the absorbing species
d	Distance between adjacent planes of atoms
ε’	Dielectric constant
ε”	Dielectric loss
I	Transmitted intensity
I_0	Intensity of the incident light
j	Complex number
K_α	Radiation of alpha component (nm)
l	Liquid content
L	Path length through the sample
L	Scherer length
m	Ground state
n	Complete number of wavelengths
n	Higher energy excited vibrational state
n	Refractive index
R	Reflectance
R_b	Bulk resistance
t	Thickness
T	Transmittance
T_f	Final temperature
T_i	Initial temperature
v	Velocity of light in vacuum (3×10^8 ms^{-1})
v	Volume
z	Zeta potential

Z’	Real part of the impedance
Z”	Imaginary part of the impedance
$\Delta 2\theta$	Angular for full width at half maximum (FWHM)
E	Extinction coefficient
θ	Angle
θ_b	Angle of the peak
λ	Wavelength
ζ	Zeta potential

LIST OF ABBREVIATIONS

Ag	Silver
$AgNO_3$	Silver Nitrate
DLS	Dynamic Light Scattering
DMF	Dimethylformamide
EIS	Electrochemical Impedance Spectroscopy
FESEM	FESEM Field Emission Scanning Electron Microscope
FTIR	Fourier Transform Infrared
FWHM	Full width at half maximum
IR	Infrared
MMA	Methyl methacrylate
Nm	Nanometer
PEG	Polyethylne glycol
PMMA	Polymethyl(methacrylate)
SEM	Scanning Electron Microscope
SPR	Surface plasmon resonance
TEM	Transmission Electron Microscope
TGA	Thermogravimetric
Uv-vis	UV-visible
VNA	Vector Network Analyzer
XRD	X-ray Diffractometer

LIST OF PUBLISHED PAPERS

1. **Noorsaiyyidah Darman Singho,** Nurul Akmal Che Lah, Mohd Rafie Johan, Roslina Ahmad, "FTIR Studies on Silver-Poly(Methylmethacrylate) Nanocomposites via In-Situ Polymerization Technique", *Int. J. Electrochem. Sci.*, 7 (2012) 5596 – 5603.

2. **Noorsaiyyidah Darman Singho,** Nurul Akmal Che Lah, Mohd Rafie Johan, Roslina Ahmad, "Enhancement of the refractive index of silver nanoparticles in polymethylmethacrylate", *International Journal of Research in Engineering and Technology (IJRET),*1 (4) (2012) 2277 – 4378.

3. **Noorsaiyyidah Darman Singho,** Mohd Rafie Johan, "Complex Impedance Spectroscopy Study of Silica Nanoparticles Via Sol-Gel Method", *Int. J. Electrochem. Sci.*, 7 (2012) 5604 – 5615.

CHAPTER ONE

Introduction

1.1 Background

Recently, the field of nanomaterials becomes one of the most active areas in materials science with impressive developments. New applications of nanomaterials are emerged in various sectors such as medicine, industry, defense and others.

Nanomaterials can be termed as the synthesis, characterization, exploration and application of nanosized (1-100 nm) materials. It deals with the materials whose structures exhibit significantly novel and improved physical, chemical, and biological properties, phenomena, and functionality due to their nano scaled size. Because of their size, nanomaterials have a larger surface-to-volume ratio than micro-sized materials. Nanomaterials have distinct properties compared to the bulk materials, thus offering many new developments in the fields of biosensors, biomedicine, and bio nanotechnology. Nanomaterials are also being utilized in medicine for diagnosis, therapeutic drug delivery and the development of treatments for many diseases and disorders (Pandey *et al.*, 2008).

Among the noble metal nanoparticles, silver (Ag) are in great interest due to their electronic, catalytic, magnetic and optical properties (Rane *et al.*, 2003). Silver nanoparticles have a large fraction of surface atoms (a high surface-to-volume ratio). This increases the surface energy as compared with bulk material. The high surface-to-volume ratio coupled with size effects (quantum effects) gives silver nanoparticles distinctively different properties (chemical, electronic, optical, magnetic and

mechanical). In particular, the optical properties of silver nanoparticles rely on a strong absorption in the visible spectrum, called the plasmon band, which is directly related to the size and shape of the particle (Berciard *et al.*, 2005; El-Sayed, 2001), metal species (Mulvaney *et al.*, 1996), surrounding medium (Kossyrev *et al.*, 2005), scattered (Manna *et al.*, 2001), absorbed substance (Gutierrez *et al.*, 1993; McFarland *et al.*, 2003) and agglomerations (Mandal *et al.*, 2001; Zheng *et al.*, 2002).

It is known that the improvements and controlling of key parameters will tweak the properties of silver nanoparticles, either by using different chemical synthesis or adjusting the reaction conditions such as reducing agent, stabilizer, etc. (Kim *et. al.*, 2006). Therefore, it is essential to study the preparation method and the influences of reaction conditions for fundamental understanding of the nucleation and growth of the nanoparticles.

Different synthesis methods of silver nanoparticles with different shapes have been reported elsewhere (He *et al.*, 2001; Zheng *et al.*, 2001), octahedral (Callegari *et al.*, 2003), tetrahedral (Callegari *et al.*, 2003), hexagonal (Manna *et al.*, 2001), cubic (Sun *et al.*, 2002), fibers (wires) (Zhang *et al.*, 2001; Zhou *et al.*, 1999), disks (Hao *et al.*, 2002; Chen *et al.*, 2002), triangular prisms (Pastoriza-Santos *et al.*, 2002; Chen *et al.*, 2002), shell (Jackson *et al.*, 2001), among others (Yin *et al.*, 2002; Metraux *et al.*, 2003).

Nowadays, polymeric nanocomposites are new class of materials that combine the properties of inorganic particles with the processability and flexibility of an organic polymer matrix. The resulting hybrid materials offer the possibility of a new generation of nanostructured materials with diverse applications such as electronic or photonic

devices, sensors, and catalysts (Mitzi, 2001; Vossmeyer *et al.*, 2002; Chen *et al.*, 1999). In such materials, organic polymer generally is a continuous phase, and the nanoparticles the dispersed phase. When the nanoparticles are introduced into organic polymer matrix, the polymorphic crystalline would be included, giving the nano-polymer matrix composites many excellent properties. Advantages of the nano-polymer matrix composites included mainly: (1) An enhanced of polymer properties, such as higher heat distortion temperature, rapid crystallization, improved mechanical properties, etc.; (2) A resource-saving compound, using only the common raw materials, and no other new materials; (3) The original process route: a nanocomposite uses the original route of polymer processing. These features make the nanocomposites easier to produce industrially, once breakthrough was obtained. In other words, nano-polymer matrix composites can provide an epoch-making performance by adjusting the complex dispersion of the original materials.

In this study, polymer was used as stabilizer to overcome the aggregation problem. By employing special organic compounds, the particles are treated as passive, which inhibits coalescence and therefore prevents aggregation. Polymeric compounds allow the nanoparticles to be isolated and are usually known as protective agents via the interaction with small particles. There are variety polymers that can be used to prepare nanocomposites. Poly (methyl methacrylate) (PMMA) is one of the most studied in the last decade due to its promising mechanical and chemico-physical properties. It is an important member of the polyacrylic and methacrylic esters family. PMMA has several desirable properties, including exceptional optical transparency, good mechanical properties, good weatherability, acceptable thermal stability, desirable electric properties, moldability and easy shaping (Mark, 1985). There are various synthetic techniques for Ag/PMMA nanocomposites including ‘core shell’ synthesis (Wang &

Chen, 2004), vapor co-deposition in vacuum (Takele *et al.*, 2006), ion implantation (Bazarov *et al.*, 1995), and suspension polymerization (Yeum & Deng, 2005).

The incorporation of silver nanoparticles in a polymer matrix PMMA has shown significant effect to the properties of the particles itself. This study shows that silver ions take place due to the hydrated electron or hydrogen from poly (methyl methacrylate) sodium salt. Thus, it is proven that the presence of silver ions in the matrix give rise to the performance of the properties of Ag/PMMA nanocomposites. The challenges to generate zero-valent silver (Khanna & Narendra, 2007) having desired shape and size with uniform distribution within the matrix have been reported. Since it is well known that silver nanoparticles in polymers have high potential opto-electronic devices, the alteration in optical properties was studied. For examples the enhancement of refractive index is due to the incorporation of silver nanoparticles with PMMA.

In this work, the synthesis of Ag/PMMA nanocomposites via *in-situ* technique was based on the formation of mono-sized silver nanoparticles via chemical reduction methods. The combination of $AgNO_3$ as precursor, PEG as reducing agent and Daxad 19 as a stabilizer shows a high stability due to strong electron donating effect of amine, as compared to oxygen. Silver nanoparticles then are coated with PMMA via *bi-in-situ* technique. This will forms an active site, which initiates concealed polymerization and gives rise to nano dispersions of Ag/PMMA nanocomposites.

1.2 Significant of Research Problems

Nanocomposites materials with different shapes and structures can be easily synthesized by controlling the reaction conditions. However, despite controlling the reaction conditions, the resultant particles tend to grow and 'glued' together, which in turn forms cluster particles. The primary problem is to prevent the aggregation among the particles which leads to the wider size distribution. The aggregation of particles may also results in a loss of their individual characteristics and properties. This problem can be overcome by employing special organic compound such as where the particles are treated as passive. These will which inhibits coalescence and therefore prevent the particles from aggregation.

The choice of a specific polymeric protective agent is also one of the most important factors in the synthesis of Ag/PMMA nanocomposites. The modification can improve the interfacial interaction between the particles and the polymer matrix. Furthermore, the homogeneity of the colloidal particles is improved significantly but limited and controlled by the rate of reaction due to the medium parameters such as concentration and temperature. In this study, the key parameters are optimized and the homogeneity of particles were achieved successfully.

Synthesis of Ag/PMMA nanocomposites based on environmentally friendly materials, which are the main concern in the present world, should be employed. There has been increasing awareness on health care, and therefore it is imperative to prevent contamination to the environment because several types of toxic reducing agents have been commonly used previously to produce metal nanoparticles. Thus, in this study, the materials used are non-toxic and environmentally friendly.

1.3 Research Objectives

The objectives of this research are listed below:

a) To produce Ag/PMMA nanocomposites via *in-situ* technique.

b) To determine the properties of Ag/PMMA nanocomposites via a number of analytical techniques such as Transmission Electron Microscopy (TEM), Field Emission Scanning Electron Microscopy (FESEM), X-ray Diffraction (XRD), UV-Visible (UV-Vis), Fourier Transform Infra Red (FTIR), Thermogavimetry (TGA), Raman spectroscopy, Vector Network Analyzer (VNA), Impedance Spectroscopy (IS), Dynamic Light Scattering (DLS) and Zeta Potential.

c) To obtain the optimum key parameters in the designed Ag/PMMA nanocomposites.

1.4 Organization of the Thesis

The present chapter gives an introduction to the thesis. There are two main objectives of this thesis, first is to synthesize Ag/PMMA nanocomposites. The second objective is to investigate the influence of the parameters on the properties of the synthesized Ag/PMMA nanocomposites via characterization technique. Controlling the size, shape and structure of metal nanocomposites is technically important because of strong correlation between these parameters and theirs physical-chemistry properties.

Chapter Two presents a literature review of the synthesis techniques, characterization behavior available to reproduce the intrinsic properties and discussion of the modified synthesis technique which have been used to tweak the properties of Ag/PMMA nanocomposites.

Chapter Three describes the synthesis methods to produce the optimized conditions of Ag/PMMA nanocomposites. The *in-situ* technique was used to produce Ag/PMMA nanocomposites. Finally, the properties characterizations of Ag/PMMA nanocomposites were characterize using Transmission Electron Microscopy (TEM), Field Emission Scanning Electron Microscopy (FESEM), X-ray Diffraction (XRD), UV-Visible (UV-Vis), Fourier Transform Infra Red (FTIR), Thermogavimetry Analysis (TGA), Raman spectroscopy, Vector Network Analyzer (VNA), Electrochemical Impedance Spectroscopy (EIS), Dynamic Light Scattering (DLS) and Zeta Potential analysis were presented.

Chapter Four presents the results of characterization of Ag/PMMA nanocomposites via *in-situ* technique. The characterization results obtained from transmission electron microscopy (TEM), field electron scanning electron microscopy (FESEM), x-ray diffraction (XRD), ultra-violet visible spectroscopy (UV-Vis), fourier transform infra red (FTIR), thermogavimetric spectroscopy (TGA), raman spectroscopy, vector network analyzer (VNA), impedance spectroscopy (IS), dynamic light scattering (DLS) and zeta potential are discussed. The influence of key parameters on the size, shape and size distribution of Ag/PMMA nanocomposites is also presented.

Chapter Five draws general conclusions of the presented thesis as well as an outlook on future research directions.

CHAPTER TWO

LITERATURE REVIEW

2.1 Introduction

The history of nanomaterials is quite long. Nevertheless, major developments within nanoscience have taken place during the last two decades. Research in nanomaterials is a multidisciplinary effort that involves interaction between researchers in the field of physics, chemistry, mechanics, material science, and even biology and medicine. The term nanoparticle, which represents another form of nanomaterials, came into frequent use in early 1990's by the materials science community to represent particles that are composed of up to tens of thousands of atoms but confined to size less than 100 nm. Until then, more general terms like submicron and ultra fine particles were in use. The first nanoparticles which is heterogeneous catalysis, was developed in the early nineteenth century (Somorjai, 1978).

Properties of nanomaterials are different and often superior to their conventional counterparts. They are available in polycrystalline form and their structure is determined by the chemical composition, grain size, atomic structure, crystallographic orientation, coordination number and dimensionality. Because of the grain dimensions, significant volume fraction of atoms in nanomaterials is located at the grain boundary that confers special attributes to them. Nanoparticles, due to their smaller size and a large surface to volume ratio, exhibit interesting novel properties which include nonlinear optical behavior, increased mechanical strength, enhanced diffusivity, high specific heat, magnetic behavior and electrical resistivity, etc (Somorjai, 1978). Researchers have proposed a huge range of potential scientific applications of metal nanoparticles such as in fields of biotechnology (Gleiter, 2000), sensors (Mirkin *et al*., 1996), medical

diagnostic (Taton *et al.*, 2000), catalysis (Storhoff *et al.*, 1998), high performance engineering materials, magnetic recording media, optics and conducting adhesives (Dagani, 1999; Hamilton & Baetzold, 1979). The commonly method to produced nanoparticles are physical vapor deposition, chemical vapor deposition, aerosol processing, sol gel process, wet chemical synthesis, mechanical alloying and etc (Schmid *et al.*, 2003).

2.2 Silver Nanoparticles

Currently, metal nanoparticles are in a great interest by their electronic, catalytic, magnetic and optical properties to technological and nanometer level. In the last few years, greater attention has been paid to their preparation, determination of structure and applications. Metal nanoparticles are defined as isolated particles between 1-100 nm diameters that do not represent a chemical compound with a metal-metal bond and a particular nuclearism (Ash *et al.*, 2000). The nanoparticles represent cluster of atoms that are involved in a protective layer to prevent or to stabilize agglomeration (Ash *et al*., 2002).

Among these metal nanoparticles, silver has received considerable scientific and practical interest due to their potential use in research and industrial applications (Alan & Albrecht, 1977). Fundamental studies were carried out in the late 1980s and 1990s showed silver nanoparticles possess an interesting interaction with light due to dielectric constant which enables the occurrence of light repines in the visible regimes (Lee & Meisel, 1982). Notably, silver is one of the metals which can be tailored to respond across the full visible spectrum.

Nowadays, silver nanoparticles are one of the promising products in the nanotechnology industry. The development of consistent processes for the synthesis of silver nanoparticles is an important aspect of current nanotechnology research. One of such promising process is green synthesis (Phong *et al.*, 2009). Frequently, nanometer-size metallic particles show unique and considerably change physical, chemical and biological properties compared to their macro scale counterpart, due to high surface to volume ratio.

Silver nanoparticles exhibit size and shape dependent properties that are of interest for applications ranging from catalysts and sensing to optics, antibacterial activity and data storage (Sudrick *et al.*, 2006, Choi *et al.*, 2007; Yoosaf *et al.*, 2007; Hutter & Fedler, 2004; Sun *et al.*, 2000; Vilchis Nestor *et al.*, 2008). Hence, the properties of silver nanoparticles are strongly dependent on their size and shape. For example, when spherical metal particles are transformed into nanoscale dicks or triangular prism, their surface plasmon resonance (SPR) are strongly affected-typically red-shifted and splitting into distinctive dipole and quadruple plasmon modes may even occur (Maillard *et al.*, 2002; Jin *et al.*, 2001; Sun *et al.*, 2003). The stability of the nanoparticles is another important factor-in addition to their sizes and shapes that affects applicability. Stabilization is usually accomplished by capping the particles with suitable surface passivating agents. The choice of capping agent is very critical because it determines the stability, solubility, reactivity and even the size and shape of the nanoparticles during the synthesis (Caruso, 2001; Kamat, 2002; Graf *et al.*, 2003).

The choice of solvent-in addition to the stabilizing surfactant is also significantly important, especially when the synthetic environment requires a high concentration of metal ions. In the absence of a stabilizing surfactant, the stability of silver nanoparticles

synthesized in glycerol is much higher than that in ethylene glycol or aqueous solutions (Rele *et al.*, 2004). The higher stability of the nanoparticles in glycerol is due to higher viscosity leading to the slower diffusion. Performing the synthesis of silver nanoparticles in organic media is preferable because the selective media may serve as both solvents and reducing agents without the need for adding an extra reducing agent (Rele *et al.*, 2004; Sun *et al.*, 2002; Silvert & Tekaia-Elhsissen, 1995; Pastoriza-Santos & Liz- Marzan, 2002; Kim *et al.*, 2001).

Generally, specific control of shape, size, and size distribution is often achieved by varying the synthesis method, reducing agents and stabilizers (Yeo *et al.*, 2003; Chimentao *et al.*, 2004; He *et al.*, 2004). Silver nanoparticles can be prepared by two routes; the first one is a physical approach that utilizes several methods such as evaporation/condensation and laser ablation. The second one is chemical approach in which the metal ions in solution is reduced in conditions favoring the subsequent formation of small metal clusters or aggregates (Khomutov & Gubin, 2002; Oliveira *et al.*, 2005; Egorovo & Revina, 2000).

Both methods are needed to alter the physical, chemical, mechanical and the surface structure of nanoparticles. The surface modification is carried out in order to improve the dispersion and compatibility of the nanoparticles with other materials. The surface modification of nanoparticles can be divided into mechanical and chemical modification, external membrane modification (ie, capsule), high-energy surface modification, surface modification using precipitation, etherification, coupling and grafting reactions. The use of ultraviolet ray for the plasma surface modification of particle belongs to the physical modification. The surface structure and state of nanoparticles are changed by the chemical reactions between the nanoparticles surface

and modifier. Surface chemical modification of nanoparticles plays a very important role to reduce the aggregation. Due to modifier adsorption or bonding on the particle surface, which reduces the surface force of hydroxyl groups, the hydrogen bonds between particles are eliminated to prevent the formation of oxygen bridge bonds when nanoparticles are drying. Thereby it prevents the occurrence of agglomeration.

2.3 Synthesis of Silver Nanoparticles

The works involving synthesis of nanoparticles have a long story. The first description was developed in the late 1857 by Faraday, who discovered the first metallic nanoparticles colloids (An *et al.*, 2007). Faraday focused on understanding the behavior of optical properties of metal in nanometer scale which suspended in the solution. Major strides towards the nanoparticles synthesized then were credited in Feynmann in 1940, who generalized the influence of the self-assembly approach on synthesized nanoparticles (Gleick, 1992). NASA researches gave priority attention towards the development of synthesized nanoparticles in the early sixtieth (Peterson, 2000). They discovered that nano-sized magnetic particles known as ferro-fluid could be dispersed in oil or water. In 1960, Plank and Rosinski found the use of zeolites in speeding up the synthesized process of nanoparticles reaction.

There are two approaches for synthesis of nanoparticles that is bottom-up and top-down approach. The top-down approach involves chopping down the bulk metals by mechanical means (Gaffet *et al.*, 1996; Amulyavichus *et al.*, 1998). Example like metal vapor techniques (Blackborrow *et al.*, 1979; Klabunde, 1980; Klabunde *et al.*, 1991), provides a versatile route for the production of a wide range of nanostructured metal colloids (Bradley, 1994; Klabunde *et al.*, 1994). However, this method has a few

drawbacks such as difficult to obtain a narrow particle size distribution, and the samples involving impurities.

On the other hand, bottom-up approach such as of wet chemical nanoparticles preparation basically relies on the chemical reduction of metal salts, electrochemical pathways, or the controlled decomposition of metastable organo metallic compounds in solution. Control over the growth of the primarily formed nanoclusters and their agglomeration is effected using a variety of stabilizers, in the form of donor ligands, polymers and surfactants. Current nanomaterials research rests heavily on bottom-up approach compared to the top-down approach (Cao, 2004). The bottom-up approach offers better flexibility and versatility in terms of material design. Figure 2.1 shows the bottom-up and top-down approach of synthesizing nanoparticles.

The synthesis of nanomaterials from atomic or molecular sources depends on the control of variety of nanoscale attributes desired in the final product. Though a plethora of methods have been reported for the synthesis of metallic nanoparticles, some of them have been extensively studied, because of their ease to apply for large-scale production and also to a wide range of materials (Edelstein *et al.*, 1997). Chemical synthesis of nanomaterials is a rapidly growing research area with a great potential to make technologically advanced and useful materials. Chemical methods have been widely used to produce nanostructured materials due to their straight forward nature and their potential to produce large quantities of the final product.

Synthesis techniques require the development of methods for nanoparticles to be assembled and dispersed in various media. Major effort in nanoparticles synthesis can be classified into two different approaches, namely gas phase and liquid phase

synthesis. Initial development of nanocrystalline materials was based on nanoparticles generated by nucleation and growth process via evaporation and condensation in a sub-atmospheric inert-gas environment (Gleiter, 1989; Siegel, 1991). However, at this technology matures and product prices become more competitive, the processing technique involves optimal cost production as well as time consuming shortage (Eickmans *et al*,. 1996). Liquid phase synthesis has shown significant advantages over the gas phase synthesis route. For the past few years, the trend towards miniaturization and the necessity on modernization of technologies processes led to the substantial increase in the number of scientific publications devoted to the synthesis and properties of silver nanoparticles (Jiang *et al.,* 2005). Chemical reduction synthesis is the most simplest and economical technique for nanoparticles production (Navaladian *et al.,* 2007).

Many chemical reduction methods have been used to synthesize silver nanoparticles from silver salts (Hying *et al.*, 2001; Sondi *et al.,* 2003; Lim *et al.*, 2006). Silver nitrate has been used as the starting material. The methods are varying in the choice of reducing agent, the relative quantities and concentrations of reagents, temperature, mixing rate and duration of reaction. The diameters of the resulting particles are depends upon the conditions. Examples like greenish-yellow (λ_{max} 420 nm) colloidal silver with particle sizes from 40 - 60 nm has been reported from reduction with sodium citrate at boiling (Kamat *et al.*, 1998). Silver colloids, described as brownish or yellow-green with maximum absorption at 400 nm and particle size of about 10 nm, are resulted from reduction of ice-cold sodium borohydride (Lee & Meisel, 1982). A method using both sodium citrate and sodium borohydride at boiling gives a greenish colloid absorbing at 438 nm with particle size 60 - 80 nm (Nair & Pradeep, 2003).

Commonly used reductants are borohydride, citrate, ascorbate, and elementalhydrogen (Ahmad *et al.*, 2003). The reduction of silver ions (Ag^{+}) in aqueous solution generally yields colloidal silver with particle diameters of several nanometers. When the colloidal particles are much smaller than the wavelength of visible light, the solutions have a yellow brown color with an intense band in the 380–400 nm range and other less intense or smaller bands at longer wavelength in the absorption spectrum (Tessier *et al.*, 2000; Rosi *et al.*, 2005). This band is attributed to collective excitation of the electron gas in the particles, with a periodic change in electron density at the surface (surface plasmon absorption) (Henglein, 1989; Ershov *et al.*, 1993).

Previous studies showed that the use of a strong reducing such as borohydride, resulted in small particles that were somewhat monodisperse, but the generation of larger particles was difficult to control (Creighton *et al.*, 1979; Schneider *et al.*, 1994). Use of a weaker reducing such as citrate, resulted in a slower reduction rate, but the size distribution was far from narrow (Shirtcliffe *et al.*, 1999). Controlled synthesis of silver-NPs is based on a two step reduction process. In this technique a strong reducing agent is used to produce small silver particles, which are enlarged in a secondary step by further reduction with a weaker reducing agent (Lee *et al.*, 1982). Different studies reported the enlargement of particles in the secondary step from about 20–45 nm to 120–170 nm (Schneider *et al.*, 1994; Schirtcliffe *et al.*, 1999; Rivas *et al.*, 2001). Moreover, the initial sol was not reproducible and specialized equipment was needed (Nickel *et al.*, 2000). The synthesis of nanoparticles by chemical reduction methods is therefore often performed in the presence of stabilizers in order to prevent unwanted agglomeration of the colloidal silver nanoparticles solution.

2.4 Silver Polymer Nanocomposites

Nanocomposite materials are the combination of the nano-sized powders or liquids and the polymer matrix. In such materials, organic polymer generally is a continuous phase, and the nanoparticles the dispersed phase. In the new century, the rapid development of nanocomposites materials becomes one of the most advanced composites materials. When the nanoparticles were introduced into organic polymer matrix, the polymeric crystalline would be introduced, giving the nano-polymer matrix composites many excellent properties. Advantages of the nano-polymer matrix composites mainly include: (1) An enhanced of polymer properties, such as higher heat distortion temperature, rapid crystallization, improved mechanical properties, etc.; (2) Resource-saving compound, using only the common raw materials, and no other new materials; (3) The original process route: nanocomposites use the original route of polymer processing. These features make the nanocomposites easier to produce industrially, one breakthrough was obtained. In other words, nano-polymer matrix composites can provide an epoch-making performance by adjusting the complex dispersion on the original materials.

Polymer-inorganic nanocomposites own the machinability of organic materials and the functional and structural properties of inorganic materials, becoming the hot spot of today's science and technology. In the nanocomposites, a large part of the nanomaterials is functional. In addition, nanomaterials provide directional characteristic, and its direction- related features, including the coupling characteristics, can be used in design process. Since the presence of anisotropy and coupling characteristics, the direction and sequence can be designed and tailored, according to the mechanical characteristics and function. With the interface of a dual nature,

nanomaterials can be more evenly dispersed in the matrix by adjusting the interaction of the interface of the two roles. The intervention of nanowiskers, nanorods, and nanobeam offers the possibility of the enhanced orientation and maintains the processing facilities of the filler nanoparticles. In the polymer-inorganic nanocomposites, different interfaces also create synergies. To maximize the beneficial effects and synergies of different interfaces of the nanocomposites, the surface modification or treatment is generally appropriated, which forms a link with the substrates (eg. covalent, hydrogen bond, intermolecular force, etc.), maximizing the dispersion and the appropriate combination.

Polymer based composite materials containing metal nanoparticles have attracted great attention of scientists owing a number of properties useful for different practical applications based on quantum size effect. Dispersion of nanoparticles into polymers has changed properties of both polymer matrix and the particles. Polymers are considered as a good host material for metal (Zhu *et al.*, 1997; Dirix *et al.*, 1999; Akamatsu *et al.*, 2000) and semiconductor (Godovsky, 2000; Qian *et al.*, 2001; Kumar *et al.*, 2001) nanoparticles, which, on the other hand, exhibit exceptional optical and electrical properties. At the same time, because of their high surface-to-bulk ratio, dispersion of nanoparticles into polymers has changed properties based on quantum size effect. Therefore, the investigation of the influence of nanoparticles on the properties of a polymer matrix is necessary in order to be able to better predict the final properties of the composite.

Among metal nanoparticles, renewed interest arises in tailoring the properties of silver (Ag) nanoparticles embedded within the polymers due to their unusually enhanced physiochemical properties and biological activities (Tolymat *et al.*, 2010). The properties of silver polymer nanocomposites are very sensitive to small changes in

the silver content and in the size and morphology of the nanoparticles. It was reported that the silver nanoparticles could act as conductive junctions between the polymer chains which result in increase of the electrical conductance of the composites (Gangopadhyay & Amitabha, 2000). The size, morphology and the type of silver nanoparticles incorporated within the polymer matrix would result in variation of properties of the silver nanocomposites.

The synthesis techniques for silver polymer nanocomposites have advances rapidly with the development of nanotechnology. Silver polymer nanocomposites have been prepared by many synthetic routes such as polymer blending (Ghosh and Maiti, 1996), metal ion-polymer complexes reduction process with reducing agents (Kunzs *et al.*, 1993), and reducing metal ions in the polymer matrix by high-energy radial irradiation (Liu *et al.*, 2001). Mbhele *et al.*, (2003) prepared silver-polyvinyl alcohol (PVA) nanocomposites by mixing a colloidal solution consisting of silver nanoparticles with a water solution of PVA in appropriate ratios. Zhao *et al.*, (1999) reported a new approach using phenolic resin via *in-situ* reduction method using external reducing agent where the interaction took place simultaneously.

In general, there are two synthesis approaches of silver-polymer nanostructures: *in-situ* and *ex-situ* methods (Carotenutu *et al.*, 2004). The *ex-situ* method involves silver nanoparticles formation first, followed by dispersion into a polymer matrix (Lim & Ast, 2001). In the *in-situ* approach, silver nanoparticles can be generated inside a polymer by reduction of metallic precursor which is dissolved in the polymer or the polymerization solution (Porel *et al.*, 2005).

Recently, Chujo *et al.,* (2002) synthesized silver dendritic structure by a redox reaction between a π-conjugated polymer and silver ions in solutions. They showed that a π-conjugated polymer containing a strong electron-donating unit should reduce silver ions. Yu and co-workers fabricated flexible silver-cross linked poly (vinyl alcohol) (PVA) coaxial nanocables by *in-situ* reduction of silver ions and cross linking of PVA (Luo *et al.,* 2005). They explained that PVA was responsible for both the formation of silver nanoparticles and growth of silver nanowires in an axial direction. In addition to these *in-situ* metallization in polymeric solutions, a monomer and a radical initiator have been used to form silver nanostructures during polymerization. Chemical oxidative polymerization of a pyrrole monomer was performed by reducing silver ions in a redox system (Chen *et al.,* 2005). Moreover, *in-situ* formation of silver nanoparticles occurred onto the polymer microsphere surface due to the reduction potential of the generated radicals (Chen *et al.*, 1998).

Since the polymers prevent agglomeration and precipitation of the particles, they have been employed as stabilizers in chemical synthesis of metal nanoparticles. The embedding of such particles in polymer matrix is also advantageous from the point of view of film casting. The polymer films having nanoparticles in them can be considered as potential candidates for their use in electronic and optoelectronic devices. The properties of polymer composites depend on type of incorporated nanoparticles, their size and shape, their concentration and interaction with polymer matrix.

There are a number of studies focusing on the synthesis of silver nanoparticles in polymers with the possibility of varying the optical properties generated from the optical activity of the polymer. Fragale *et al.*, (1999) have prepared silver nanoparticles of mean size 32 nm and dispersed them inside a polyimide matrix. It has been reported

that matrix allowed these silver nanoparticles to remain trapped in the polymeric cage. Structural and compositional analysis of nanocomposites films have been carried out by XRD, TEM and XPS. XRD data have not shown silver oxide diffraction contribution suggesting that oxygen interaction has affected the cluster at the surface only. The dispersion process of silver nanoparticles of size 5 nm into vapor-deposited nylon-11 thin films has been investigated by Akamatsu *et al.*, (2002). A strong correlation between the optical spectra features dispersion state of the nanoparticles and structural changes of the polymer matrix have been established. This behavior of nanocomposites has been attributed to the changes in the effective dielectric constant of the film due to reduction of the effect of dipole interaction between neighboring particles. Silver nanoparticles have been found penetrated from surface into bulk phase of the nylon matrix when the samples were heated. Dispersion mechanism has been discussed in terms of surface energy of silver nanoparticles, which has been found reduced upon dispersion in the polymer matrix. Zeng *et al.*, (2002) have reported synthesis of 14 nm silver nanoparticles by chemical reduction, and latter dispersed in polystyrene (PS) and acrylonitrile-styrene (AN) polymers for formation of thin nanocomposites films by static casting at room temperature. The optical absorption of polymer films has been found influenced by the incorporation of silver nanoparticles and the filler-matrix interfacial interactions. Optical extinction of polymers films with embedded silver nanoparticles has been examined by Heilmann *et al.*, (1998). It has been presented in this study that optical properties of these nanocomposites depend on the nanoparticles material, size and shape. They have report used Rayleigh-Gans theory first time to compute the optical extinction of silver nanocomposites with experimentally determined particle size and shape. The electron irradiation has caused the hardening of polymer matrix and prevented reshaping in the affected areas.

Among polymer materials, PMMA is well known as a polymeric glass with a wide range of applications. The poly (methyl methacrylate) (PMMA) has been one of the most widely studied in the last decade due to its promising mechanical and chemico-physical properties. PMMA is an important member of the polyacrylic and methacrylic esters family. PMMA has several desirable properties, including exceptional optical transparency, good mechanical properties, good weather ability, acceptable thermal stability, desirable electrical properties, moldability, and easy shaping (Mark, 1985). Use of PMMA offers two fold advantages such as availability to carboxylate functional group for a chemical bonding with the metal ions and high solubility of PMMA in solvent like DMF for silver nitrate reduction. Organic solvents such as dimethylformamide (DMF) and Daxad 19 have been successfully used for reduction of silver salts (Che Lah & Johan, 2011).

Earlier report on the synthesis of silver nanoparticles in poly (methyl metacrylate) (PMMA) utilized sodium salt of acrylic acid via radiolysis method (Longenberger & Mills, 1995; Monti *et al.*, 2004). They described that the reduction of silver ions takes place due to the hydrated electrons or hydrogen coming from the long chain of PMMA. Silver nanoparticles have been embedded by Stepanov *et al.*, (2002) in poly (methyl metacrylate) (PMMA) by ion implanation near surface layer. Weak SPR bands in some samples have been attributed to their dependence on the implanation dose. The increased absorbance with ion dose especially near the ultraviolet range has been explained in terms of degradation of polymer under ion beam irradiation. Modeling of extinction spectra of the Ag/PMMA nanocomposites has given a reasonably good agreement with features of the experimental optical data.

Deng *et al.*, (2008) prepared Ag/PMMA nanocomposites by considering silver nanoparticles colloids suspension drying on the quartz substrates using PMMA and DMF via *in-situ* polymerization techniques. They observed that the behavior of linear and nonlinear optical properties were different compared to the pure PMMA film. A novel strategy has been achieved by Yang *et al.*, (2008), which were based on *in-situ* synthesis technique using free radical metallic precursor suspension and bulk polymerization technique. They described that the metal nanoparticles were uniformly distributed inside the polymer matrix and the inclusion of the metal precursor had no significant influence on the polymerization process. Following this, improved stability of silver nanoparticles has been achieved in the polymer.

2.5 Synthesis of Ag/PMMA Nanocomposites via *In-situ* Technique

Material Scientists are conducting research to develop novel materials with better properties, more functionality and lower cost than the existing ones. Several physical, chemical and biological synthesis methods have been developed to enhance the performance of nanoparticles displaying improved properties with the aim to have a better control over the particle size, distribution and morphology (Shankar *et al.*, 2003). Synthesis of nanoparticles to have a better control over particles size, distribution, morphology, purity, quantity and quality, by employing environment friendly economical processes has always been a challenge for the researchers (Hahn, 1997).

Feldman (2003) demonstrated the desirous for selected synthesis to form homogeneous and well dispersions of silver nanoparticles. Notwithstanding the fact that as compared with gold nanoparticles, silver nanoparticles non-stabilized in a proper way undergo fast oxidation and easily aggregate in solutions, which complicates their

use in the development of sensors and optical instruments. Silver is more reactive than gold; hence, the method for synthesis and effective stabilization of silver nanoparticles with narrow size distribution must be elaborated. This is intrinsically important in metastable thermodynamics, where the stability encountered with their high surface areas represents a positive contribution to the free enthalpy of the silver nanoparticles system. Nonetheless, if the activation energies are not sufficiently high, the disperse evolution of silver nanoparticles causes an increase in nanoparticles size. The highly dispersed nanoparticles can be kinetically stabilized and prepared under proper conditions via the most preferred technique, which is the chemical reduction technique. Via chemical reduction technique, the well-known problem of coupling the synthesis of silver nanoparticles using an appreciate modifier on their surface is by no means an insurmountable obstacle in the production of stable silver nanoparticles and for their future applications.

The use of chemicals for nanoparticle synthesis has been proven to work and been widely studied. For example the use of chemicals and electricity as a combination has also managed to yield nanoparticles such as that of silver nanoparticles by electrochemical (Hu & Easterly, 2009; Khaydarov *et al.*, 2009; Jian *et al.*, 2005; Starowicz *et al.*, 2006) and sonochemical means (Liu *et al.*, 2001; Salkar *et al.*, 1999). Many methods have been suggested and refined over time to yield nanoparticles of much finer sizes. Jiang *et al.*, (2005) mentions that chemical reduction methods for nanoparticle synthesis can be divided into two subgroups; first of which is the co-reduction of two different kinds of metal salts and the second method is the successive reduction of two metal salts. The second method is usually carried out to prepare a core – shell structure of bimetallic nanoparticles. Based on Figure 2.1, it is seen that the conventional wet chemical route includes the elements of organic synthesis, self

assembly and colloidal aggregation. These three elements are representative of the various stages in the bottom-up strategy. It involves molecular components as starting materials which are linked with chemical reactions, nucleation and growth processes to promote the formation of complex nanoclusters (Yon & Jamie, 2008).

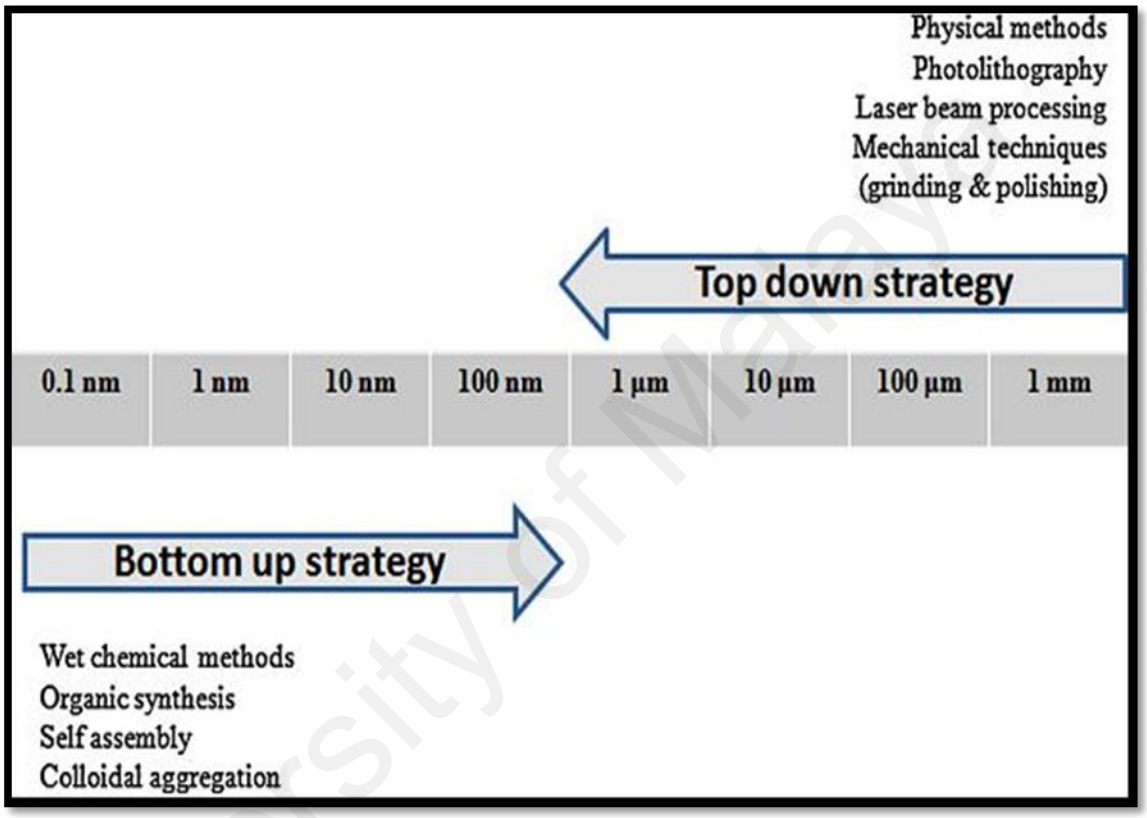

Figure 2.1: Strategies for manufacturing nanomaterials (Manikam *et al.*, 2011)

The distinct feature from Figure 2.1 is the fact that the wet chemical route demonstrates much finer particle synthesis as compared to that of the physical method. Material reactions via use of chemical precursors can readily produce bulk quantities of nanoparticles (Edelstein *et al.*, 1997). The chemical reduction of salts for metal nanoparticle synthesis is the simplest method possible and can be easily scaled up for bulk volume production (Guzman *et al.*, 2008). Thus, taking into consideration the three major factors of finer nanoparticle size synthesis, bulk quantity possibility during synthesis as well as the ease of using the method, many researchers have focused on

utilizing chemicals for nanoparticle synthesis. This includes the discussed method of chemical reduction in this literature work. According to Zhang *et al.* (2007), chemical reduction does have its own disadvantage in terms of toxic chemical usage which is harmful to the environment and health. The chemical reduction method traditionally utilizes three main items; a precursor, a reducing agent and a stabilizer or protective agent. Occasionally, a certain catalyst may be added to speed up a reaction. A solvent may also be introduced to create a more soluble, interacting media for the chemicals. Additionally, heating may be required to mix the precursors prior to the addition of reduction and surfactant agents. A simple comparison of the chemical synthesis route versus other synthesis methods for all types of nanoparticles and it highlights the advantages and disadvantages of each method in general, which can be taken into consideration when selecting a method for synthesis.

It is also critical to study the effects of nanoparticle structures and how they can influence the properties and applications associated with them. It is a well conceived idea that the type of surfactant and reducing agent influences the particle size. A stronger reducing agent such as $NaBH_4$ or hydrazine typically generates narrower particles, and is usually coupled with strong retarding agents or surfactants for example PVP or PVA to maintain the particle sizes as well as avoid agglomeration when dispersed. Also, nanoparticles are classified as 0, 1, 2 and 3D having different shapes such as rods, spheres and tubes (Yon & Jamie, 2008). Each shape may be used for different applications; spheres for interconnect in electronic applications as closer packing is needed or rods in structural applications for generating higher strength (Salkar *et al.*, 1999; Rotello, 2004; Gleiter, 2000).

Two of the most prominent synthesis methods to produce silver nanoparticles are the Creighton *et al.* method (1979) and the Lee and Meisel (1982) method. These methods are said to produce poly-disperse particles with a variety of shapes and sometimes unstable suspensions (Lundahl *et al.*, 2008). The Creighton method utilizes the reduction of silver nitrate ($AgNO_3$) by sodium borohydride ($NaBH_4$) whereas the Lee and Meisel method is generally accepted as the reduction of silver nitrate by sodium citrate. Another method which has been adapted and refined to produce silver nanoparticles is the Turkevich method (Krutyakov *et al.*, 2008). The Turkevich method, which also utilizes sodium citrate as a reduction agent was originally suited for gold nanoparticle synthesis. However, it also works on silver nanoparticle synthesis. The drawback of this method is that the particle size range is rather wide, between 20 and 200 nm (Krutyakov *et al.*, 2008). $AgNO_3$ is the most common source or precursor of silver ions due to its low cost and stability (Lee *et al.*, 2007) although Ag_2SO_4, 2 silver 2-ethylhexonate and silver perchlorate has also been used.

According to Tolaymat *et al*., (2010), a reducing agent is a chemical agent, plant extract, biological agent or means of irradiation, which is needed to reduce a particular salt during nanoparticle production. Sodium citrate, sometimes commonly known as trisodium citrate ($Na_3C_6H_5O_7$) is actively used in the aforementioned Lee and Meisel method (Lee & Meisel, 1982) when synthesizing silver nanoparticle. In this method (Lee & Meisel, 1982), $AgNO_3$ is added to water and brought to a boiling point before 1 percent of sodium citrate is added to the solution. Tan *et al.*, (2003) also utilized sodium citrate to reduce silver sulphate in the presence of aniline. The method produced considerably large-sized, polydisperse, and somewhat aggregated silver nanoparticles between the ranges of 35 and 100 nm. The authors believe that the amount of aniline added into the starting solution influenced the morphology of the silver nanoparticles.

Sileikaite *et al.,* (2006) reported that the synthesized silver nanoparticles from $AgNO_3$ salt was 100 nm when sodium citrate was used as the reduction agent and the surface plasmon resonance peak in the absorption spectra of the silver colloidal solution showed an absorption maximum value at 450 nm.

Another reduction agent – ascorbic acids ($C_6H_8O_6$) –was studied by Sondi *et al.*, (2003) and Suber *et al.,* (2005). Suber *et al.,* (2005) noted that during the experiment, when the ascorbic acid was discontinued or slowed in terms of addition to the silver ion solution, the resulting particles were more anisotropic in nature. Suber *et al.*, (2005) noted further that ascorbic acid is powerful as a reducing agent in acidic conditions. It managed to completely convert silver ions to metallic silver. Suber *et al.*, (2005) compared the reactions of ascorbic acid to that of Daxad 19 in the same experiment. The authors (Suber *et al.*, 2005) noted that rather uniform particles were formed in the absence of ascorbic acid, when only Daxad 19 and $AgNO_3$ were left to age for some time possibly due to the strong interaction of the sulfonic groups of Daxad 19 and the surface of silver. Also at a higher concentration of $AgNO_3$, finer particles were formed. The sizes of the synthesized silver nanoparticles were strongly dependent on the concentration and volume of the stabilizer and reducing agents, respectively. Such modifications enabled the authors to create a wide range of silver nanoparticles.

Surfactants and stabilizers both promote the same basic cause; they are added to avoid nanoparticles from aggregating and enhance size control of the particles. Stabilizers help to avoid excessive reactions between chemicals as well as inhibit separation in suspensions. A surfactant on the other hand helps to lower the surface tension in a suspension or liquid which makes it easier to disperse particles in it.

Surfactants fall under the category of stabilizers (Tolymat *et al.*, 2010; Luo *et al.*, 2005; Rao *et al.*, 2005 & 2006).

Agglomeration is caused by the high surface energy and thermodynamic instability exhibited by the surface of the particle (Tolaymat *et al.*, 2010). Sodium dodecyl sulphate (SDS) (Tolaymat *et al.*, 2010; Guzman et al., 2008; Wang *et al.*, 2008), and PVA (Tolaymat *et al.*, 2010) for instance are widely used as stabilizers and surfactants. Chen & Huang (2002) showed in their work that PEG held a dual role in silver nanoparticle synthesis; as a reducing agent and stabilizer in a dimethylacetamide (DMAC) solution. The authors (Chen & Huang, 2002) pointed out that in a solution of pure DMAC with silver salts, no silver nanoparticles were found unless PEG was added into it. This finding strongly confirms the role of PEG as a reducing agent. When varying molar mass of PEG was used on the silver nanoparticles, as the molar mass of PEG increased, the mean diameter of the silver nanoparticles reduced accordingly. This finding directly indicates that surfactant molar mass can be used to control the resulting nanoparticle sizes. Based on the preceding discussions, it can be seen that chemical reduction methods for silver nanoparticles is widely studied and has gained popularity amongst researchers (Biswas *et al.*, 2006).

However, most of the procedures described, yield stable silver dispersion only at relatively low concentrations of metal. Hence, they are not suitable for large scale manufacturing. This chemical reduction describes a simple method to produce silver nanoparticles in continuous media. The silver nanoparticles are obtained from $AgNO_3$ chemical reduction in selected solvent, using catalysts and colloidal suspension stabilizers. As mentioned before, surfactants work as surface modifiers that avoid particles agglomeration, and their action allows future manipulation of nanoparticles.

Therefore, large scale synthesis of nanosized silver particles using removable reductants and stabilizers is worth investigation.

Synthesis of silver nanoparticles consists of mixing two inverse emulsion (of the 'water-in-oil' type), in which one contains a silver salt ($AgNO_3$) dissolved in solubilised water and the other contains a reducing agent, which employ the reduction of silver nitrate using polyethylene glycol (PEG). Silver nitrate ($AgNO_3$) is the most common source of silver ions and polyethylene glycol (PEG) been usually used as reducing agents. Hence, to protect the particles from aggregation and to achieve long- term stability, surfactants or polymers are usually employed and in this study we select Daxad 19. These high activity dispersants are used to disperse finely divided insoluble particles in water.

The reduction of silver nitrate with Daxad 19 can lead not only to uniform, highly dispersed spheres in concentrated solutions, but also to isolated particles of other shapes (Sondi *et al.*, 2003). The performance of Daxad 19 was recognized when it was combined with ascorbic acid and sulphuric acid (Suber *et al.*, 2005). Based on their findings, the silver nanoparticles formation process can be tailored by increasing the time for the solution to be in basic and neutral conditions. In addition, a change in morphology of silver nanoparticles can be controlled when the reaction of Daxad 19 at high temperature was implemented. Nevertheless, the time constraint is critically important. Instead of combining the Daxad 19 with any acid, the use of PEG, polyethylene glycol is considered. In this work, the reducing agent involving silver nitrate ($AgNO_3$) and PEG (Luo *et al.*, 2005) as well as the possible reaction including Daxad 19 are:

Reducing

$$-CH_2CH_2OH + Ag^+ \rightarrow -CH_2CHO + H_2O + \text{Silver nanoparticles} \quad (2.1)$$

Stabilizing

$$\text{Daxad 19} + \text{Silver nanoparticles} \longrightarrow \text{Stable Silver nanoparticles} \quad (2.2)$$

Tuval *et al.*, (2007) discovered that the role of PEG significantly inhibits the reduction reaction. In this synthesis, PEG serve as an environmentally benign reducing agent. However, the chain length of PEG was shown to play a key role in the formation of silver nanoparticles (Kumar *et al.*, 2001). According to Luo *et al.*, (2005) ethylene glycol used as a reducing agent for the preparation of metal nanoparticles at high temperature (170 °C) was inactive for reducing of silver ions (Ag^+) at 80 °C. Nonetheless, silver ions can be smoothly reduced to silver nanoparticles at the same condition in PEG 2000. Thus, this study demonstrated the use of PEG 8000 upon the reaction condition since the reducing rate of silver ions to silver nanoparticles was enhanced remarks, with the increase in polymer length.

Therefore, as described by Sileikaite *et al.*, (2006), the chemical reduction technique has been proven to give better control over the process in order to tailor the properties at molecular level. Spherical, prism and hexagonal silver nanoparticles having better size distribution are synthesized successfully using the chemical reduction method. In addition, Reddy *et al.*, (2007) showed that silver nanoparticles prepared via this technique could eliminate problems such as poor stability and reproducibility due to the colloid aggregation.

However, the colloid aggregation problems can be overcome by using the polymer as the capping agent that plays a role of size controlling. It is now well established that the polymer are excellent host materials for nanoparticles of metal and semiconductor (Mbhele *et al.*, 2003; Zeng *et al.*, 2002; Zhang & Han, 2003; Mullick *et al.*, 2004; Firth, 2004). When the nanoparticles embedded or encapsulated in polymer, the polymer will act as a surface capping agent. Incorporation of inorganic nanoparticles in a polymer matrix can significantly affect the properties of the matrix (Kickelbick, 2003; Caseri, 2000). The obtained nanocomposites might exhibit improved optical, thermal, mechanical, electrical, magnetic, and flammability properties. The properties of polymer composites depend on the type of incorporated nanoparticles, their size and shape, their concentration and interaction with polymer matrix.

Many different synthetic procedures for preparation of Ag/PMMA nanocomposites such as "core-shell" synthesis (Wang & Chen, 2004; Quaroni & Chumanov, 1999), ion implantation (Stepanov *et al.*, 2000), vapor phase co-deposition in vacuum (Yeum & Deng, 2005) and suspension polymerization (Marutani *et al.*, 2004). The main problem in polymer nanocomposites technology is the prevention of the particles aggregation. This problem can be overcome by modification of the surface of the particles. The modification improves the interfacial interaction between the inorganic particles and the polymer matrix (Kickelbick, 2003; Zhang *et al.*, 2005; Vodick *et al.*, 2009).

In general, the silver/polymer nanocomposites were prepared in two steps. Firstly, the polymer was synthesized, and then the silver ions introduced into the polymer matrix were reduced to zerovalent state by a reducing agent or by post-heating. In recent years, much effort was devoted to the studies on the *in-situ* synthesis of metal

nanoparticles in polymer matrices (Hatchett *et al.*, 1999; Huang *et al.*, 1991; Gotoh *et al.*, 2000). This method is based on the reduction of metal ions that are dispersed in polymer matrices. The synthesis involving methyl-methacrylate (MMA) in the presence of external reducing agent and the addition of the appreciate amount of silver nanoparticles was achieved successfully (Vodick *et al.*, 2009). Organic polymer materials exhibit significant fast nonlinearities and low absorption across the visible and infrared spectral regions. It was described earlier that the reduction of silver ions from silver nitrate took place due to hydrated electron and hydrogen (Monti *et al.*, 2004). However, Khanna and Singh (2007) found that besides the reduction of silver ions, the availability of sodium ions from the poly (methyl methacrylate) need to be considered. The presence of silver ions can alter the optical and electronic properties of nanocomposites. Therefore, it is essential to obtain pure silver nanoparticles with the desired morphology and uniform size distribution within the composites. Nonetheless, these challenges were not fully tackled since the use of the external reducing agent and the silver salt did not induce a complete reaction. These problems can be eliminated by employing simpler and easier synthetic methods which can generate zero-valent silver in the composites (Khanna & Singh, 2007). Ershov and Heglein (1998) found that during the formation process of silver nanoparticles, bands at 345 and 420 nm were observed due to the presence of silver ions (Ag^{+}) and silver nanoparticles. Khanna and Singh (2007) produced Ag/PMMA nanocomposites with bands observed at 452 nm due to agglomerations of particles and change in dielectric properties of nanocomposites. Yan Deng *et al.*, (2006) reported that the SPR peak of Ag /PMMA nanocomposite was observed at 428 nm due to collective excitation of the free electron of silver nanoparticles. The linear absorption properties of the films demonstrate that silver nanoparticles were successfully incorporated into and stabilized in the PMMA matrix. From the electrical studies, the value of dielectric constant, ε' is higher for low

frequency and lower at high frequency range since PMMA is a polar material (Bhargav et al., 2010; Mardare & Rusu, 2004; Fuyuki & Matsunmi, 1986). This may be attributed to the tendency of dipoles in polymeric samples to orient themselves in the direction of applied field in the low frequency range. On the other hand, the value of dielectric constant is decreases due to polarization effects and smaller tendency of dipoles to orientation themselves according to the field vibration at high frequencies (Ramya et al., 2008). The reaction of the MMA and silver nanoparticles is (Khanna & Singh, 2007):

Initiator

$$CH_2C(CH_3)COOCH_3 \rightarrow [CH_2C(CH_3)COO^-]_n \quad (2.3)$$

In-situ technique

$$-CH_2C(CH_3)COO^- + Ag^+ \rightarrow -CH_2 - C(CH_3)(COO^-)(Ag^0) - CH_2 - \quad (2.4)$$

In-situ technique has been proven to give significant improvement to the modification of the interfacial between inorganic particles and the polymer matrix (Marutini *et al.*, 2004; Zhang *et al.*, 2005). Vodick *et al.*, (2009) used *in-situ* bulk polymerization using chloroform as a solvent to produce PMMA sphere surrounded silver nanoparticles. The particles distribution was quite agglomerated due to incorporation of silver nanoparticles into the PMMA matrix. The *in-situ* technique involves the deposition of silver nanoparticles into dielectric PMMA matrix (Singh & Khanna, 2007; Thomas *et al.*, 2008; Garcia *et al.*, 2009). In this process, silver nanoparticles and PMMA are developed simultaneously, and leads to uniform particle size distribution. This modification improves the interfacial interaction between silver nanoparticles and the PMMA, which inhibits the particles from agglomerated.

This is a class of the simplest and most representative method for the preparation of composite materials. Polymers and inorganic hybrid precursors were dissolved in a suitable solvent, and the molecules of polymer and precursors combined together. Via a reaction, such as metal alkoxide hydrolysis, oxidation and reduction reactions, and so on, inorganic nanoparticles were *in-situ* formed in the polymer. Using the adsorption and complexation of metal ions of polymer-specific functional groups or the space constraints between polymer and reactant, nanocomposites were prepared *in-situ*. The methods for generating nanoparticles can be radiation, heat, light, gas reactions and so on. By this way, the obtained inorganic particle was usually nanometer size, and uniformly dispersed in polymer. Therefore, the compounds own transparent stable structures. Moreover, the polymer plays a role of size controlling and aggregation preventing of inorganic nanoparticles.

In this research, the precursors used were silver nitrate ($AgNO_3$) as a source of silver ion, polyethylene glycol (PEG) as reducing agent and Daxad 19 (sodium salt of poly naphthalene sulfonate formaldehyde condensate) as the stabilizer. Doubly distilled water was used in the preparation of aqueous solutions. The chemical composition was determined based on previous study (Luo *et al.*, 2005). The variation in composition of $AgNO_3$ was needed in order to provide an ultimate condition for producing silver nanoparticles. The PEG composition was constant throughout the experiment since the main focus is towards the effects of Daxad 19 on the silver nanoparticles. Various surfactants and different concentrations of Daxad 19 and of silver nitrate were used to establish their effect on the size and the stability of the resulting dispersions of silver particles. While in the *in-situ* technique, PMMA was used as a stabilizer that acted as the protection from agglomeration of nanoparticles. The stabilizer attached to the silver nanoparticles by chemical bonding and prevented nanoparticles to agglomerate to form

bigger particles. Dimethylformamide (DMF) was used as a solvent for chemical network between silver nanoparticles and PMMA (Pastoriza-Santos & Liz-Marzan, 1999).

2.6 Silver nitrate ($AgNO_3$)

Silver nitrate is an inorganic compound with chemical formula $AgNO_3$. The silver ions are three-coordinated in a trigonal planar arrangement in the solid silver nitrate. It is clear that their size and shape are particularly important in explaining their physical properties and chemical reaction mechanism. The molecular structure of silver nitrate is shown in Figure 2.2, which show the arrangement of atoms around the 'central atom'.

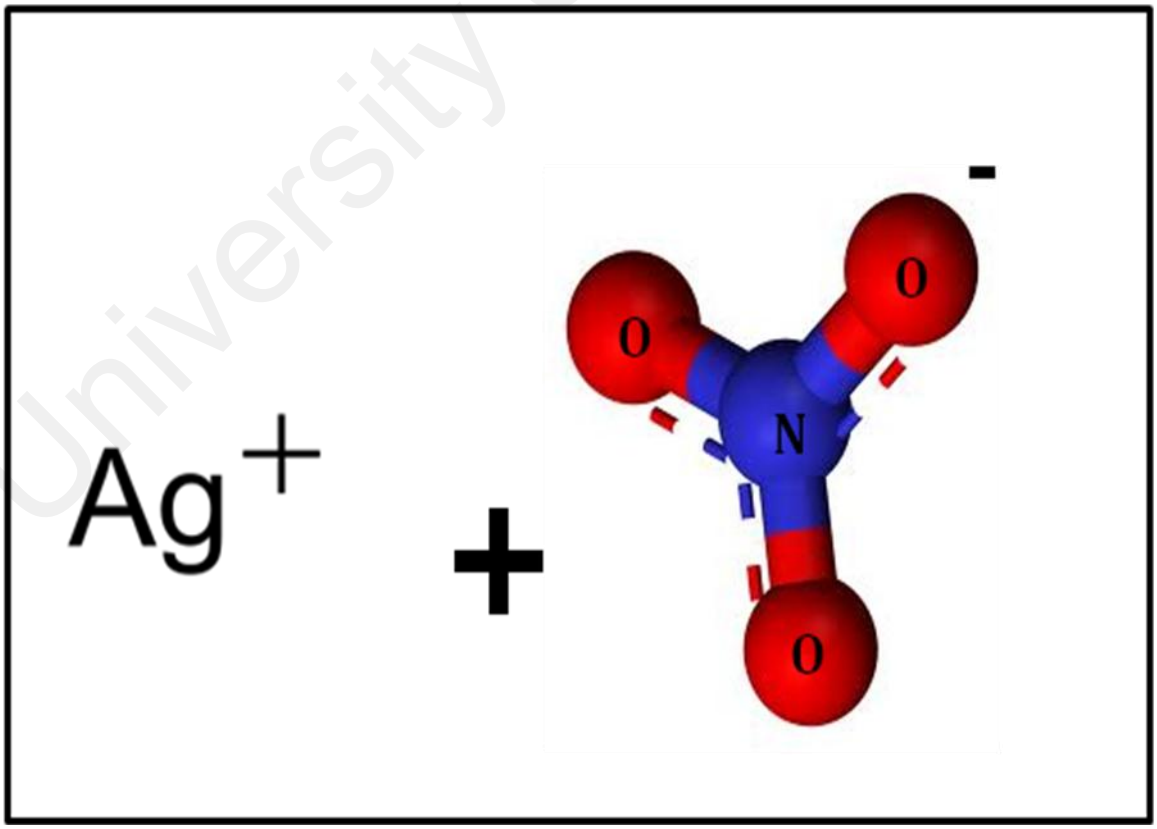

Figure 2.2: The arrangement of trigonal planar of silver nitrate

Silver nitrate can be prepared by reacting silver, such as a silver bullion or silver foil, with nitric acid, resulting in silver nitrate, water, and oxides of nitrogen.

$$3Ag + 4HNO_3 \rightarrow 3AgNO_3 + 2H_2O + NO \quad (2.5)$$

Silver nitrate is the least expensive salt of silver; it offers several other advantages as well. It is non-hygroscopic, in contrast to silver fluoroborate and silver perchlorate. It is relatively stable to light. Finally, it dissolves in numerous solvents, including water. The nitrate can be easily replaced by other ligands, rendering $AgNO_3$ versatile.

To obtain highly concentrated stable dispersions of nanosized silver particles, the chemical reduction in aqueous solutions of the most common silver compound, silver nitrate, was used. Different concentrations of silver nitrate were used to establish their effect on the size and the stability of the resulting dispersions of silver nanoparticles.

2.7 Polyethylene glycol (PEG)

Polyethylene glycol (PEG) is a polyether compound with many applications from industrial manufacturing to medicine. PEG refers to an oligomer or polymer of ethylene oxide with a molecular mass below 20,000 g/mol. PEGs are prepared by polymerization of ethylene oxide and are commercially available over a wide range of molecular weights from 300 g/mol to 10,000,000 g/mol. PEG with different molecular weights find use in different applications and have different physical properties (e.g., viscosity) due to chain length effects, their chemical properties are nearly identical.

Different forms of PEG are also available dependent on the initiator used for the polymerization process. Lower-molecular-weight PEGs are also available as purer oligomers, referred to as monodisperse, uniform or discrete. Very high purity PEG has recently been shown to be crystalline, allowing determination of an x-ray crystal structure. PEG has the following molecular formula and its arrangement position is shown in Figure 2.3.

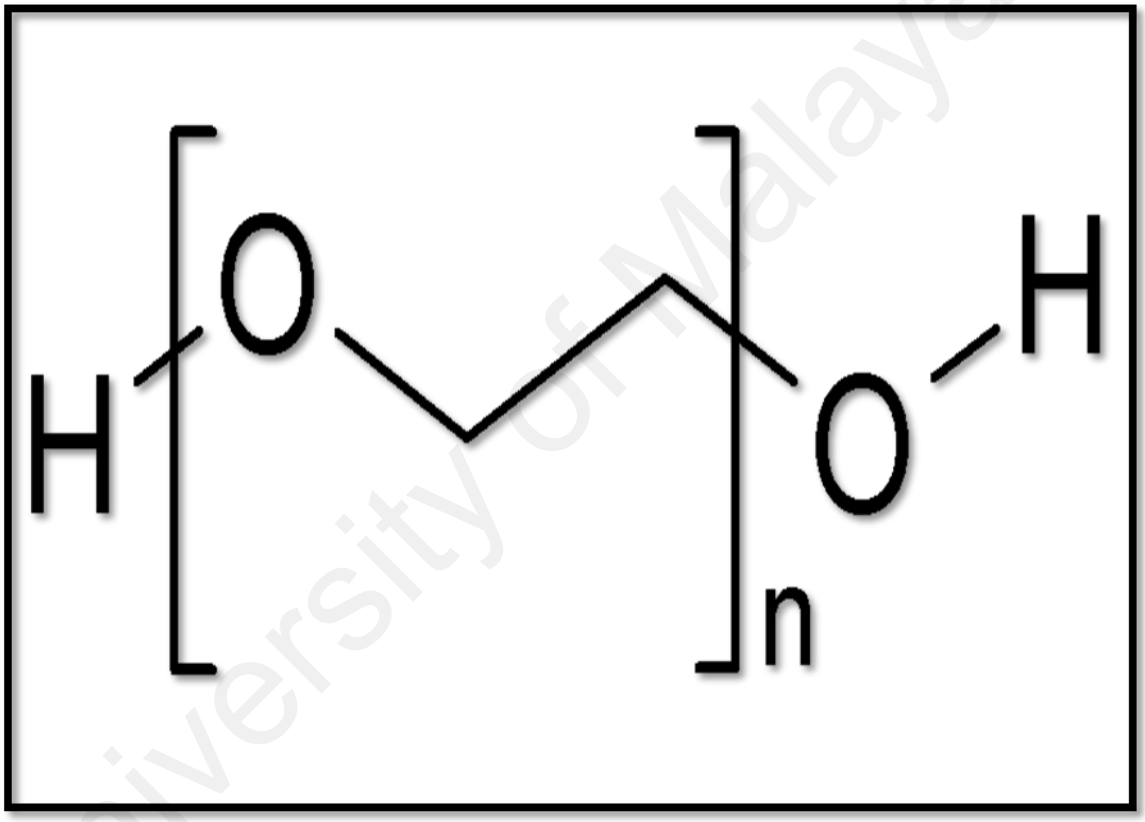

Figure 2.3: The arrangement of PEG structure, whereby value of n depends on the molecular weight of PEG

Polyethylene glycol is produced by the interaction of ethylene oxide with water, ethylene glycol, or ethylene glycol oligomers. The reaction is catalyzed by acidic or basic catalysts. Ethylene glycol and its oligomers are preferable as a starting material instead of water, because they allow the creation of polymers with a low polydispersity

(narrow molecular weight distribution). Polymer chain length depends on the ratio of reactants as shown in Equation 2.6:

$$HOCH_2CH_2OH + n(CH_2CH_2O) \rightarrow HO(CH_2CH_2O)_{n+1}H \quad (2.6)$$

PEG is also a good stabilizer for synthesis silver nanoparticles based on the conclusions made by several research studies (Chen *et al.*, 2007; Popa *et al.*, 2007; Shkilnyy *et al.*, 2009). In one of these research works, Luo *et al.*, 2005 reduced $AgNO_3$ in the presence of PEG. The researchers suggested that stabilization can be obtained due to the free polymer chains in solution, where formation of aggregates is denied because of steric hindrance. From their observation, they also proposed that increasing the molecular weight of the polymer would help in forming stable silver nanoparticles (Luo *et al.*, 2005).

2.8 Daxad 19

Daxad 19 consists of 85 percent sodium napthalene sulphonate, 10 percent sodium sulphate and 5 percent of water (Figure 2.4). These high activity dispersants are used to disperse finely divided insoluble particles in water. Furthermore, they are used to improve suspension, decrease viscosity, increase color intensity, and provide better grinding properties in emulsion polymerization, dyes, ceramic slips, cemets and many other industries. In this studies, Daxad 19 play as a dual role; as a reducing agents as well as stabilizer. Che Lah & Johan, 2011 stated that a light grey transparent solution was formed in the solution of silver nanoparticles without Daxad 19, indicating that the reduction of Ag^+ to Ag^0 nanoparticles did not occur. The disappearance of peaks indicates that the silver nanoparticles would not develop without Daxad 19 as a stabilizer.

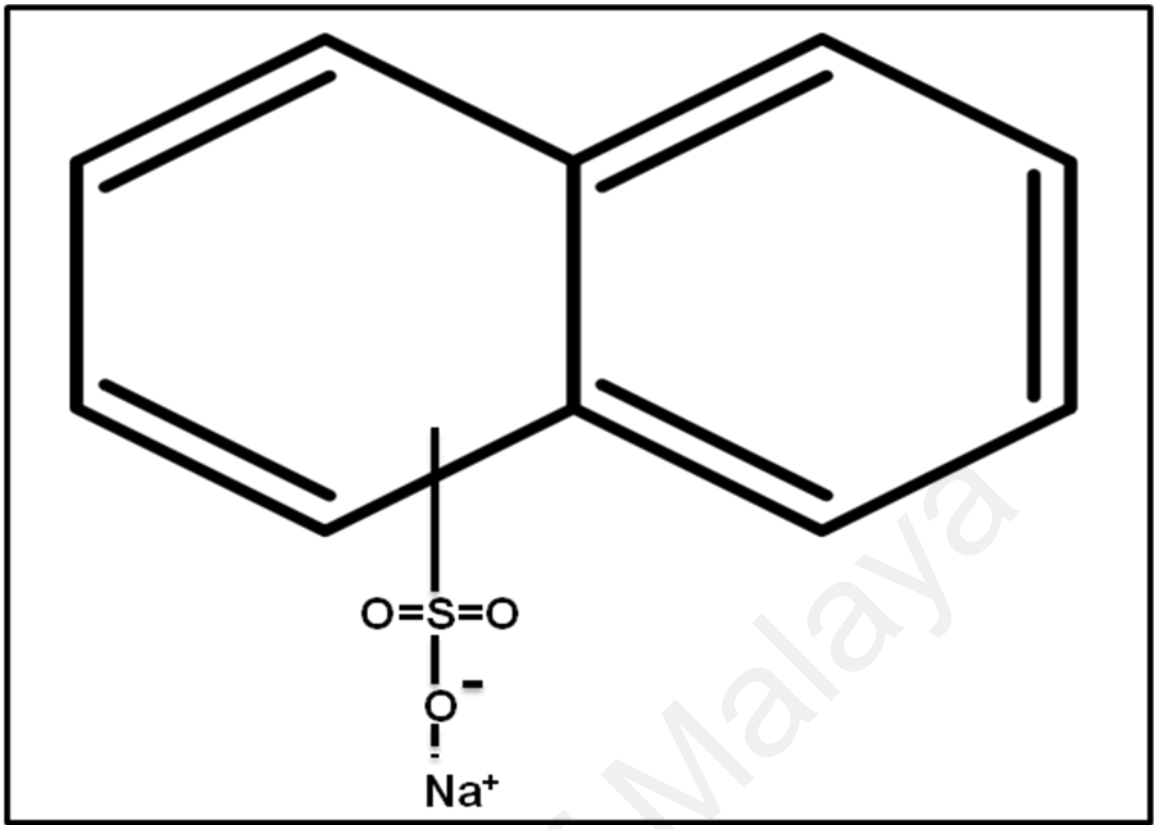

Figure 2.4: The general structure of Daxad 19

2.9 Dimethylformamide (DMF)

Dimethylformamide (DMF) is an organic compound with the formula $(CH_3)_2NC(O)H$. This colorless liquid is miscible with water and the majority of organic liquids. Pure DMF is odorless whereas technical grade or degraded DMF often has a fishy smell due to impurity of dimethylamine. DMF is a common solvent for chemical reactions. Its name is derived from the fact that it is a derivative of formamide, the amide of formic acid. DMF is a polar (hydrophilic) aprotic solvent with a high boiling point (Figure 2.5). DMF can be synthesized from methyl formate and dimethylamine or by reaction of dimethylamine with carbon monoxide.

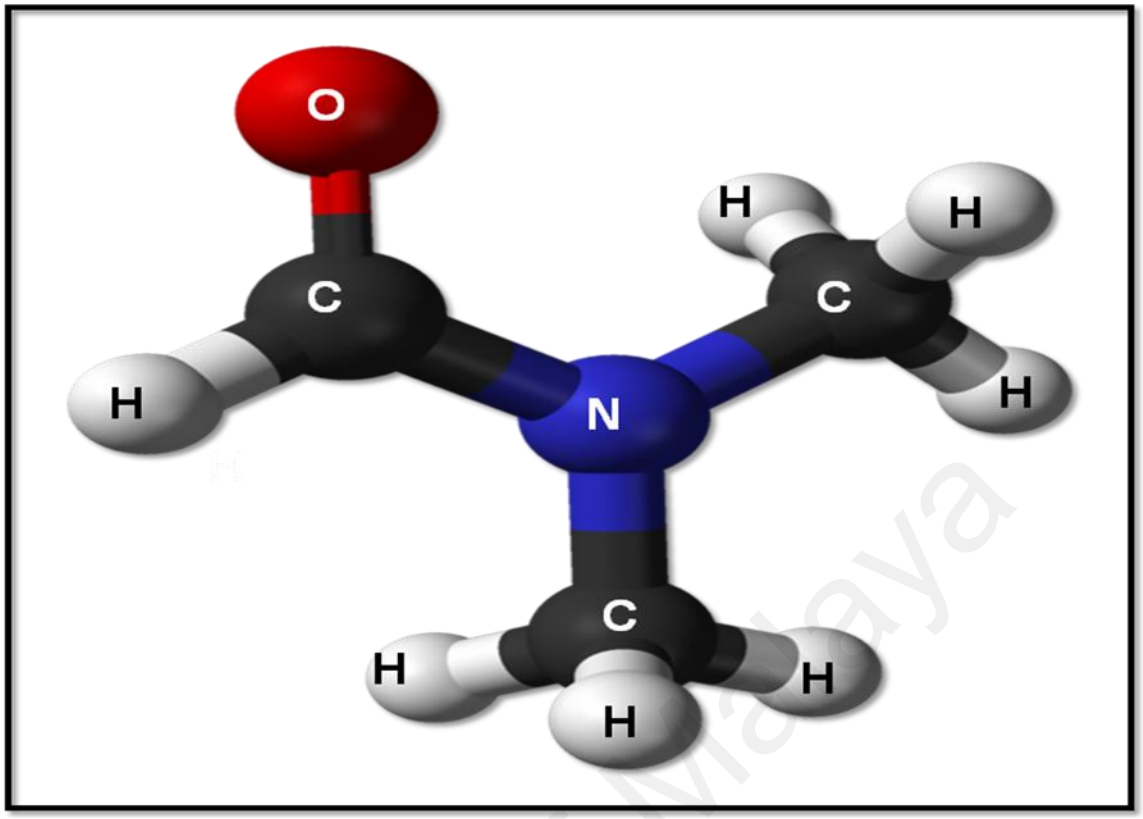

Figure 2.5: Molecular arrangement of dimethylformamide (DMF)

DMF is a polar substance with a large dipole moment (μ = 3.86 D). It is an eminently suitable solvent for compounds with a high molecular weight owing to the combined action of its high dielectric constant, electron donor properties and ability to form complexes. As a result, many reactants can be brought together in suitable concentrations in a DMF medium. This molecule has a fairly strong proton acceptor group and no proton donor groups. Further, the hydrogen atom of the C–H group is able to provide only a weak hydrogen bond. Therefore even if there are aggregates with intermolecular hydrogen bonds in the liquid DMF, they cannot be treated as stable moieties. DMF, as pure solvent, is to some extent associated by means of non-specific dipole–dipole interactions due to the large dipole moment of the DMF (Tukhcvatullin *et al.*, 2003).

However, DMF is not stable in the presence of strong bases like sodium hydroxide or strong acids such as hydrochloric acid or sulfuric acid and is hydrolyzed back into formic acid and dimethylamine, especially at elevated temperatures. Due to the contribution of the two possible resonance structures of an amide, the bond order of the carbonyl C=O bond is reduced, while that of the carbon-nitrogen bond is increased as shown in Figure 2.6. DMF is produced either via catalyzed reaction of dimethylamine and carbon monoxide in methanol or via the reaction of methyl formate with dimethylamine.

DMF was chosen as a solvent for synthesize Ag/PMMA nanocomposites. This is because it has high solubility when PMMA is use as a matrix as well as use of DMF being more suitable for silver nitrate reduction (Khanna *et al.*, 2005; Santos & Marzan, 1999).

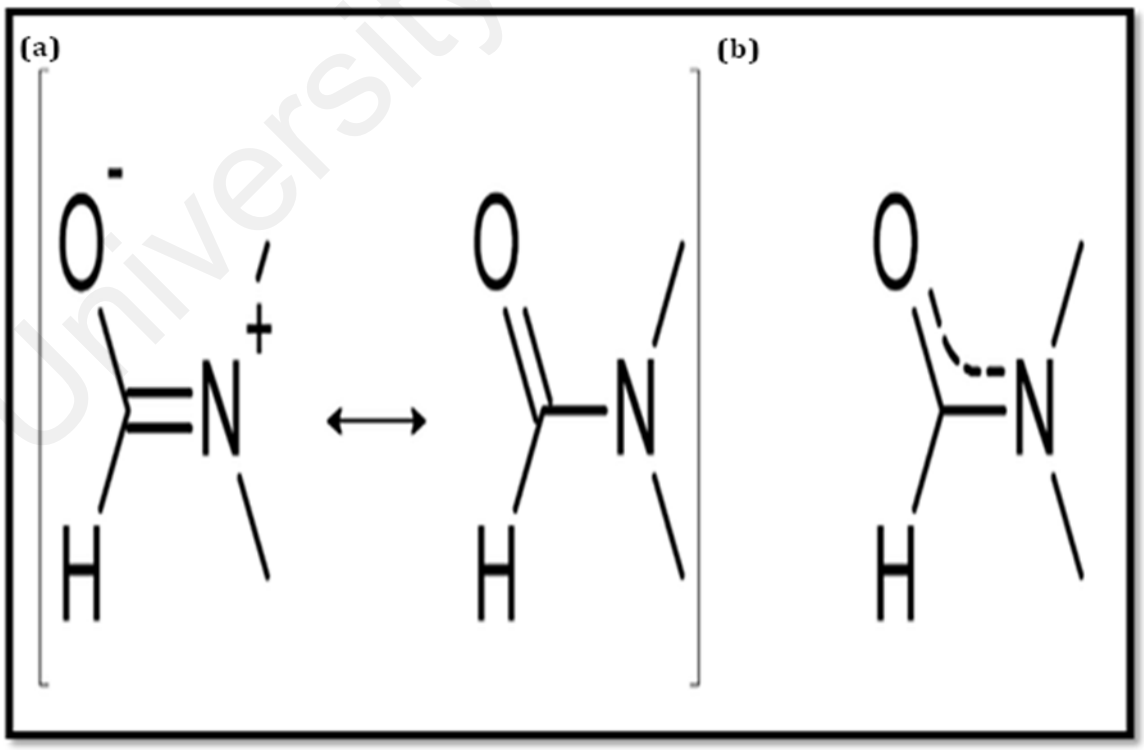

Figure 2.6: (a) The mechanism of two DMF resonance form (b) DMF molecular arrangement (Internet source, Wikipedia)

2.10 Polymer

Polymers are defined as macromolecules which are composed of long molecule chains of large, strong molecules bonded through chemical reaction. The word "polymer" is derived from greek words ("poly" means many and "mer" means part or segment). Polymer chains are formed from the polymerization of monomers which are small and light molecules. These chains can be linear or branched.

Polymers are found in countless applications in day to day life because of their properties such as light weight, ease of fabrication, highly corrosion resistance, non-toxic (some were non toxic), and capability to make polymer composites. However, the they possess disadvantages including their brittle nature (some thermosets), low temperature stability, and low electrical conductivity (PMMA shows electrical conductivity as low as 10-12 ohm/cm). Some of these problems can be solved by making polymers into the composites such as carbon nanotube/ polymer composites which show an improved electrical conductivity and good mechanical strength (Ajayan *et al.*, 2004 & 2007; Balberg *et al.*, 2004).

Poly (methyl methacrylate) (PMMA) is a linear thermoplastic with amorphous structure. It is known as transparent polymer Perspex which is also denoted as poly (methyl 2- methylpropanoate). The molecular formula (Figure 2.7) is $(C_5O_2H_8)n$. PMMA was first developed in the year 1928, brought to the market by Rohm and Haas Company. It has specific gravity 1.18 g/cc, softens over 130 °C, boiling point is around 200 °C, and has low resistance to scratchiness compared to glass. The electrical conductivity of PMMA is about 1×10^{-13} S/cm (Park *et al.*, 2005).

The thermal degradation process of PMMA has been a subject of numerous studies (Jellinek, 1995; Kashiwagi *et al.*, 1995) and usually involves multiple steps assigned to: presence of relatively weak head-to-head linkage, the scission of unsaturated end groups, and to the random scission. It is generally considered that most PMMA thermally degrade through depolymerization; therefore, the kinetics of mass loss is determined by the mode of depolymerization initiation (Neill, 1968). The TGA curve for pure PMMA has peak 276 and 430 °C, respectively. This behavior can be explained by the dual function of oxygen in PMMA degradation (Vodnik *et al.*, 2009). At lower temperatures, oxygen exhibits PMMA degradation by reacting with a polymeric radical and forming a stable peroxy radical. At higher temperatures (above 270 °C), peroxy radical degrades and release a more reactive radical resulting in the acceleration of PMMA decomposition (Peterson *et al.*, 1999). Under these condition, the peak corresponding to the week head-to-head linkage (100-200 °C) disappears, and the peak belongs to the scission of the unsaturated end groups (100-200 °C) merges with the random scission peak at 300-450 °C.

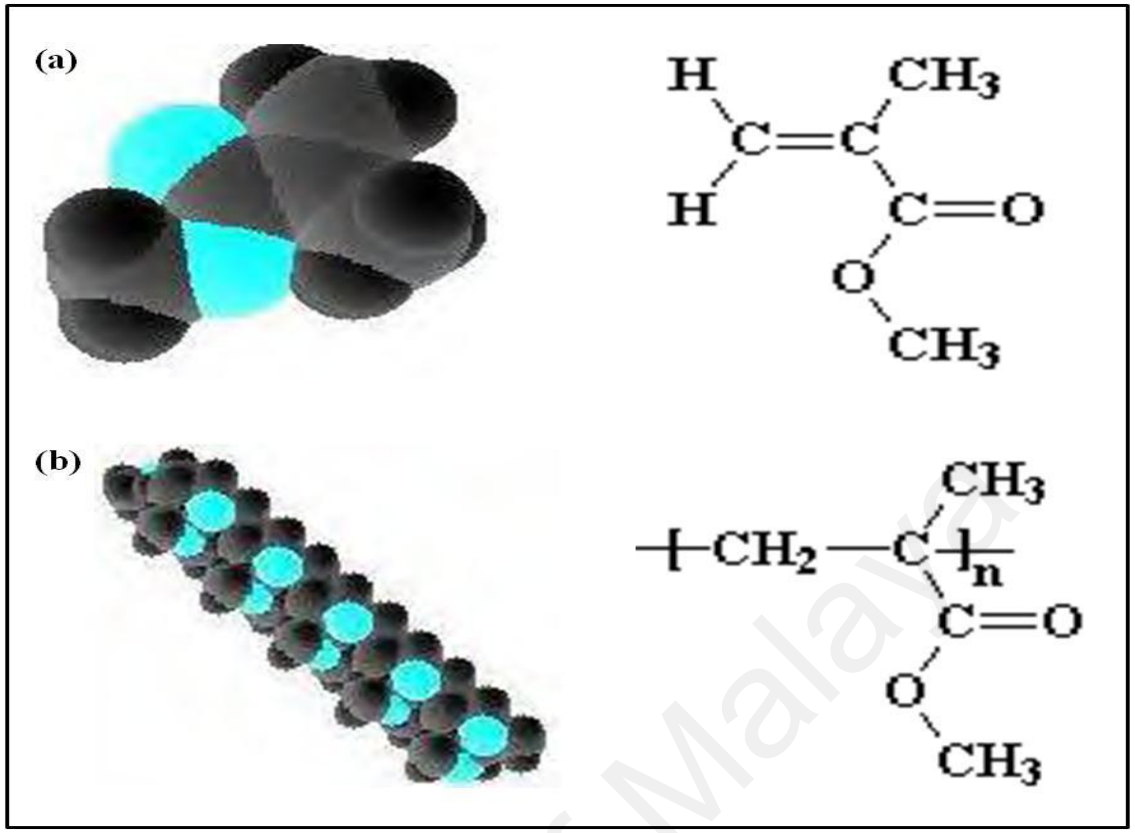

Figure 2.7: Atomic structure and chemical formula of a) Methyl Methacrylate b) Poly Methyl Methacrylate (Brydson, 1995).

Preparation of PMMA:

PMMA is prepared through free radical polymerization of methyl methacrylates. The methyl methacrylate monomers were polymerized to get poly (methyl methacrylate) (Figure 2.8). PMMA is used as matrix for many electrically conducting composites such as carbon coated cobalt-PMMA composites (Lueshinger *et al.*, 2008). In this dissertation, PMMA is used as a matrix and also as a capping agent.

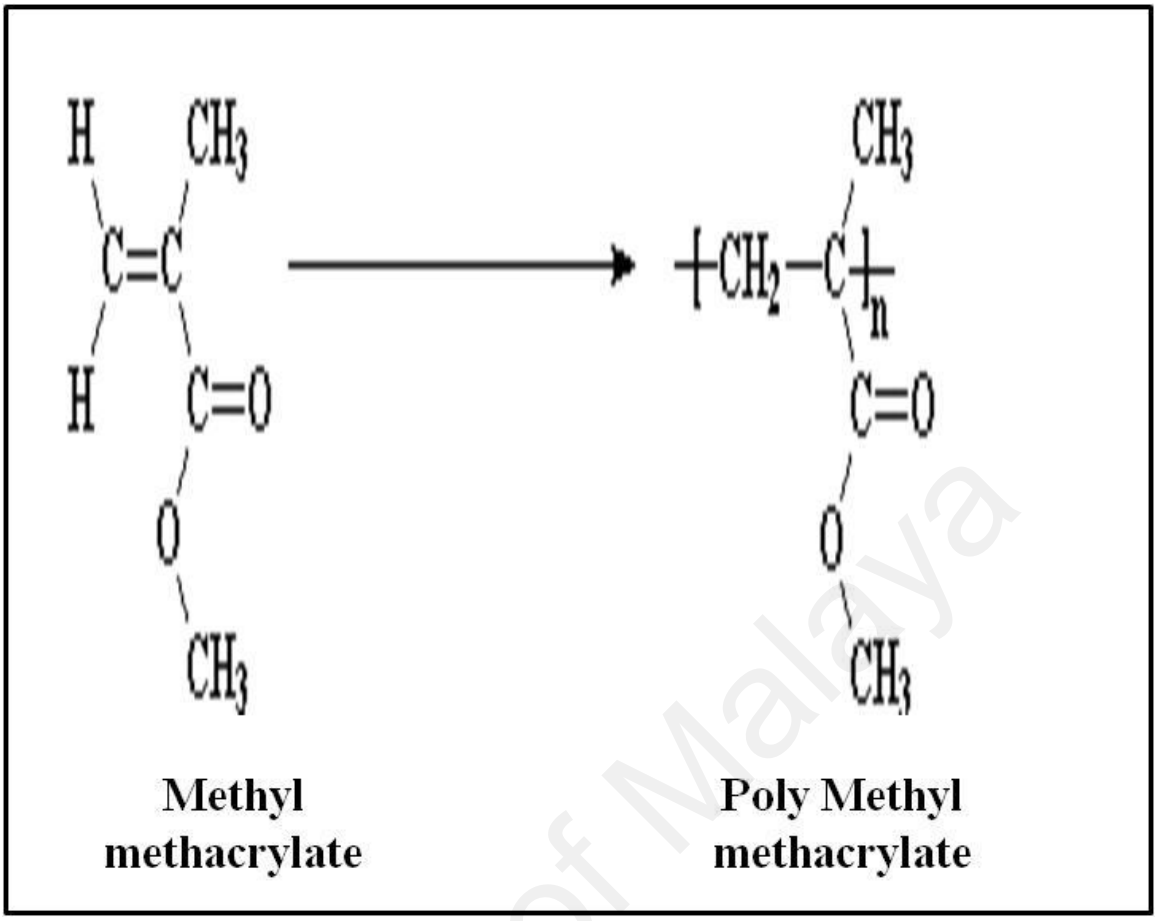

Figure 2.8: Free radical polymerization of methyl methacrylate gives poly (methyl methacrylate) (Brydson, 1995).

CHAPTER THREE

METHODOLOGY

3.1 Materials

All the chemical reagents were analytical graded and used without purification. Silver nitrate ($AgNO_3$) (Fisher Scientific) was selected as a source of silver. Polyethylene glycol (PEG) (Acros Organics) was used as a reducing agent. Daxad 19 (sodium salt of polynaphtalene sulfonate formaldehyde condensate) (Canamara United Supply Company) was used as stabilizer and reducing agent. Poly (methyl methacrylate) (PMMA) (Acros Organics, New Jersey, USA) was used as a capping agent. Doubly distilled water was used in the preparation of silver nanoparticles aqueous solution and dimethylformamide (DMF) (R & M Marketing, Essex, UK) was used as solvent in the synthesis of Ag/PMMA nanocomposites. Table 3.1 summarizes the materials used in this work.

Table 3.1: Precursor materials for synthesis of Ag/PMMA nanocomposites

Chemical Name	Chemical Structure	Molecular Weight	Function
Silver nitrate	$AgNO_3$	NA	Source of silver ion
PEG	$HO\text{-}CH_2\text{-}(CH_2\text{-}O\text{-}CH_2\text{-})n\text{-}CH_2\text{-}OH$	8000	Reducing agent
Daxad 19	$C_{10}H_7NaO_3S$	8000	Reducing agent and stabilizer
DMF	C_3H_7NO	NA	Solvent
PMMA	$(C_5O_2H_8)n$	35 000	Capping agent (matrix)

3.2 Samples Preparation

3.2.1 Synthesis of Ag/PMMA nanocomposites via *in-situ* technique

Figure 3.1 shows the silver nanoparticles preparation using reduction method, 4 g of $AgNO_3$ was dissolved in a mixture of 100 mL distilled water, 4.5 g of PEG and 5 g of Daxad 19 at 80 °C and stirred for 1h. The color of Daxad 19 solution changed from colorless to light brown upon the addition of $AgNO_3$. This indicates the formation of preliminary silver nanoparticles due to the reduction of Ag^+ ions by Daxad 19. The solution was then centrifuged at a 15,000 rpm, washed with distilled water (Erchov & Henglein, 1998) and heated at 100 and 120 °C.

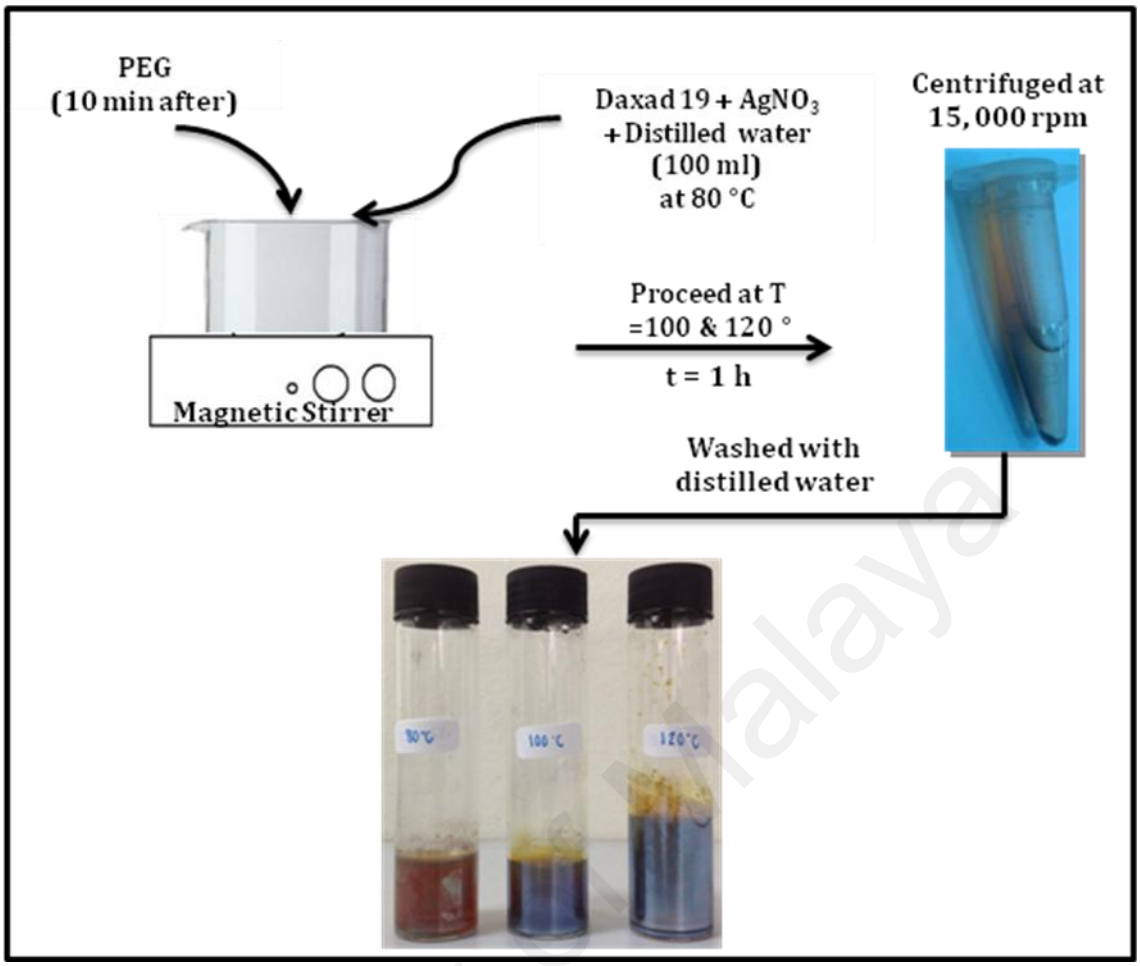

Figure 3.1: Schematic diagram of silver nanoparticles preparation procedure

Beside PEG as a reducing agent, Daxad 19 plays a dual role as a reducing agent and a stabilizer. The combination of Daxad 19 and PEG forms an optimum condition for producing silver nanoparticles. The details of the experimental conditions used are listed in Table 3.2.

Then, 6 g of PMMA was dissolved in 50 mL of DMF. Approximately 3 mL of freshly prepared solutions of silver nanoparticles were added in such a way to obtain 6 percent loading of silver nanoparticles in PMMA. The entire processing was carried out in a fume hood under constant stirring at 80 °C. The mixture was further stirred for 1 hour in order to mature the reaction. The samples were heated at two temperatures, 100 and 120 °C. The process of synthesis Ag/PMMA nanocomposites using *in-situ*

technique is illustrated in Figure 3.2. The color of the composite material depends on the nature and concentration of the silver particles as well as on the synthesis conditions. Evidently, as the percentage loading of silver nanoparticles and reactant temperatures increases, the color become more intense, changing from light brown to dark reddish brown due to the formation of silver colloids. The reduction of the Ag^+ ions occurred simultaneously via heating (Khanna & Singh, 2007).

Table 3.2: Experimental conditions for the the silver nanoparticles and Ag/PMMA nanocomposites

Reactant temperature (°C)	**Reaction time (h)**	**$AgNO_3$ (g)**	**Daxad 19 (g)**	**PEG (g)**	**Silver Nanoparticles (mL)**	**PMMA (g)**
80	1	2	3	4.5	3	6
80	1	3	4	4.5	4	8
80	1	4	5	4.5	5	10
100	1	2	3	4.5	3	6
100	1	3	4	4.5	4	8
100	1	4	5	4.5	5	10
120	1	2	3	4.5	3	6
120	1	3	4	4.5	4	8
120	1	4	5	4.5	5	10

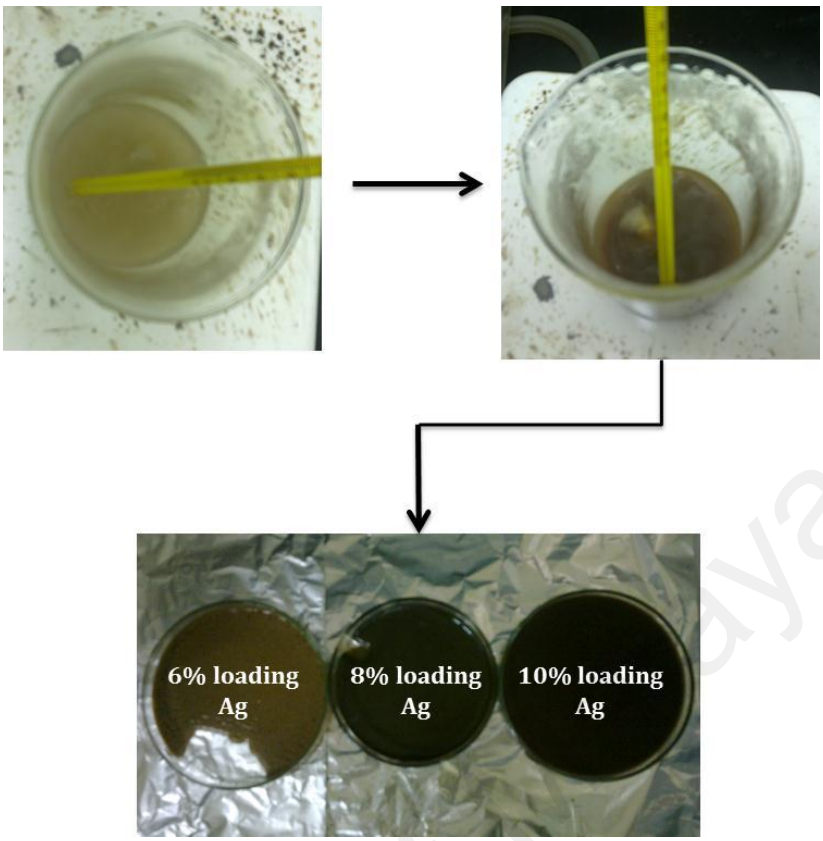

Figure 3.2: *In-situ* synthesis process routes for Ag/PMMA nanocomposites

In-situ technique offers two folds advantages: (i) The availability of carboxylate functional group, i.e. the acrylates in PMMA are considered to be better suited for chemical bonding with the metal ions, (ii) high solubility of PMMA in DMF is more suitable for $AgNO_3$ reduction (Che Lah & Johan, 2011). The reduction of Ag^+ ions occurred simultaneously via heating. The details of the the experimental conditions are listed in Table 3.2. Figure 3.3 shows the flowchart of sample preparation.

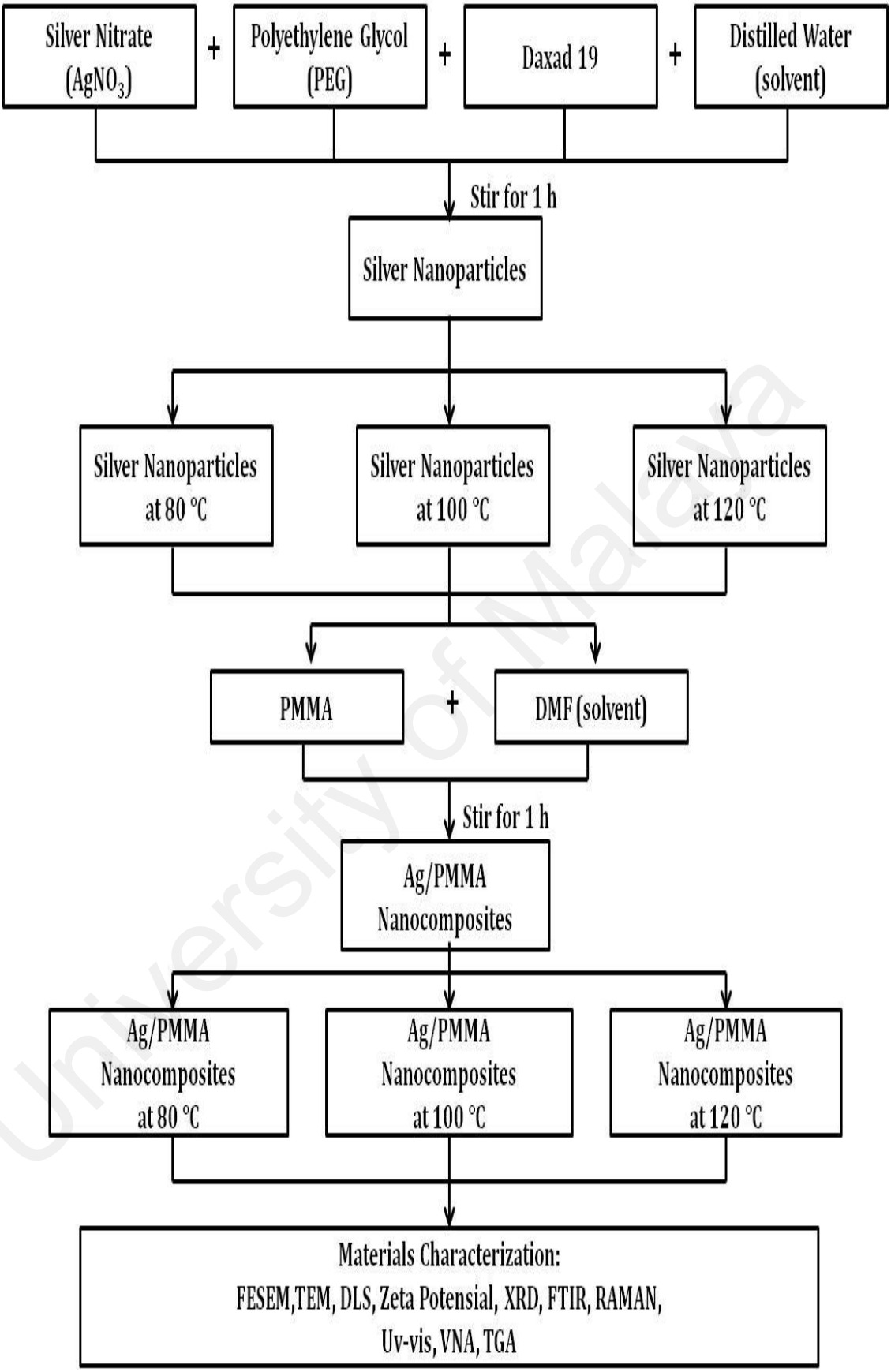

Figure 3.3: Flowchart of sample preparation for silver nanoparticles and Ag/PMMA nanocomposites

3.3 Material Characterization

3.3.1 Field Emission Scanning Electron Microscopy (FESEM)

Figure 3.4 shows the field emission scanning electron microscopy (FESEM), (AURIGA, ZEISS, Germany) used in this research. High beam energies were used to achieve good resolution and small probe diameters when non-conductive materials have been coated, to avoid charging problems.

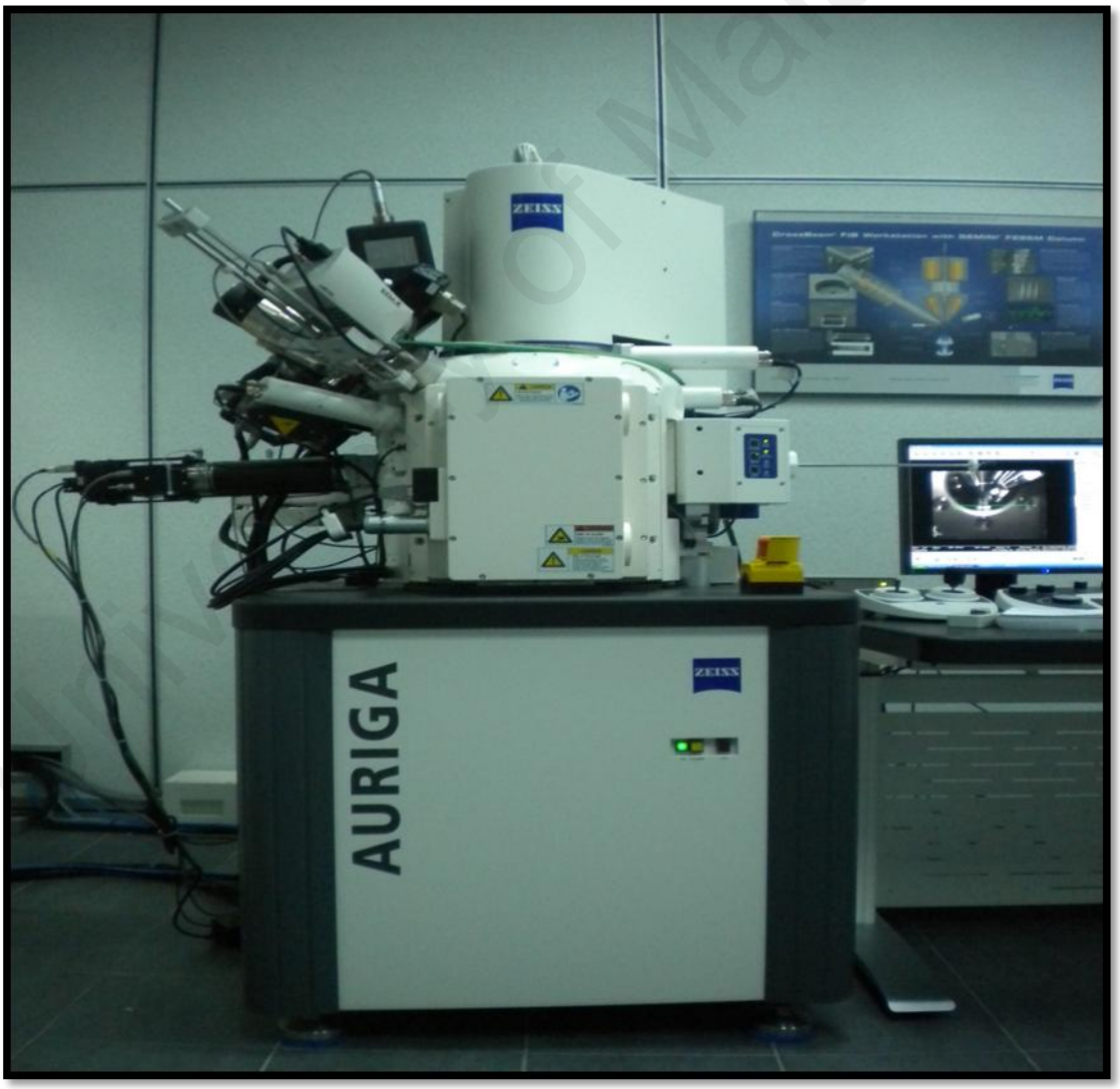

Figure 3.4: FESEM machine

In this work, the surface and morphology of Ag/PMMA nanocomposites were conducted using FESEM with an electron beam generated by 3 kV. A thin layer of gold was coated to make the samples conductive. It operated at a vacuum of the order of 10^{-5} torr. The accelerating voltage of the microscope was kept in the range 10-20 kV. Compositional analysis on the sample was carried out by the energy dispersive X-ray spectroscopy (EDX) attached with the FESEM. The EDX normally reveals the presence of phases. The sample preparations for FESEM analysis were shown in Figure 3.5.

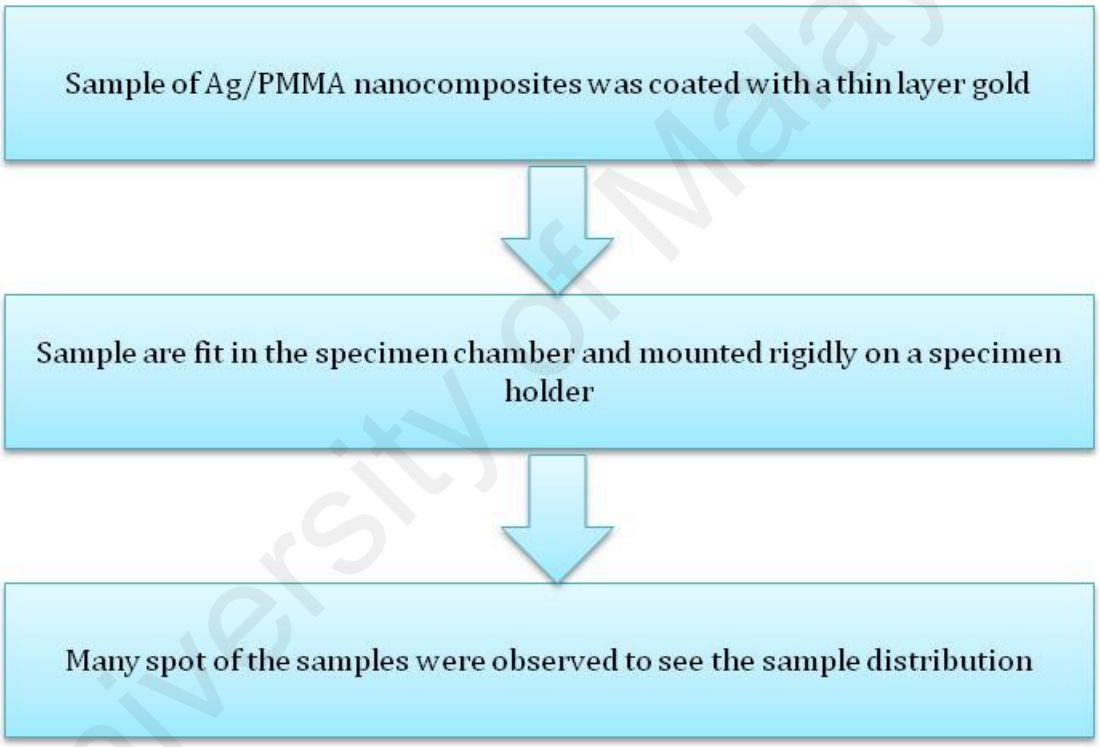

Figure 3.5: FESEM sample preparation

3.3.2 Transmission Electron Microscopy (TEM)

The particle size and distribution of Ag/PMMA nanocomposites were carried out in a LEO LIBRA electron microscope (Figure 3.6) operated at 200 kV.

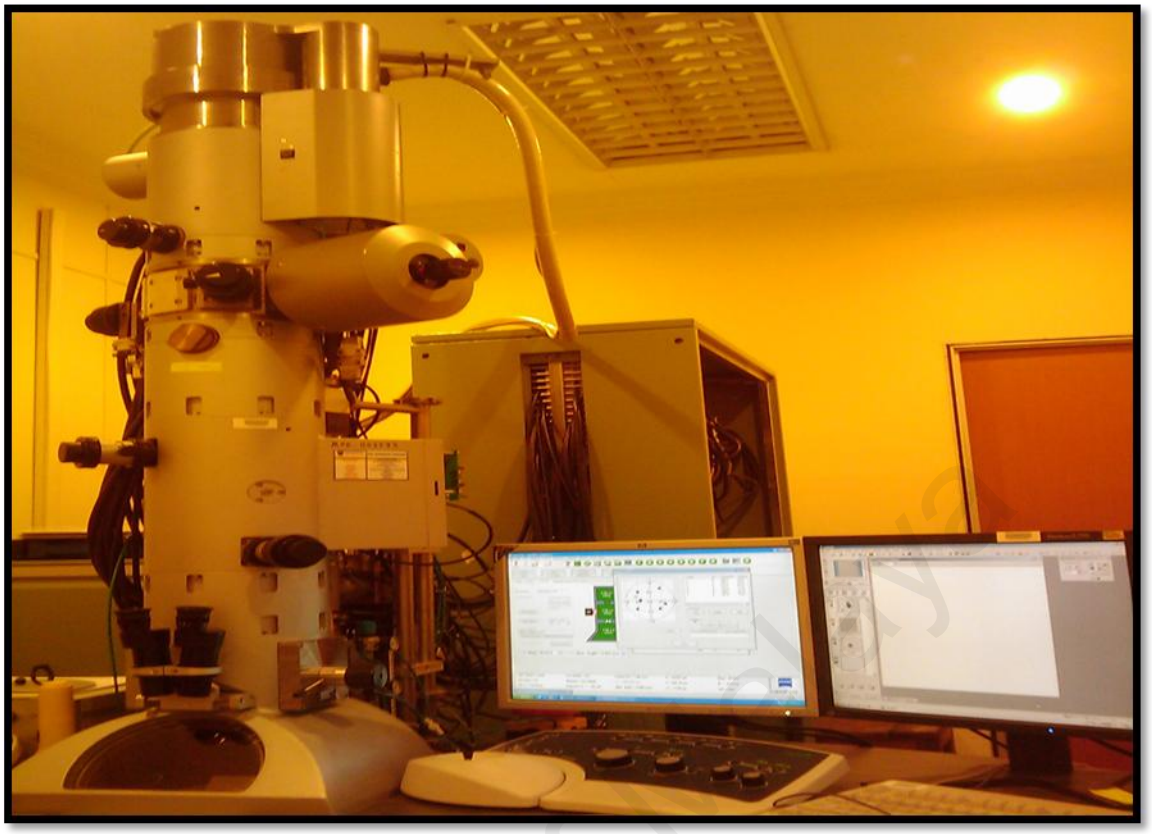

Figure 3.6: TEM machine

Samples were diluted in DMF. Then, the samples were partly submerged in water in an ultrasonic bath for sonication in duration 30 minutes. A drop of solution was placed on a 300-mesh lacy carbon-coated copper grid, which was allowed to dry before being used for analysis. Samples on the copper grids then were fixed in the specimen holder. Vacuum pumping was set up to a minimum of four cycles before the samples were fully inserted. The power supply was turned on after the vacuum pressures reach a range of 10^{-7} torr to fix the acceleration voltage at 200 kV. The filament was heated by increasing the current so that it reached the saturation current value of 113 µA. The apertures were selected and the samples images were viewed on the computer screen. The samples grids were focused at appropriate locations and at specific magnifications to record micrographs in the bright field image made on the photographs plate. The

average size and distribution of Ag/PMMA nanocomposites were obtained by image analysis of these micrographs. The TEM sample preparations were shown in Figure 3.7.

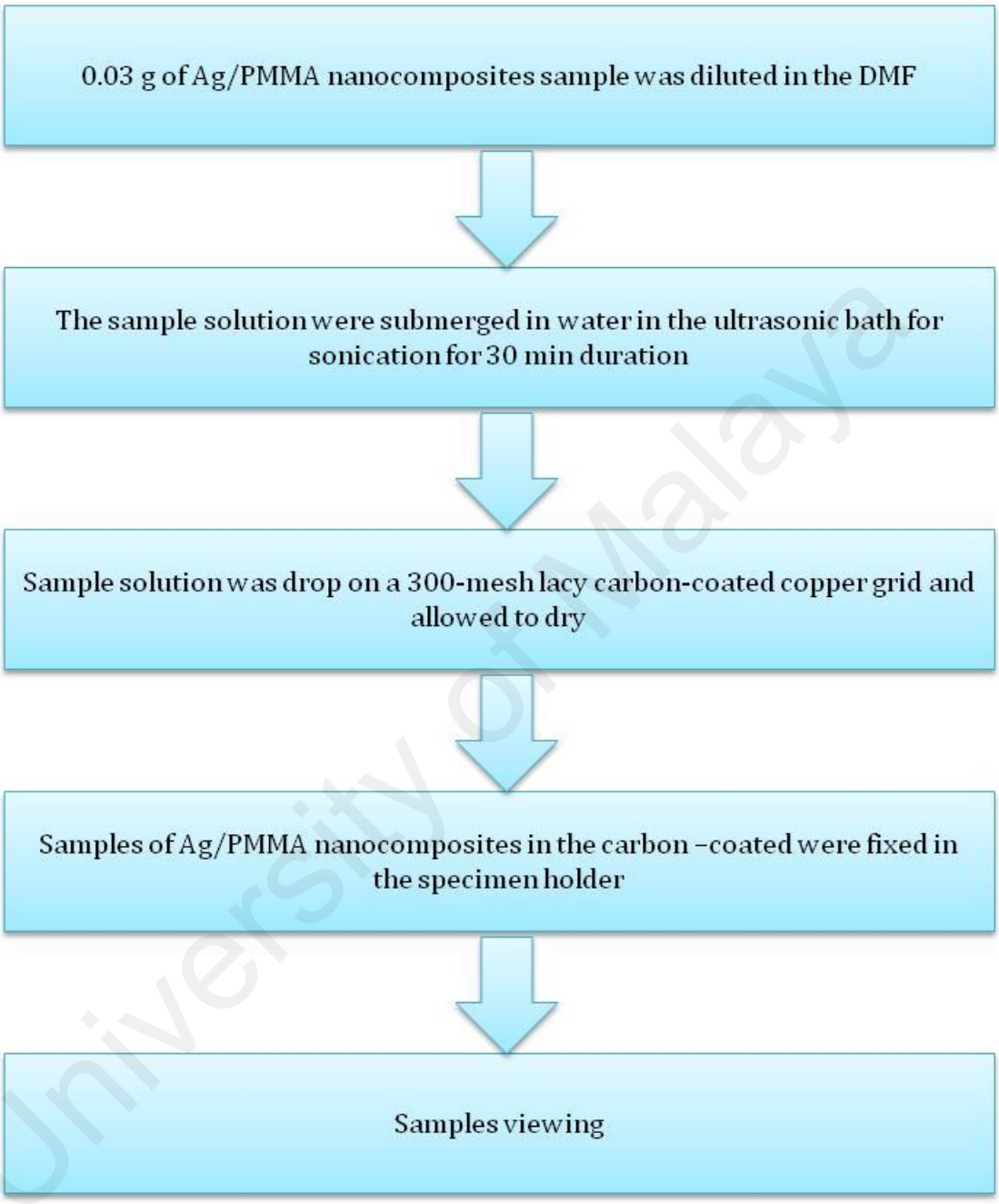

Figure 3.7: TEM sample preparation

3.3.3 Dynamic Light Scattering (DLS) Analysis

In this study, DLS ZETA Sizers 3000HSA (Malvern Instruments) (Figure 3.8) was used to measure the size distribution of Ag/PMMA nanocomposites in the solution.

Several parameters such as solvent viscosity, solvent refractive index and sample temperature can affect the analysis of DLS, (Wolfgang, 2007).

Figure 3.8: DLS ZETA Sizers 3000HSA Spectroscopy

Samples should be diluted to suppress interparticulate interactions and in liquid dispersions such as an emulsion or suspension. The scattering intensity depends on mass or size of the particles, solute particle concentration and refractive index differences between the solute and solvent. In order to avoid a Columbic interaction between the charged systems (polyelectrolytes), low concentrations of salt such as NaCl, KBr or NaBr are recommended for aqueous systems. For organic solvents, tetrahydrofuran (THF), dimethyl formamide (DMF) and chloroform are used. In addition to these factors, sample purification is another critical step in order to obtain reliable data. Air bubbles are removed by ultrasonication while dust particles are removed by filtration or by centrifugation. The DLS sample preparations were shown in Figure 3.9.

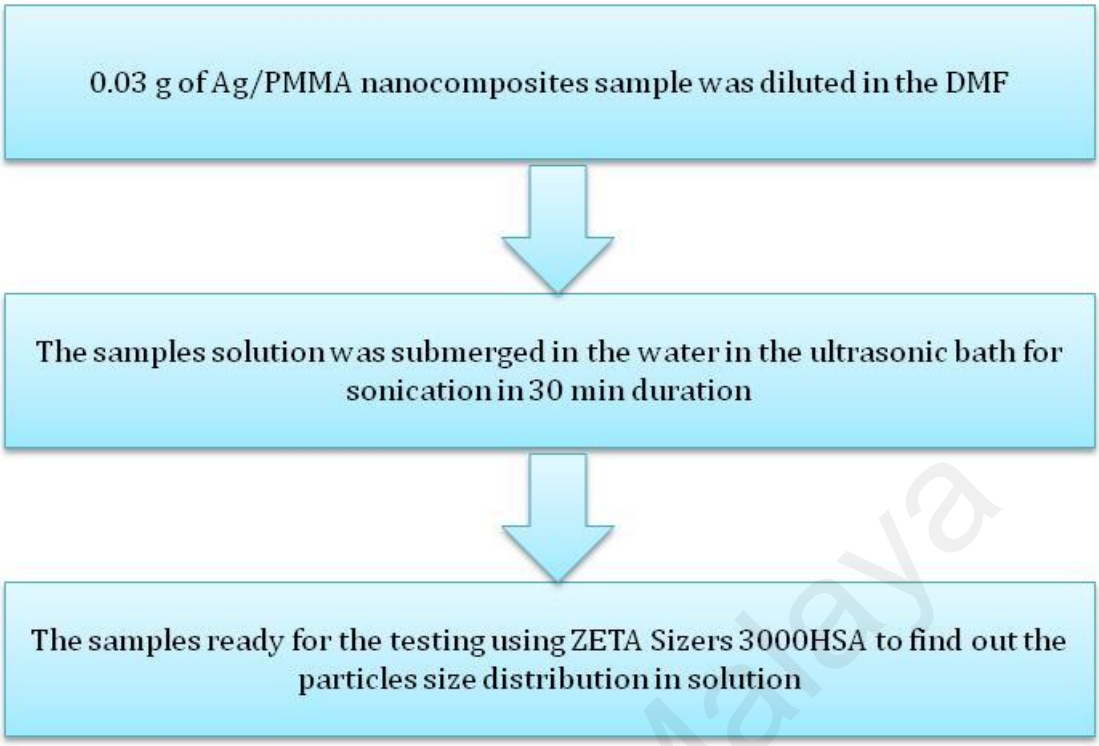

Figure 3.9: DLS sample preparation

3.3.4 Zeta Potential Analysis

Zeta potential (ζ) is a measure of the surface electrostatic potential of the nanoparticles. It is related to the electrophoretic mobility and stability of the nanoparticles suspension (Dougherty *et al.*, 2007). The stability of particle dispersion will depend upon the balance of the repulsive and attractive forces that exist between particles as they approach one another. If the particles have a mutual repulsion then the particles will remain dispersed. However, if the particles have little or no repulsive force, then flocculation, aggregation or coalescence will eventually take place. The development of a nett charge at the particle surfaces affect the distribution of ions in the surrounding interfacial region, resulting in an increased concentration of counter ions close to the surface. Thus an electrical double layer exists around each particle. The liquid layer surrounding the particle exists as two parts; an inner region, called the Stern layer, where the ions are strongly bound and an outer, diffuse, region where they are

less firmly attached. Within the diffuse layer there is a notional boundary inside which the ions and particles form a stable entity. When a particle moves (e.g. due to gravity), ions within the boundary move with it, but any ions beyond the boundary do not travel with the particle. This boundary is called the surface of hydrodynamic shear or slipping plane. The potential that exists at this boundary is known as the zeta potential. Figure 3.10 shows the development of the zeta potential and electrical double layer.

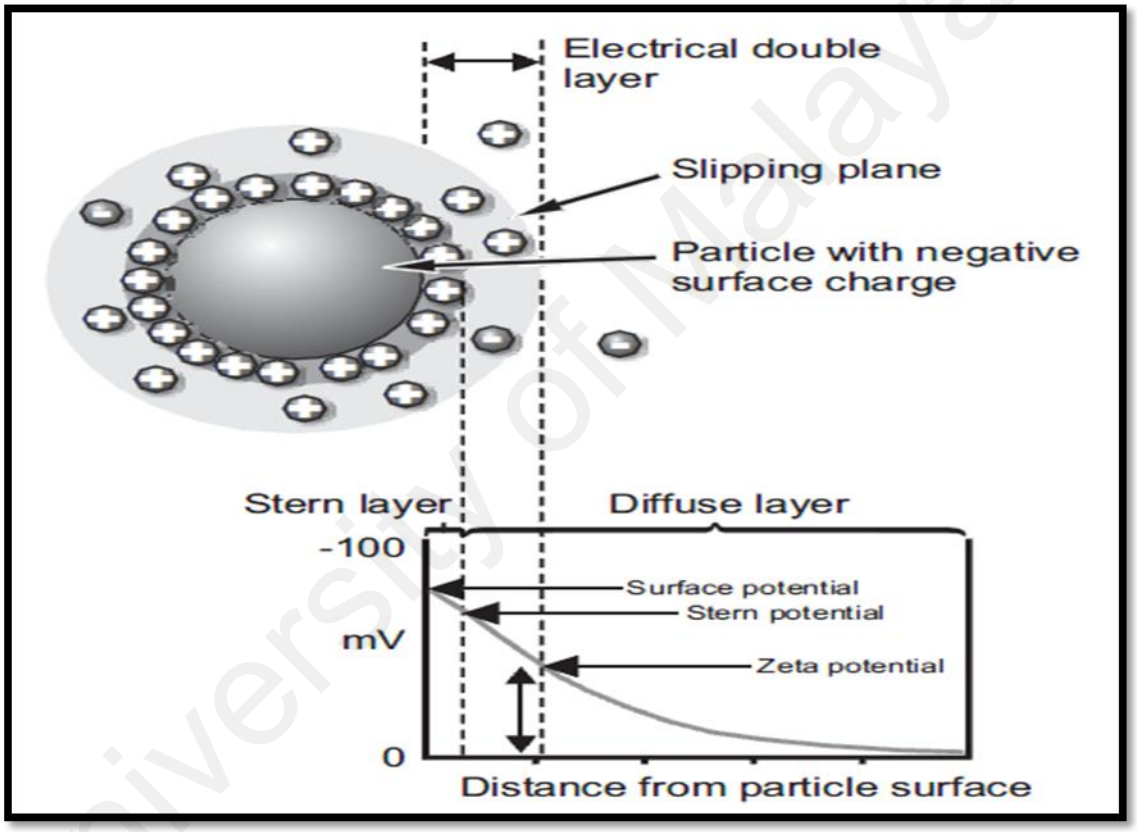

Figure 3.10: Development of the zeta potential and electrical double layer

The zeta potential of a particle is the overall charge that the particle acquires in a particular medium. The magnitude of the measured zeta potential can be used to predict the long-term stability of the product. If the particles in a suspension have a large negative or positive zeta potential then they will tend to repel each other and resist the formation of aggregates. However, if the particles have low zeta potential values, i.e.

close to zero, then there will be nothing to prevent the particles approaching each other and aggregating. The dividing line between stable and unstable suspensions is generally taken at either +30 mV or -30 mV. Particles with zeta potentials more positive than +30 mV or more negative than -30 mV are normally considered stable.

Sample preparation for zeta potential analysis was similar with the sample preparation of dynamic light scattering (DLS) in previous section. 0.03g of Ag/PMMA nanocomposites sample was diluted in the DMF solution. Then, the sample solution was submerged in the water in the ultrasonic bath for sonication in 30 min duration. The sample was ready for the zeta potential testing using ZETA Sizers 3000HSA analyzer.

3.3.5 X-Ray Diffraction (XRD) Analysis

The structural analysis is focused on the investigation of crystalline structures of nanoparticles. Philips Analytical X'Pert Graphics & Identify XRD (Figure 3.11) using Cu K_α with 0.154 nm radiations was used at Department of Physics, University of Malaya for characterization of Ag/PMMA nanocomposites.

Figure 3.11: XRD machine

The sample preparation of Ag/PMMA nanocomposites were shown in Figure 3.12. The glass slide was placed into the sample holder after the dimensions were fixed to 10 x 10 x 1 mm^3. The scan parameters of the diffractometer were set with a step size of 0.05°, scan rate at 1.2° min^{-1} and 2θ range from 30 to 80°. The voltage and current were gradually increased and fix at 45 kV and 40 mA, respectively, between room temperature (25 °C) and 300 °C when the power of the X-ray tube was switched on. The shutter across the X-ray beam was opened and the samples were scanned. The data was recorded by rotating the X-ray detector about the sample; the latter being mounted on a diffractometer goniometer stage.

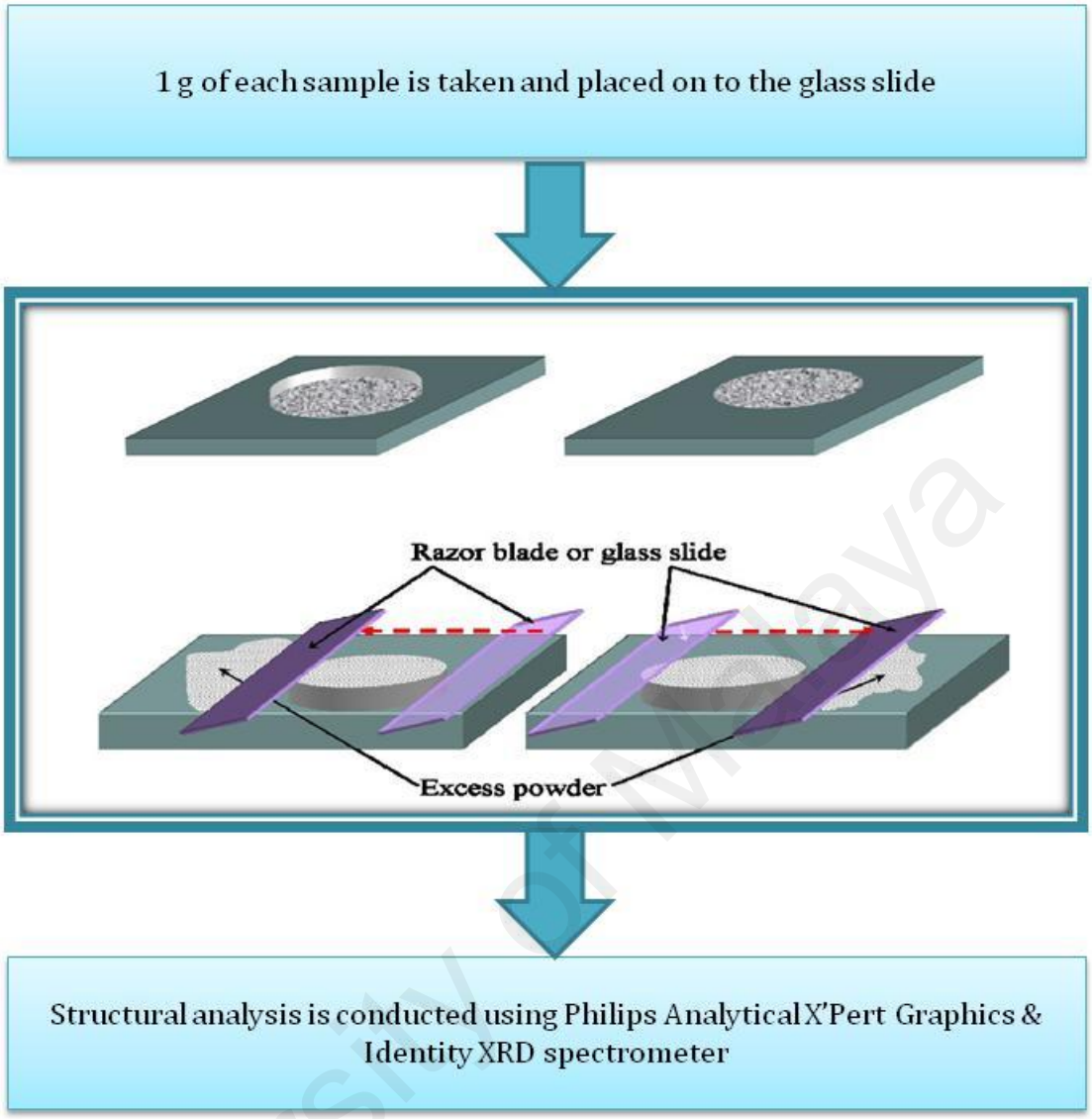

Figure 3.12: XRD sample preparation procedure

3.3.6 Fourier Transform Infrared Spectroscopy (FTIR)

The FTIR spectra of the Ag/PMMA nanocomposites were recorded using Perkin Elmer FL Winlab FTIR spectrometer (Figure 3.13) at Tribology Lab, Faculty Engineering, University of Malaya.

Figure 3.13: FTIR machine

It is equipped with an air-cooled rare earth oxide filament source, CSI beam splitter and DTGS detector. The instrument was set for ten scans at 4 cm^{-1} resolution with cosine apodisation in the mid-IR region: 4000-400 cm^{-1}. No purging was carried out. Samples were placed into the sample holder made and contacted with a diamond stub and the testing was run. The sample preparations of FTIR analysis were shown in Figure 3.14.

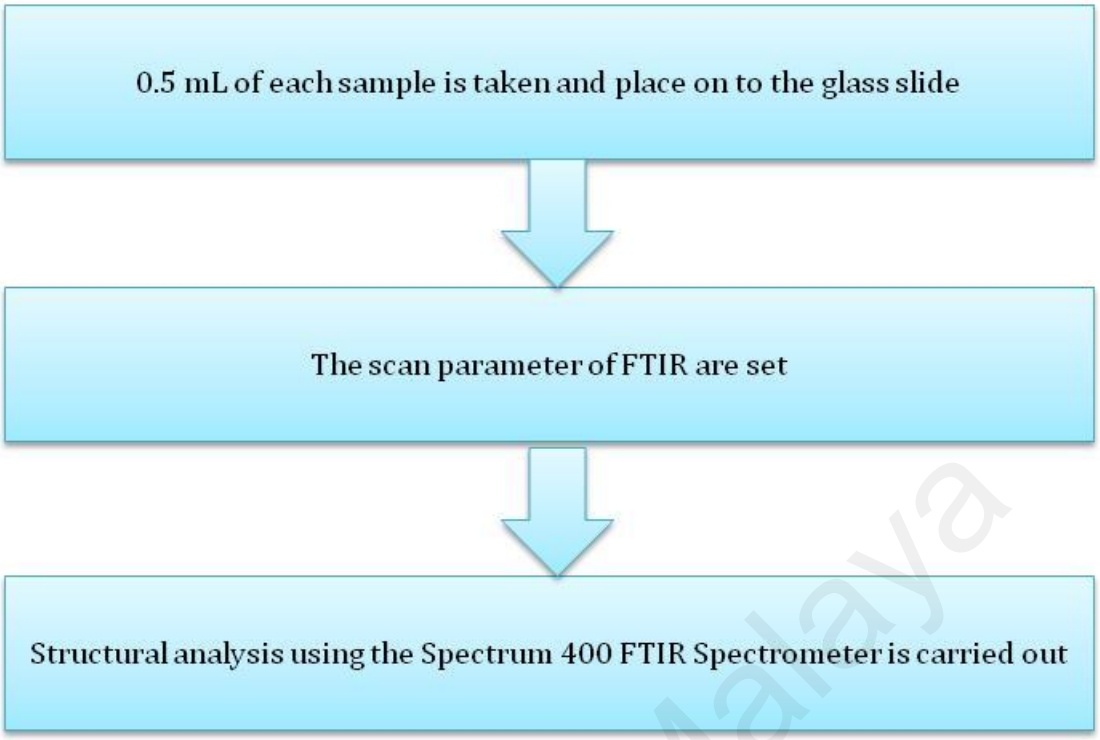

Figure 3.14: FTIR sample preparation procedure

3.3.7 Raman Spectroscopy

Raman characteristics of the Ag/PMMA nanocomposites were conducted by Raman XploRA spectroscopy (Horiba, Japan) (Figure 3.15).

Figure 3.15: Raman spectroscopy

The He-Ne laser with wavelength at 633 nm was excited to a solution containing well-dissolved Ag/PMMA nanocomposites to study the attachment of bonding groups in the nanocomposites. Using the attached microscope and camera, the instrument was focused on the powder sample through the objective lens (x10). One scan was recorded with a detector exposure time of 1 sec. Sample preparation for Raman analyses were shown in Figure 3.16.

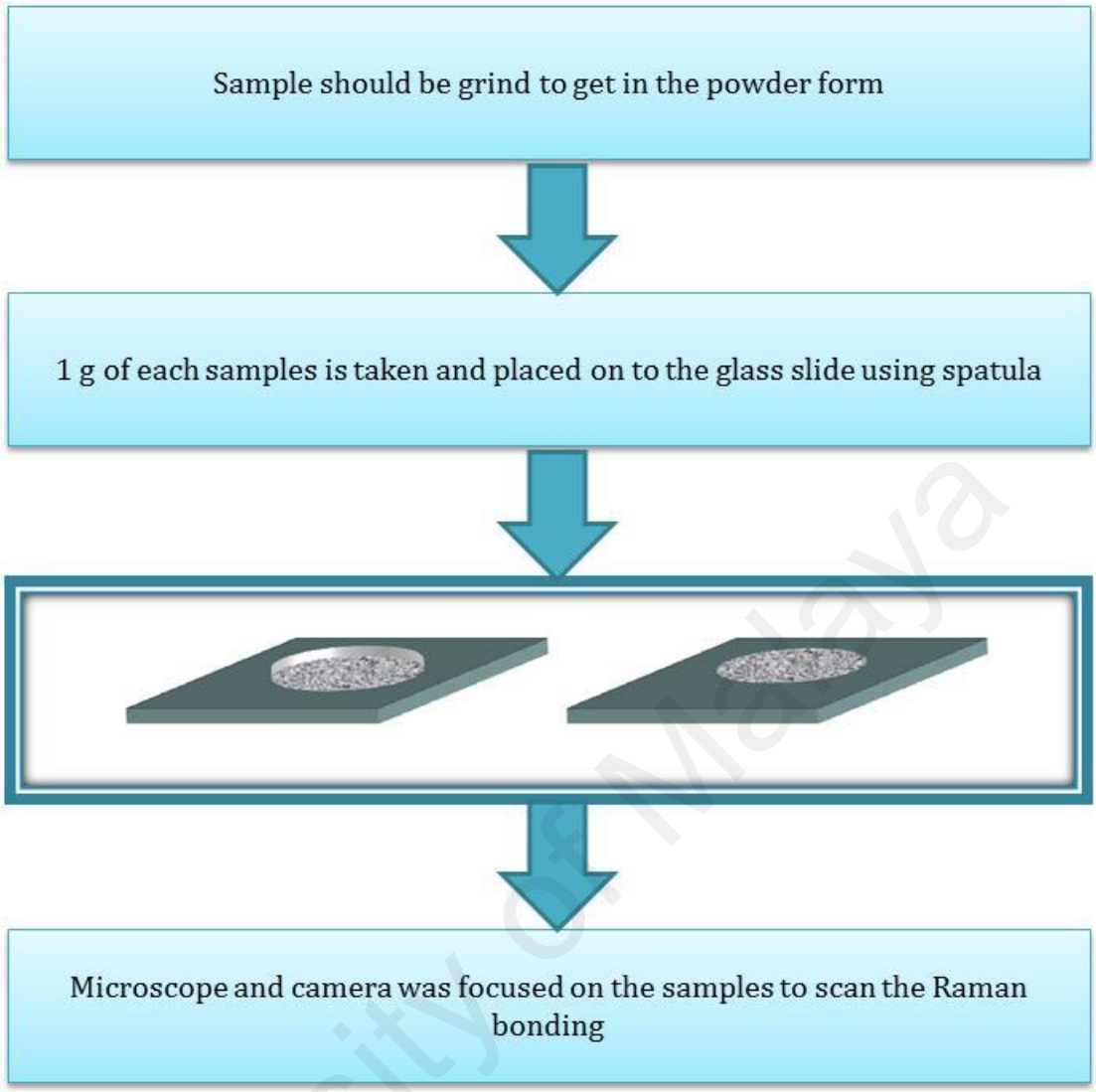

Figure 3.16: Raman analysis sample preparation

3.3.8 Ultra-Violet Visible (UV-Vis) Spectroscopy

Figure 3.17 shows the Cary 50 UV-Visible spectrophotometer used for optical characterization of Ag/PMMA nanocomposites. The wavenumbers range for this equipment is 180-900 nm, and the consideration wavenumbers considered in this research is within the range of 300-800 nm at a scan speed of 60 nm/min. The flow chart of the UV-Vis sample preparation is shown in Figure 3.18. Before using 'UVCary50' software, baseline correction of the spectrophotometer was carried out by using pure blank DMF solution for Ag/PMMA nanocomposites. I mL of Ag/PMMA

nanocomposites was diluted in 10 mL DMF and rinsed in ultrasonic bath for 15 minutes. The absorption spectra were recorded at a rate 60 nm/min, with a spectral resolution of 2 nm at room temperature in a 1 cm optical path quartz cuvette.

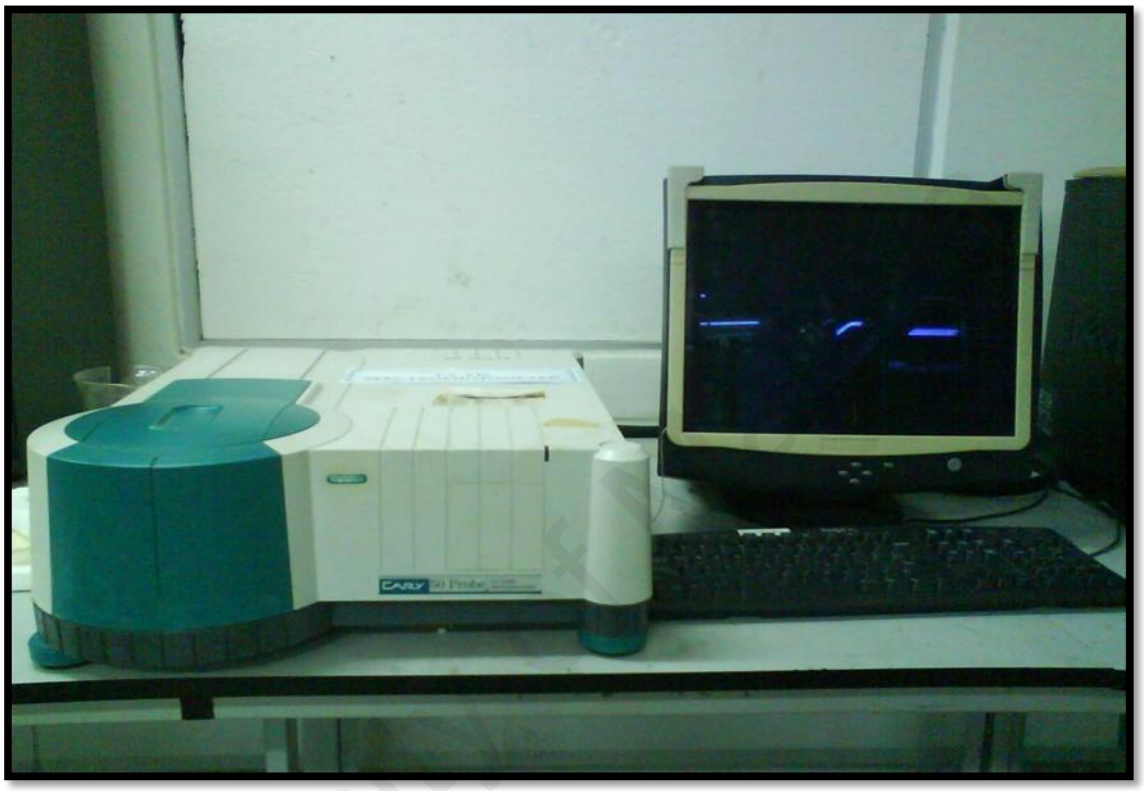

Figure 3.17: UV-Visible spectrophotometer

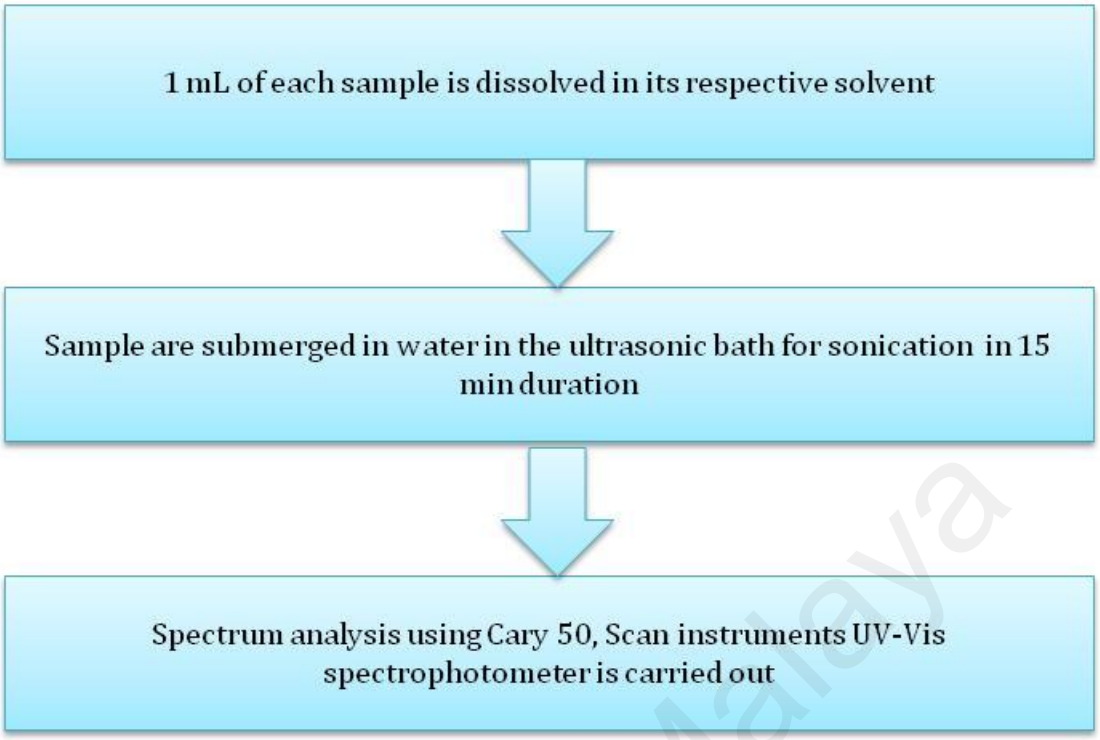

Figure 3.18: Step in UV-Vis sample preparation

3.3.9 Impedance Spectroscopy (IS)

Figure 3.19 shows the IS machine used in this work, HIOKI 3531 LCR Hi-Tester, with frequency range from 50 Hz to 5 MHz.

Figure 3.19: Impedance Spectroscopy (EIS), Hioki 3531 z Hi Tester

The results were analyzed using HIOKI software to extract the impedance, which was then used to calculate the bulk conductivity of the electrolyte. This technique is used to determine the ionic conductivity of the electrolyte. It involves the application of voltage, particularly alternating voltage in the appropriate frequency stage, to a cell containing the electrolyte and measuring the resulting current. The impedance of the electrolyte can then be calculated from this current value.

AC impedance spectroscopy involves the application of a sinusoidal voltage and the measurement of the sinusoidal current resulting from the perturbation. Since the applied voltage is indirect, the two parameter is required to relate the applied potential and current flowing in the cell are the magnitude of the resistance and the phase difference between the voltage and the current, which are both functions of the applied

frequency. The combination of these two parameters makes up the impedance of the cell, a vector quantity comprising both magnitude and phase, represented schematically in Figure 3.20.

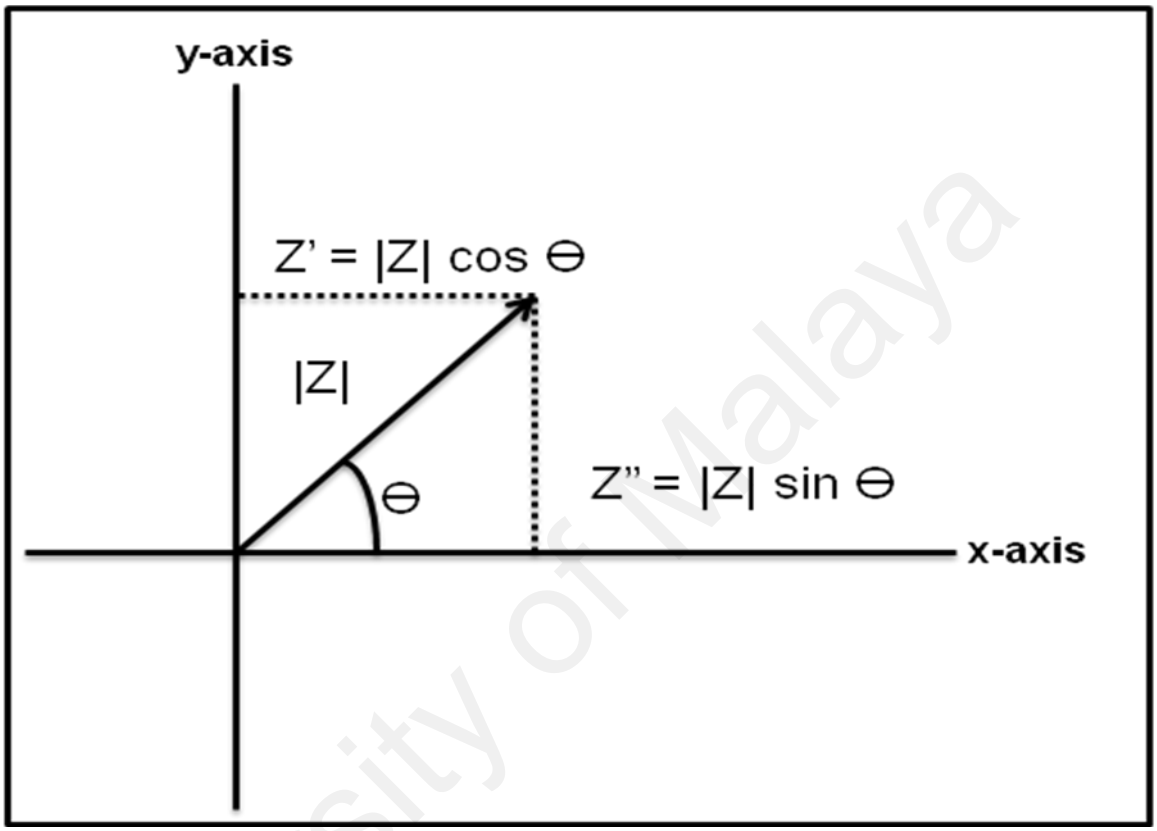

Figure 3.20: Schematic representation of the components of impedance, Z^*

The equations defining these relationships are given as:

$$Z^* = Z' - iZ'' \qquad (3.1)$$

$$Z^* = |Z|\cos\theta - |Z|\sin\theta \qquad (3.2)$$

where:

Z^* = complex impedance

Z' = real component of complex impedance

Z'' = imaginary component of complex impedance

$|Z|$ = magnitude of complex impedance

θ = phase angle

i = complex number operator = $\sqrt{i}$

A typical AC impedance experiment plot, also called Nyquist plot or Cole-Cole plot, consists of a representation of the real impedance, *Z'* on the x-axis and the imaginary impedance, *Z"* on the y-axis as a function of the applied frequency. From Equations (3.1) and (3.2), we can define the dielectric parameter as a function of frequency as described by the complex permittivity in the form:

$$\varepsilon^*(\omega) = \varepsilon'(\omega) - i\varepsilon''(\omega) \tag{3.3}$$

$$\varepsilon'(\omega) = \frac{Z''}{\omega C_o (Z'^2 + Z''^2)} \tag{3.4}$$

$$\varepsilon''(\omega) = \frac{Z'}{\omega C_o (Z'^2 + Z''^2)} \tag{3.5}$$

where ω is the angular frequency, C_o represents the vacuum capacitance of any configurations of the electrode, ε' is the real dielectric constant and ε'' dielectric loss factor.

Figure 3.21 shows the sample preparation of IS analysis. The dimensions of the palletize samples was measured, the thickness and the diameter were recorded. Then the area of the palletize samples were calculate from its diameter and the average were calculated and recorded also. After that, the samples were tested and the bulk resistance (R_b) of each sample was measured from the impedance plot through extrapolating technique.

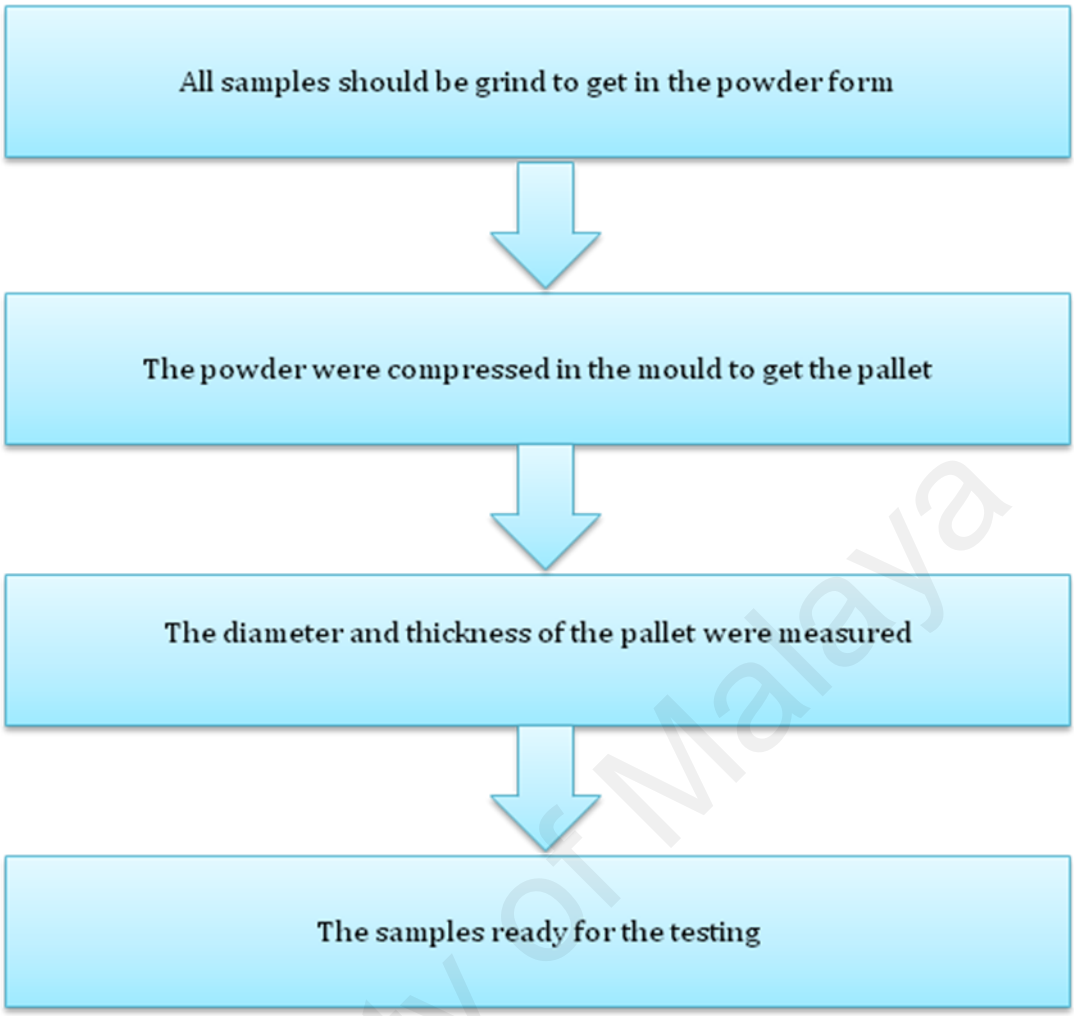

Figure 3.21: IS sample preparation

3.3.10 Vector Network Analyzer (VNA)

The real and imaginary permittivity data of the samples were recorded using Agilent E5071C Network Analyzers (Figure 3.22) in the frequency range from 500 MHz until 4.5 GHz. The sample preparation of the VNA testing is the same with the IS testing in the previous section. After the sample were prepared, the probe were touch on the pallet that generate the electric.

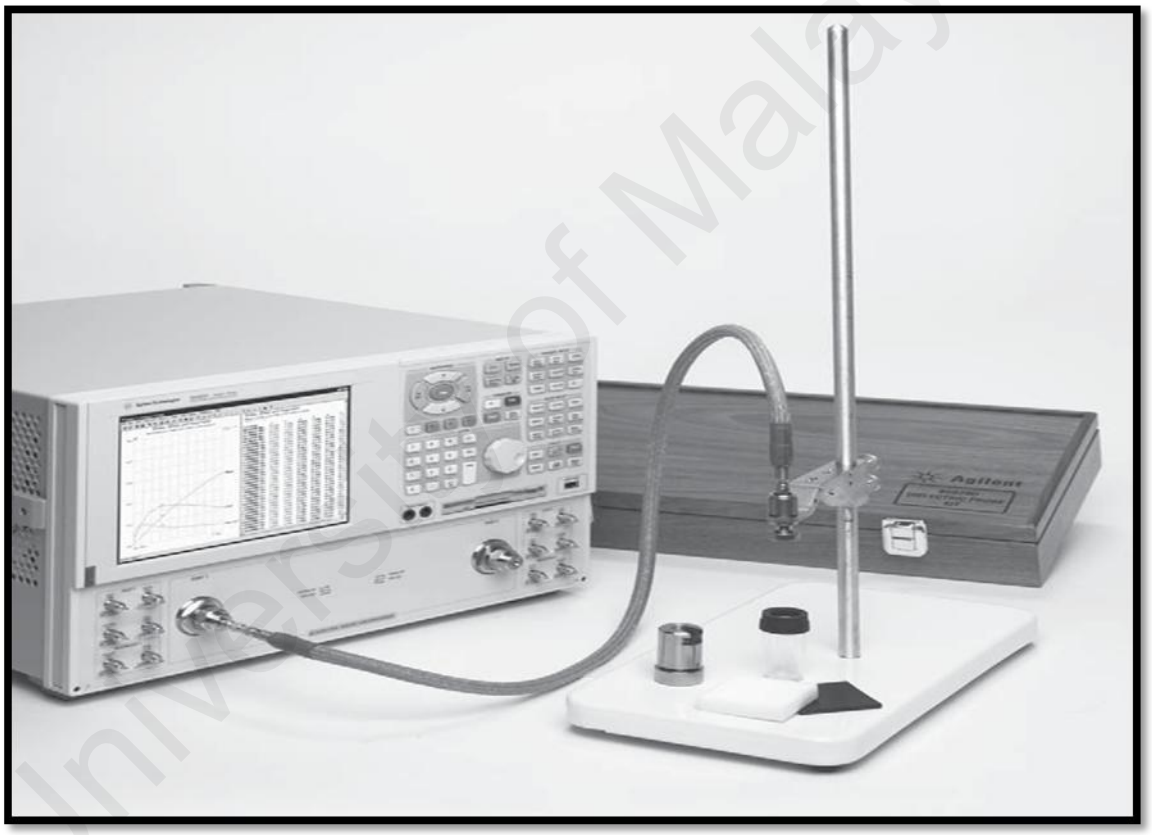

Figure 3.22: Agilent E5071C Network Analyzers

3.3.11 Thermogavimetry (TGA)

Figure 3.23 shows the TGA used in this work (TGA/SDTA 851 Mettler Toledo). This instrument is also often used to estimate the corrosion kinetics in high temperature

oxidation. Analysis is carried out by raising the temperature of the sample gradually and plotting the weight (percentage) against temperature. The temperature in many testing methods routinely reaches 1000 °C or greater. Once the data is generated, curve smoothing and other operations may be carried out such as to find the exact of inflection. A method known as hi-resolution TGA is often employed to obtain greater accuracy in areas where the derivative curve peaks. This method identified the exact temperature where a peak occurs more accurately. Several modern TGA devices can vent burn off to an infrared spectrophotometer to analyze composition.

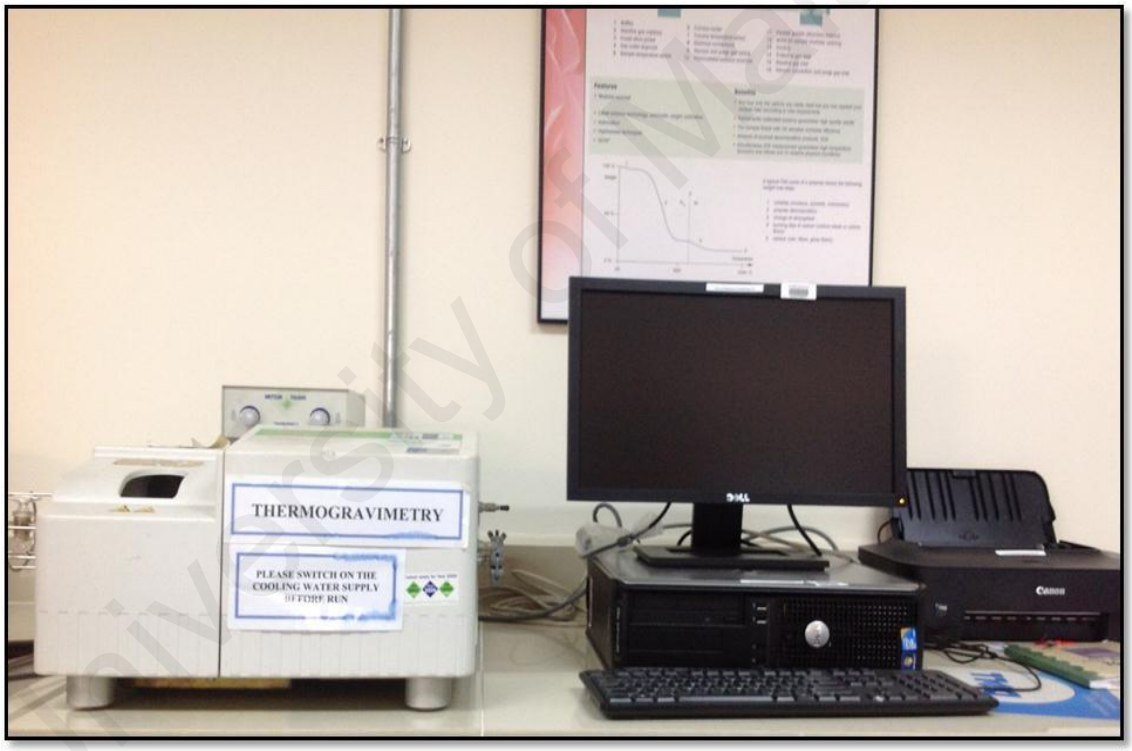

Figure 3.23: TGA machine

TGA analyzer usually consists of a high-precision balance with a pan (generally platinum) loaded with the sample. A different process using a quartz crystal microbalance has been devised for measuring smaller samples on the order of a microgram (versus milligram with conventional TGA)(Mansfield *et al.*, 2010). The sample is placed in a small electrically heated oven with a thermocouple to accurately

measure the temperature. The atmosphere may be purged with an inert gas to prevent oxidation or other undesired reactions. A computer is used to control the instrument.

CHAPTER FOUR

RESULTS AND DISCUSSION

4.1 Introduction

In this chapter, the optimum results of the silver/poly (methyl methacrylate) (PMMA) nanocomposites via *in-situ* technique are obtained. The properties of Ag/PMMA nanocomposites depend on type of incorporated silver nanoparticles such as their size and shape, concentration and interaction with polymer matrix. Therefore, the effect of temperature, percentage (%) loading of silver nanoparticles and weight percentage (%) of PMMA on the morphology, structure, optical, dielectric and thermal properties of Ag/PMMA nanocomposites are studied.

Samples subjected to higher percentage loading of silver nanoparticles at 80 °C were found to be the most effective and stable Ag/PMMA nanocomposites. The present work exhibits superior performance with the smallest mean particle size compared to the previous works (Khanna & Singh, 2007).

4.2 Morphological and Physical Size Studies

4.2.1 Field Emission Scanning Electron Microscopy (FESEM) Analysis

Figure 4.1 shows the FESEM images of Ag/PMMA nanocomposites at different reactant temperature for 10 percent loading of silver nanoparticles. The particles are almost spherical in shape and highly occupied. Their sizes are varies and significantly increase as the temperature increases. The sizes are 5.56, 7.41 and 10.96 μm at 80, 100 and 120 °C respectively. The particles start to agglomerate at 120 °C due to the attractive Van der Waals force. It may also due to their inhomogeneous spatial distribution, a certain number of Ag/PMMA nanocomposites gather without coalescence into finite aggregates.

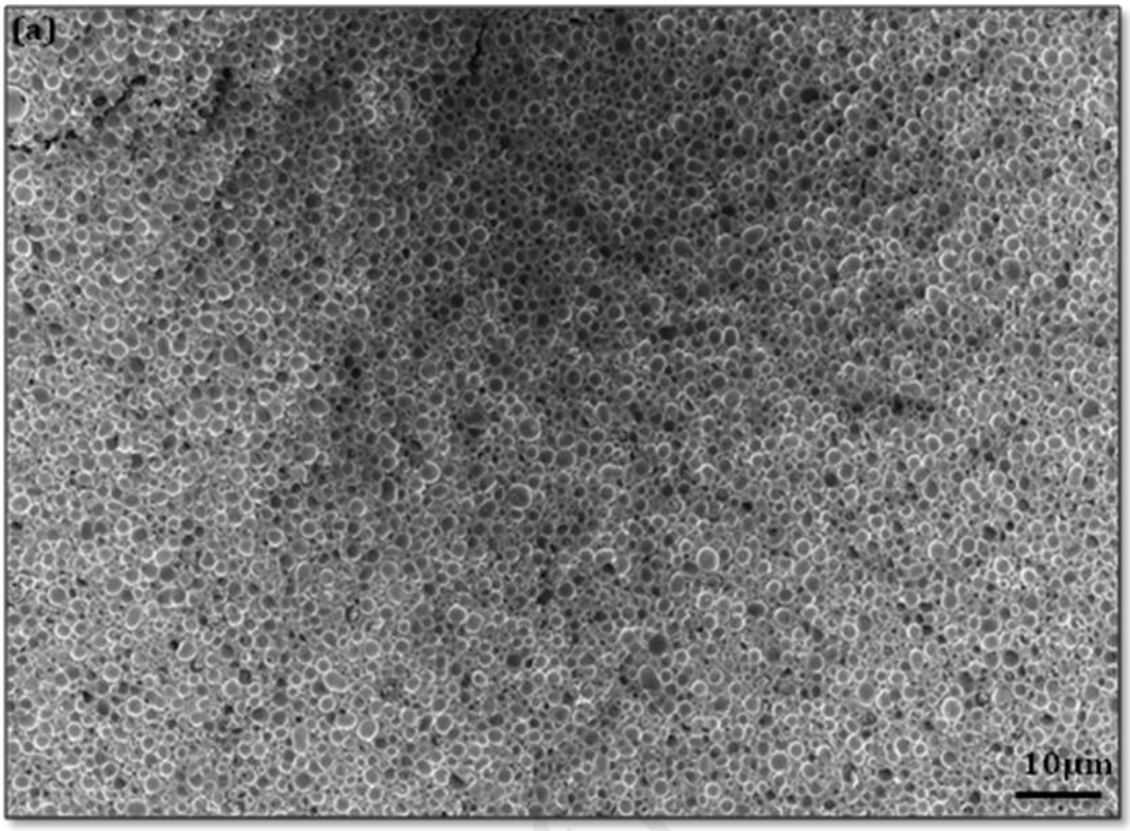
(a)
10µm

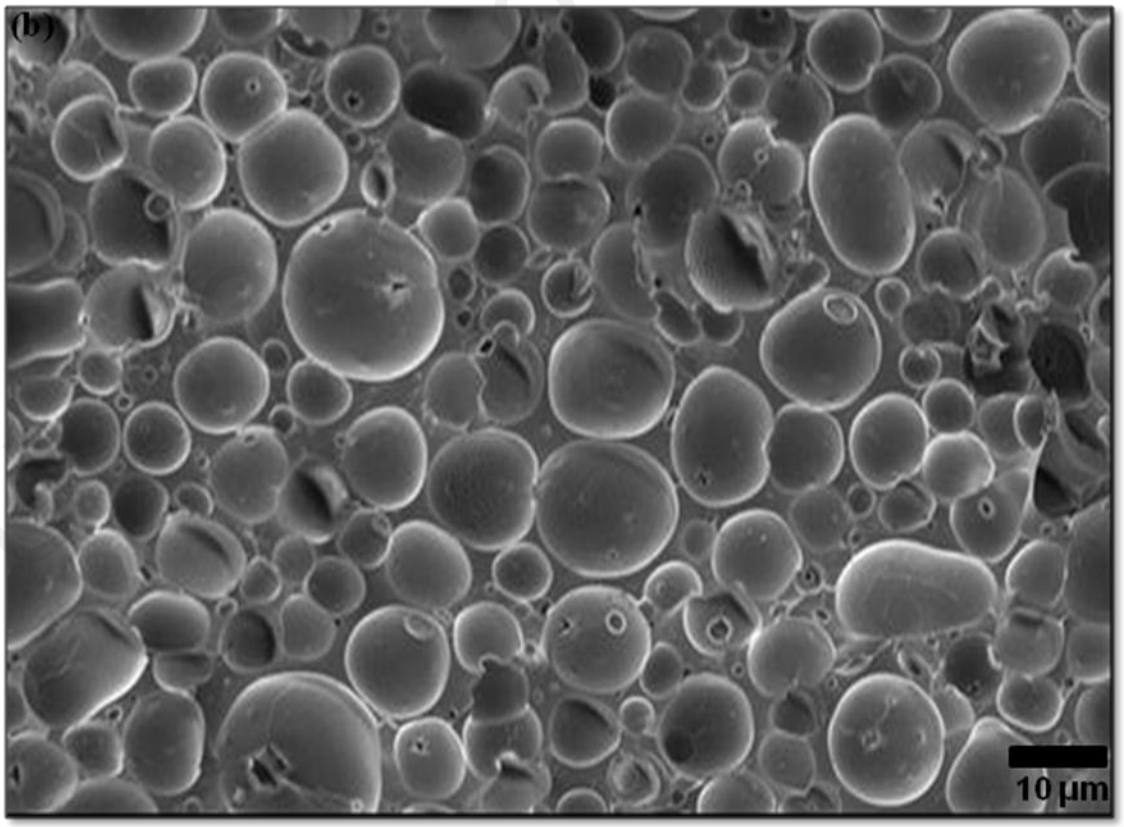
(b)
10 µm

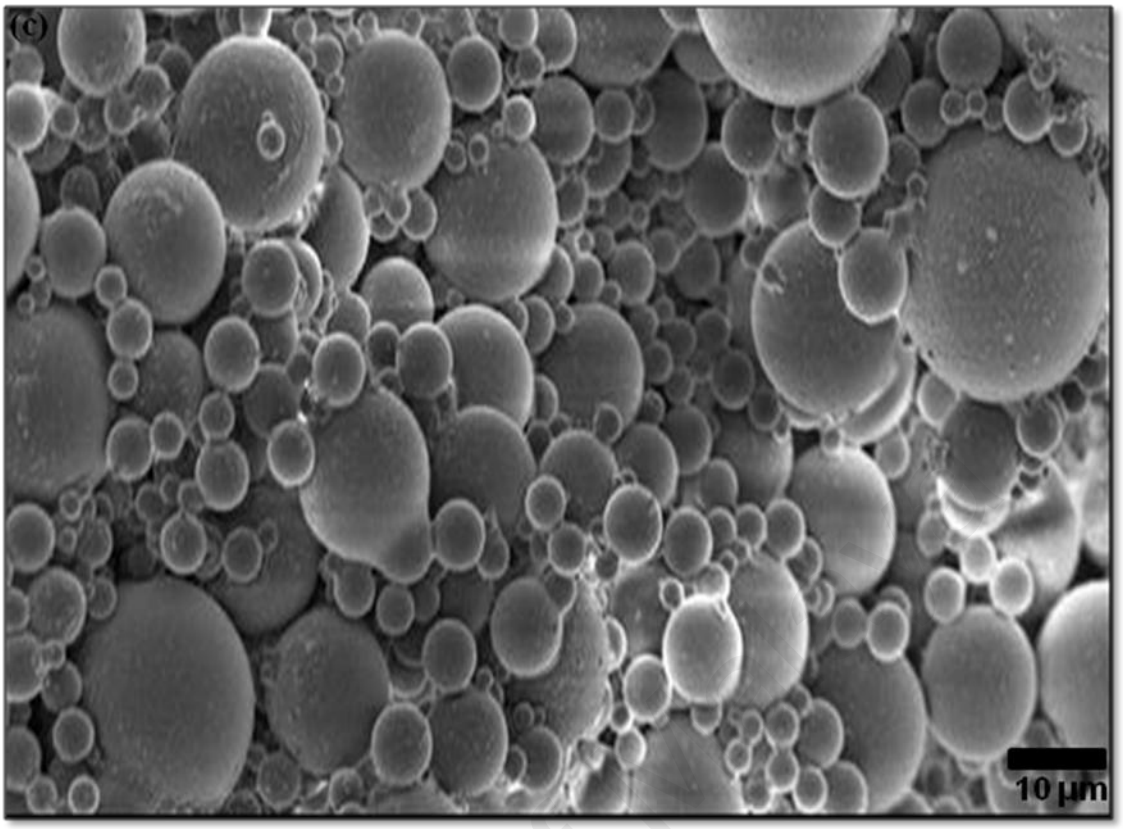

Figure 4.1: FESEM images of Ag/PMMA nanocomposites at 10 percent loading of silver nanoparticles at different reactant temperature

(a) 80 °C, (b) 100 °C and (c) 120 °C

4.2.2 Transmission Electron Microscopy (TEM) Analysis

Figures 4.2-4.4 show the TEM images for Ag/PMMA nanocomposites at various reactant temperatures for 10 percent loading of silver nanoparticles. The image reveal that the particles are nearly spherical and within the nanometer range. PMMA acts as a protective agent by encapsulated the silver particles and restrict the mobility of silver ions during the reaction. Furthermore, the addition of PMMA will increases the viscosity of the dispersion, thus reducing the possibility of particle aggregation and phase separation (Akhavan *et al.,* 2010).

The image shows the increasing of particles size with reactant temperature. The smallest size of Ag/PMMA nanocomposites is 24 nm at 80 ℃ as shown in Figure 4.2. As the reactant temperature increases to 100 ℃ (Figure 4.3), the average particle size increases to 50 nm. A similar behavior is observed at 120 ℃ as the particles size increase to 53 nm (Figure 4.4). However, moderate agglomeration of particles was observed at 120 ℃ due to the attractive van der Waals force and/or the driving force that tends to minimize the total surface energy of the system. The increase in particle size of Ag/PMMA nanocomposites also may be due to the aggregation of smaller size particles resulting from dissolution and precipitation process during synthesis. The particles size distribution in a range of 10 to 60 nm as shown in Figures 4.2(b)-4.4(b). It is interesting to note that all silver nanoparticles are in spherical shape, well bounded and separated by a white layer adsorbed on the particles surface. This represents the presence of methyl methyacrylate (MMA) (Figures 4.2-4.4).

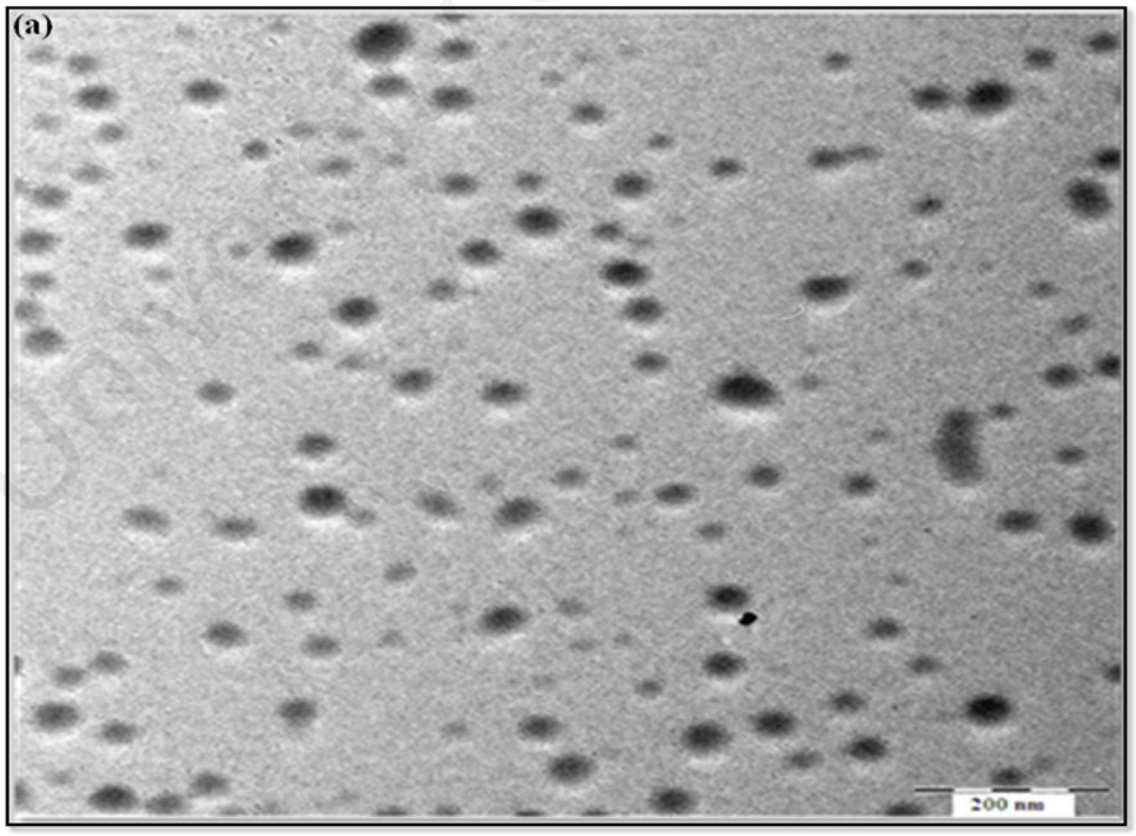

Figure 4.2: (a) TEM image of Ag/PMMA nanocomposites at 80 ℃

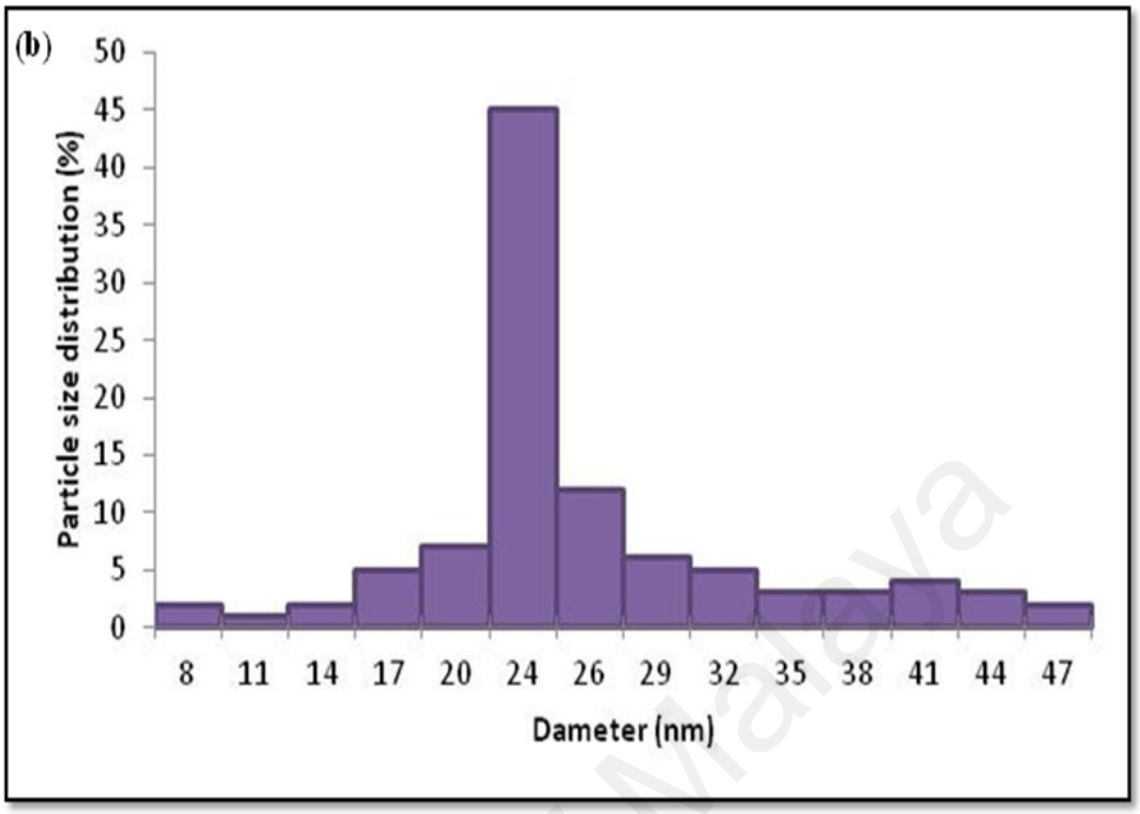

Figure 4.2: (b) Particle size distribution of 10 percent loading of silver nanoparticles at 80 °C

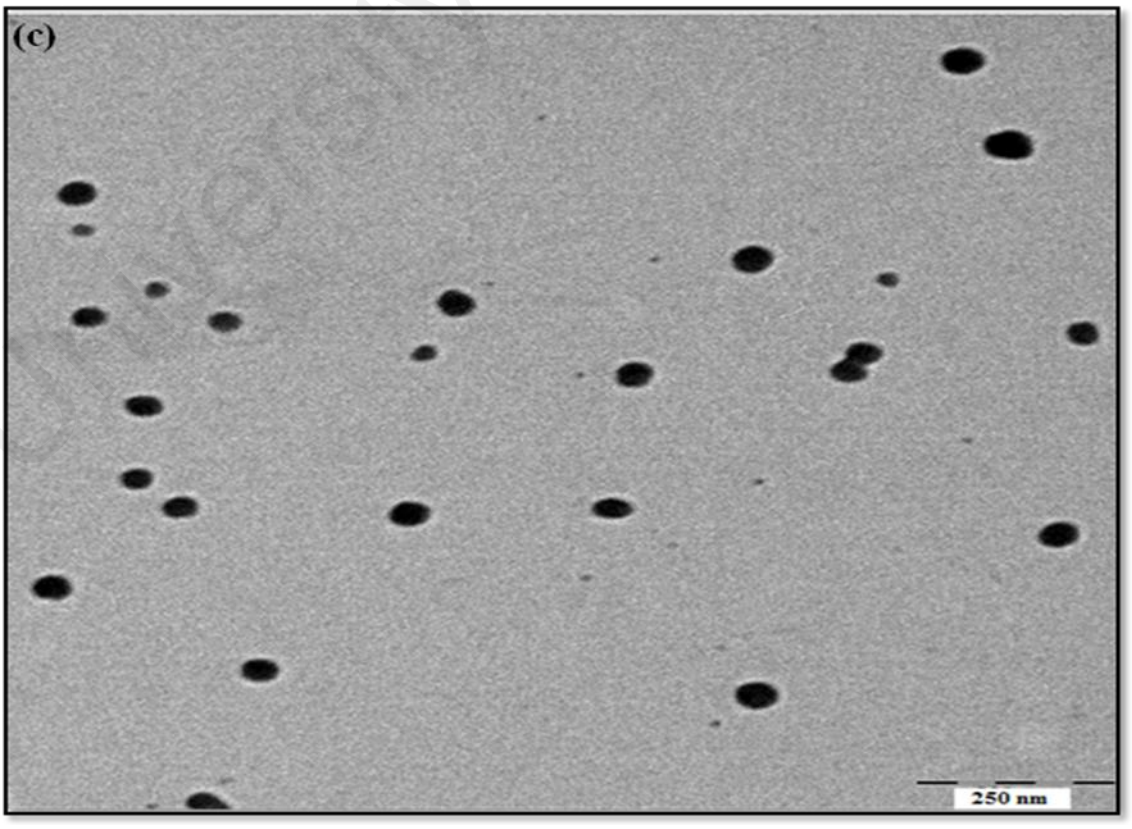

Figure 4.3: (a) TEM image of Ag/PMMA nanocomposites at 100 °C

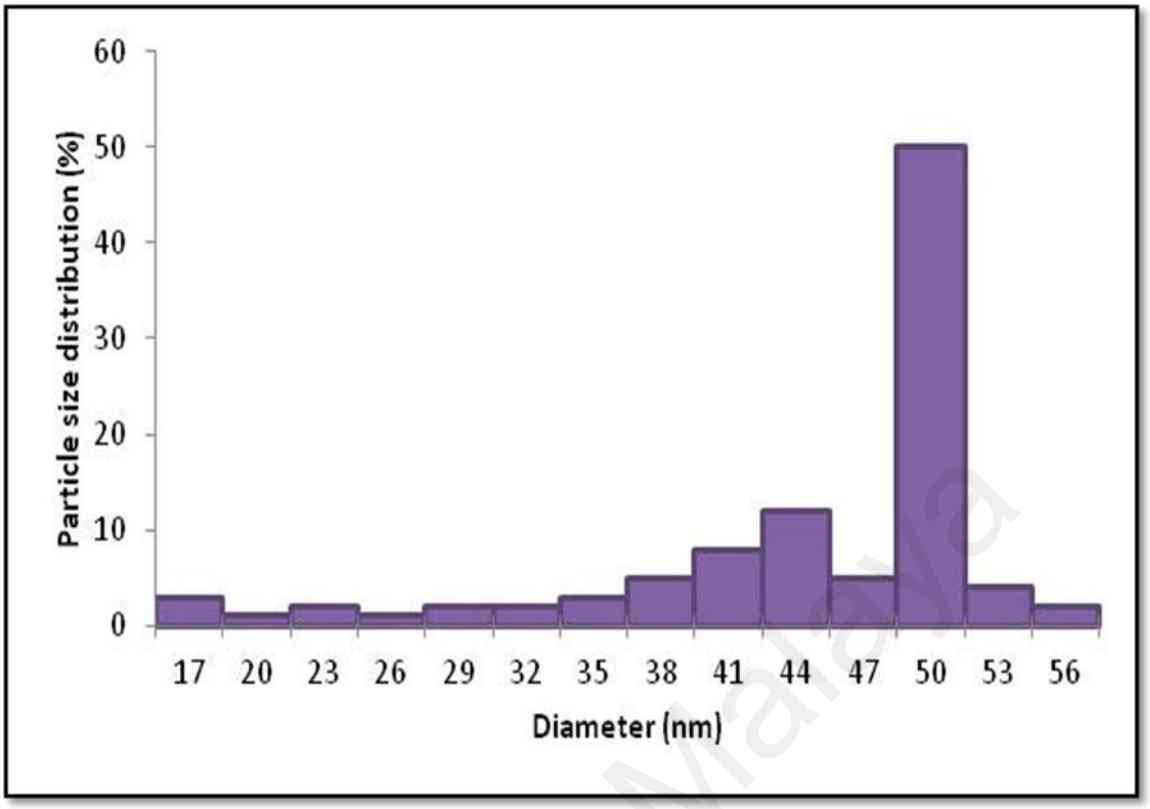

Figure 4.3: (b) Particle size distribution of 10 percent loading of silver nanoparticles at 100 ℃

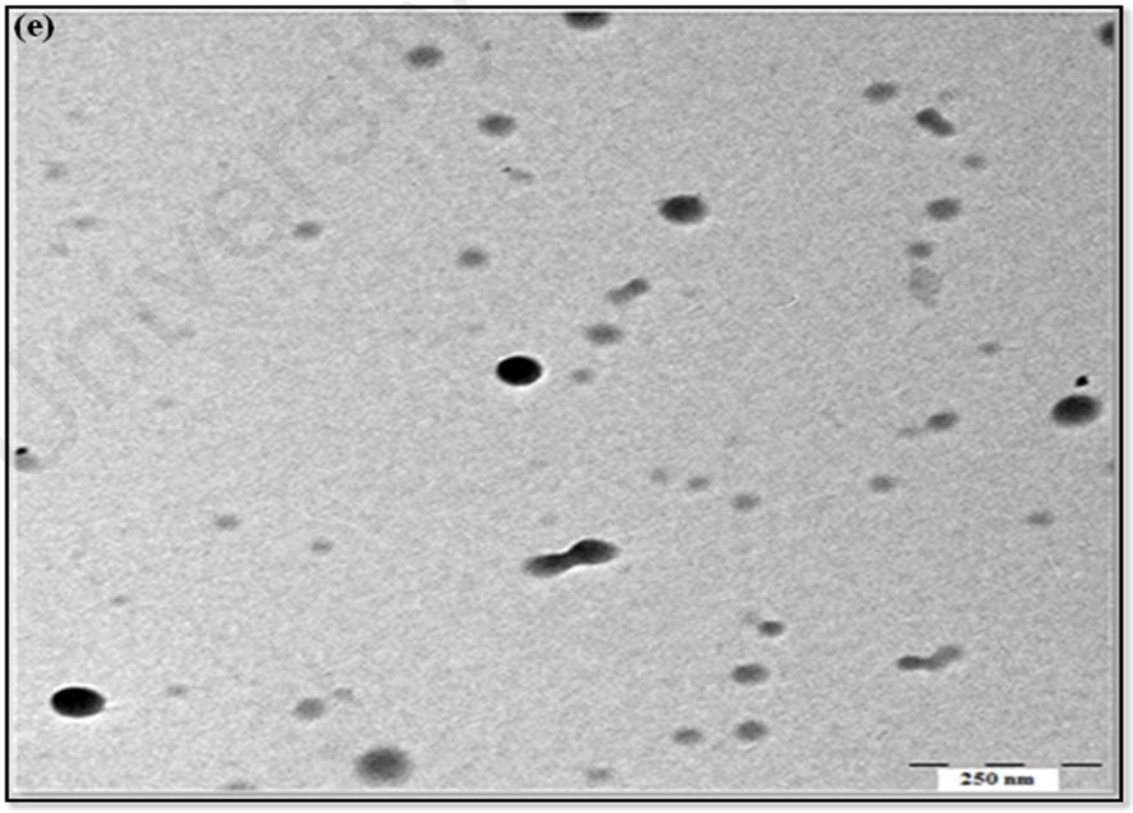

Figure 4.4: (a) TEM image of Ag/PMMA nanocomposites at 120 ℃

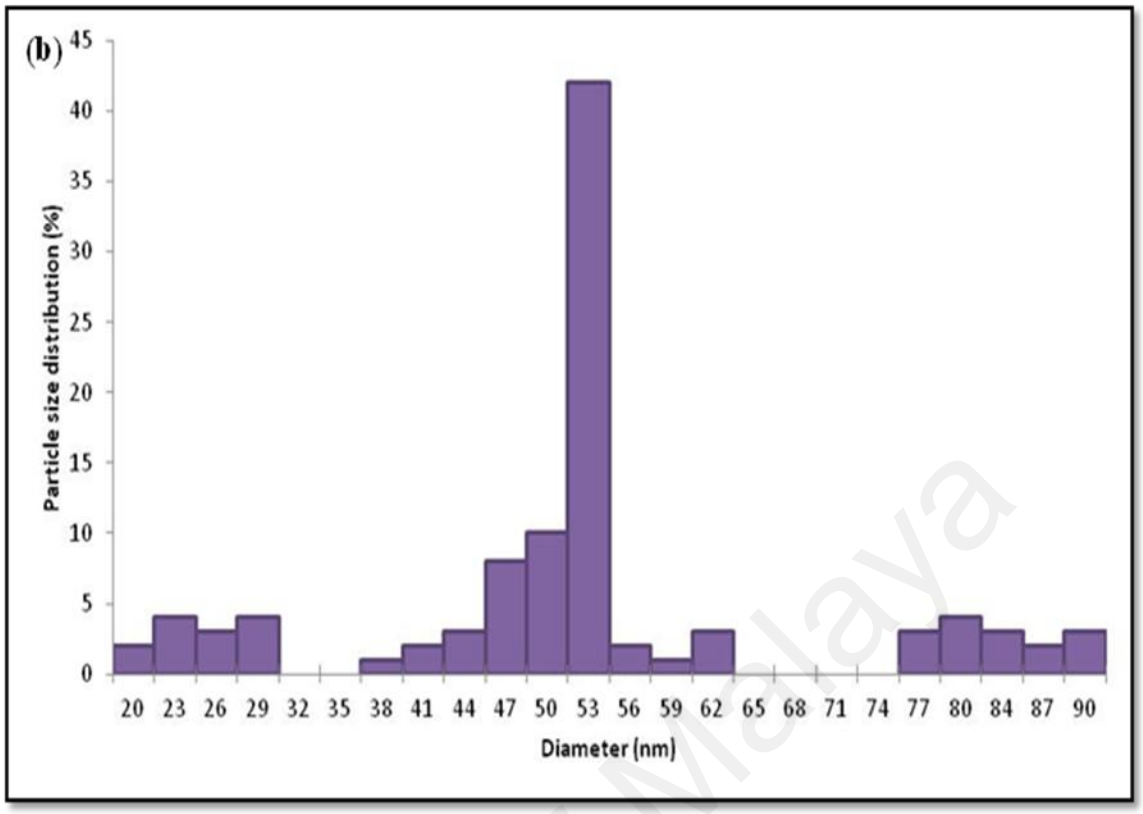

Figure 4.4: (b) Particle size distribution of 10 percent loading of Ag nanoparticles at 120 ℃

4.2.2a Effect of $AgNO_3$ content on the particle size

Figure 4.5 shows the particles size decreases with the increase of silver ion ($AgNO_3$) content. A lower concentration of $AgNO_3$ produced an unstable silver nanoparticles and leads to larger sizes of particles. The formation of larger particles could be explained by the generation of a smaller number of nuclei at lower reactant concentrations, then follow with the aggregation of the silver particles.

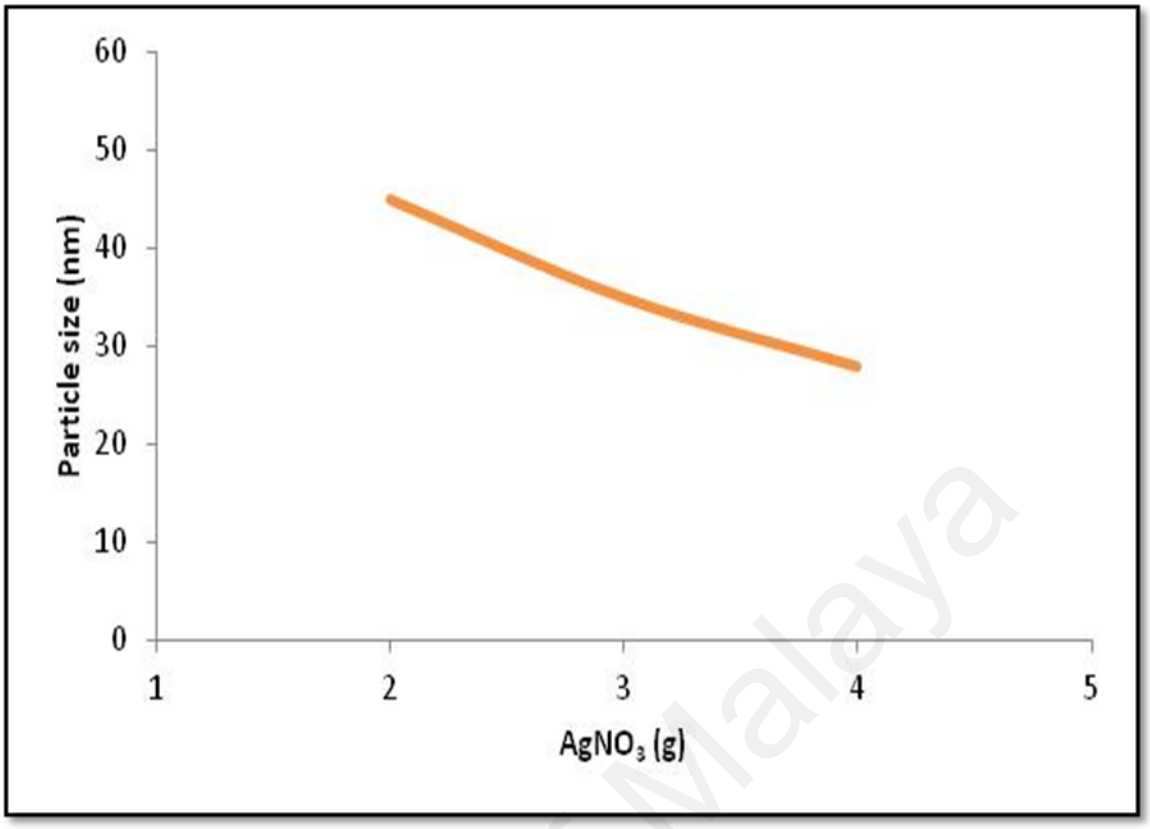

Figure 4.5: Variation of particle size as a function of $AgNO_3$ content

4.2.2b Effect of PMMA content on the particle size

Figure 4.6 shows the dependence of particles size on the PMMA content. The particle size showed a noticeable decrease with the increase of PMMA content. The size of Ag/PMMA nanocomposites decreased with the PMMA content increased. Furthermore, the addition of PMMA increased the viscosity of the dispersion, thus reducing the possibility of particle aggregation and phase separation.

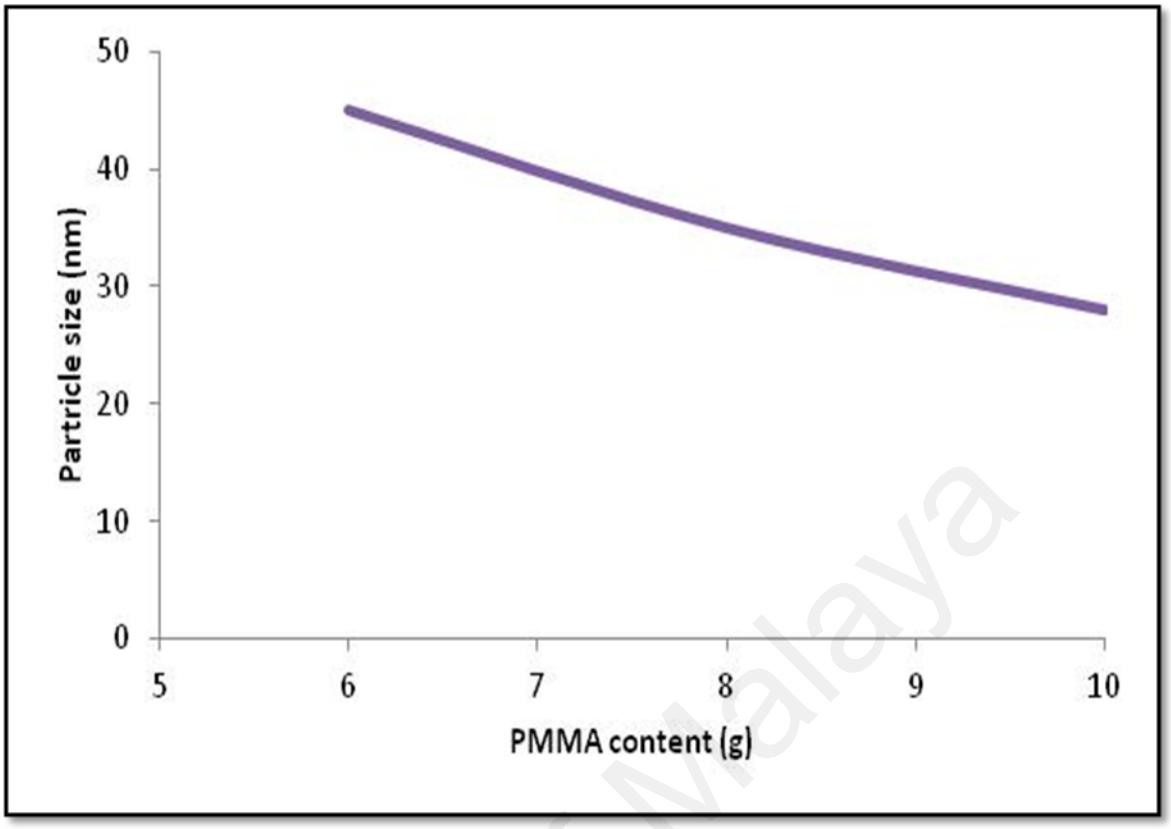

Figure 4.6: Variation of particle size as a function of PMMA content

4.2.2c Effect of reactant temperature on the particle size

Figure 4.7 shows the effect of reactant temperature on the particle. The particle size was increased significantly from 24 to 53 nm when the temperature increased from 80 to 120 °C. The particles keep growing at high temperature due to the Ostwald ripening during the heating process (Deng *et al.*, 2008). The small particles were dissolved and redeposit onto larger crystals.

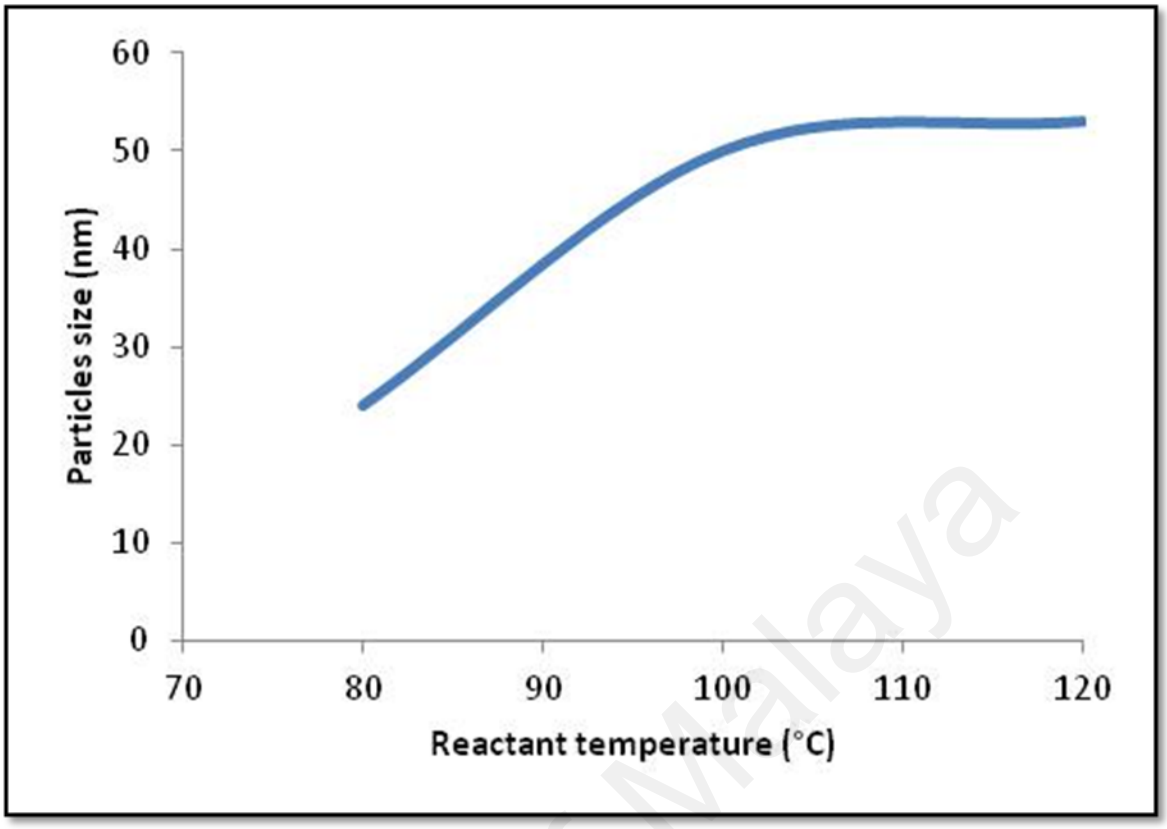

Figure 4.7: Variation of particle size as s function of reactant temperature

4.2.2d Effect of silver nanoparticles content on the particle size

The loading of silver nanoparticles in the solvent was determined by the following equation:

$$L\% = (\frac{V_1}{V_2})x100\% \tag{4.1}$$

where V_1 and V_2 are the volume of the silver nanoparticles and solvent (DMF) used in preparing Ag/PMMA nanocomposites. The effect of silver content on particle sizes is shown in Figure 4.8. The size of particle decreases as the content of silver increases.

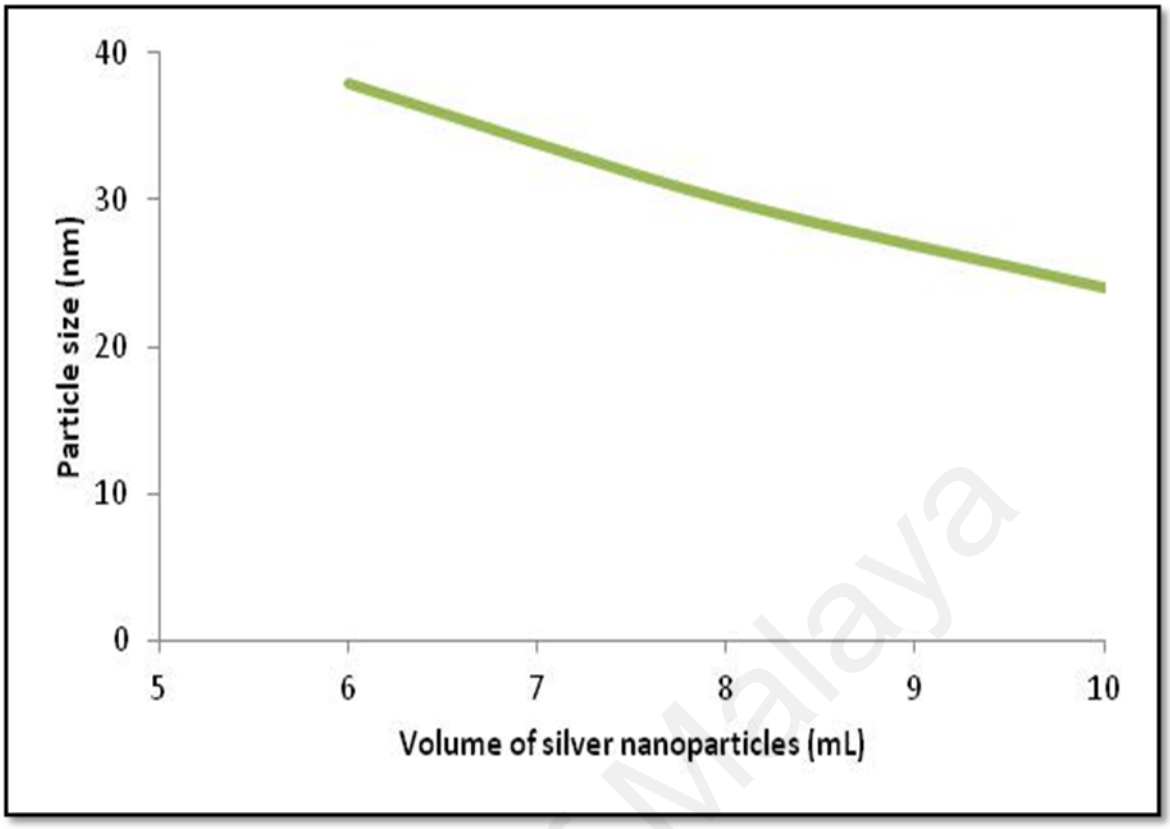

Figure 4.8: Variation of particle size as a function of silver nanoparticles content

4.2.3 Dynamic Light Scattering (DLS) Analysis

The particle size distribution of Ag/PMMA nanocomposites in solution form was measured using dynamic light scattering (DLS) method as shown in Figure 4.9. These data represent the hydrodynamic size of the particles which are affected by the surrounding and by assuming an isotropic spherical shape of particles.

Figure 4.9(a) shows decreases of particle size at 83, 74 and 72 nm for 6, 8 and 10 percent loading of silver nanoparticles at 80 °C. The particle size gradually decreases with the increasing of $AgNO_3$. On the contrary, a low concentration of silver nanoparticles is favorable to form larger particle size since the reactants will rapidly transfer from one core to another. Figure 4.9(b) shows the increases of particles size

with the temperature. This result is in good agreement with the TEM results (Figures 4.2-4.4) and FESEM results (Figure 4.1).

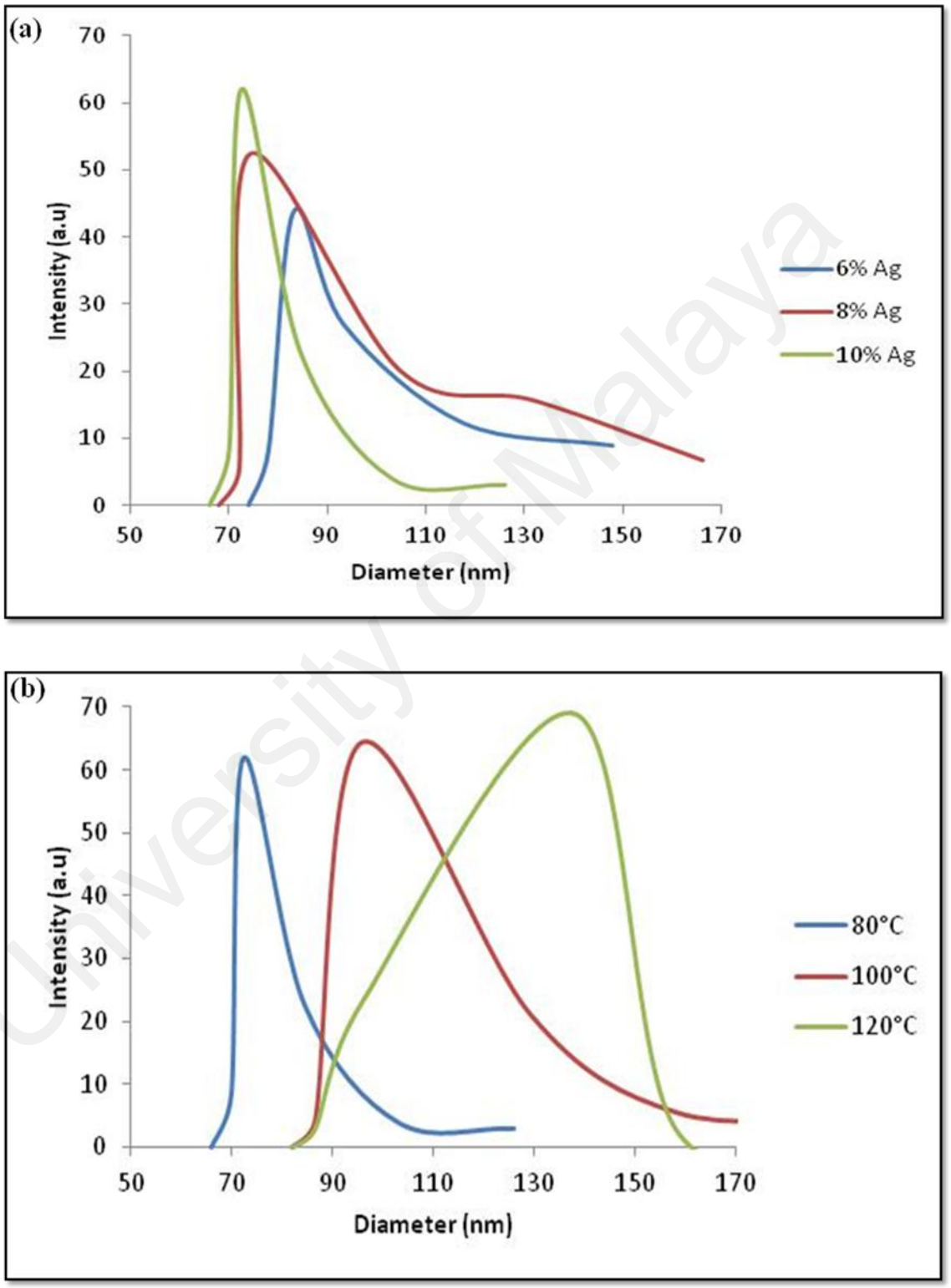

Figure 4.9: DLS size distribution of particles at difference (a) concentration of silver nanoparticles at 80 °C (b) temperature

4.2.4 Zeta Potential Analysis

The zeta potential of the Ag/PMMA nanocomposite in suspension at various percentage loading of silver nanoparticles and temperatures are summarized in Table 4.1. It was observed that all samples have negative potentials with the maximum value (-61.0 mV) at 80 ℃ for 10 percent loading of silver. Meanwhile, the minimum value of potential is -32.1 mV at 120 ℃ for 6 percent loading of silver. This indicate that sample at 80 ℃ is highly stable then the sample at 120 ℃ where it will remain suspended at 80 ℃ before being precipited at 120 ℃. Due to the negative potential, an oxidized layer is likely present on the surface of silver nanoparticles (Li *et al.*, 2010).

Table 4.1: Zeta potential of Ag/PMMA nanocomposites at different percentage loading of silver nanoparticles and temperature

Temperature (°C)	Percentage loading of silver nanoparticles (%)	Diameter (nm)	Potential (mV)
80	6	83	-58.3
80	8	74	-59.4
80	10	72	-61.0
100	6	119	-33.8
100	8	101	-45.1
100	10	96	-54.0
120	6	152	-32.1
120	8	144	-33.2
120	10	139	-35.1

4.3 Structural Studies

4.3.1 X-Ray Diffraction (XRD) Analysis

Figure 4.10 shows the XRD patterns for all samples at different reactant temperature. Figure 4.10(a) shows the XRD pattern of silver nanoparticles. All the prominent peaks appeared at angle of 2Θ = 38°, 44.44°, 64.54° and 77.38° are corresponding to the (111), (200), (220) and (311) miller indices of face center cubic (fcc) of silver. Figure 4.10(b) shows the XRD pattern for pure PMMA containing a broad peak at 19.62°. Meanwhile, Figures 4.10(c-e) show the XRD pattern of Ag/PMMA nanocomposites at different reactant temperature, 80, 100 and 120 °C which exhibit a two-phase (crystalline and amorphous) structure. The peak for (111) plane increases as the temperature increases up to 120 °C. Silver nanoparticles preferred alignment in PMMA is at the (111) plane. This can be explained from a viewpoint of thermodynamics since the preferred orientations of solid particles are known to be the perpendicular directions to the planes of lowest surface energy, which corresponds to the most densely packed planes for metallic materials (Fukuda *et al.*, 2003; Herrero & Guillen, 2002). Accordingly, the FCC structure of silver (111)-preferred orientation, and (111) planes have the highest packing density. However, not every grain is oriented to (111) direction. There is other factor may influencing the preferred orientation which is initial orientation of nuclei at the early growth stage. The initial orientation of nuclei is governed by the adsorption energy of adatoms to substrate and bonding energy between adatoms (Jung, 2004).

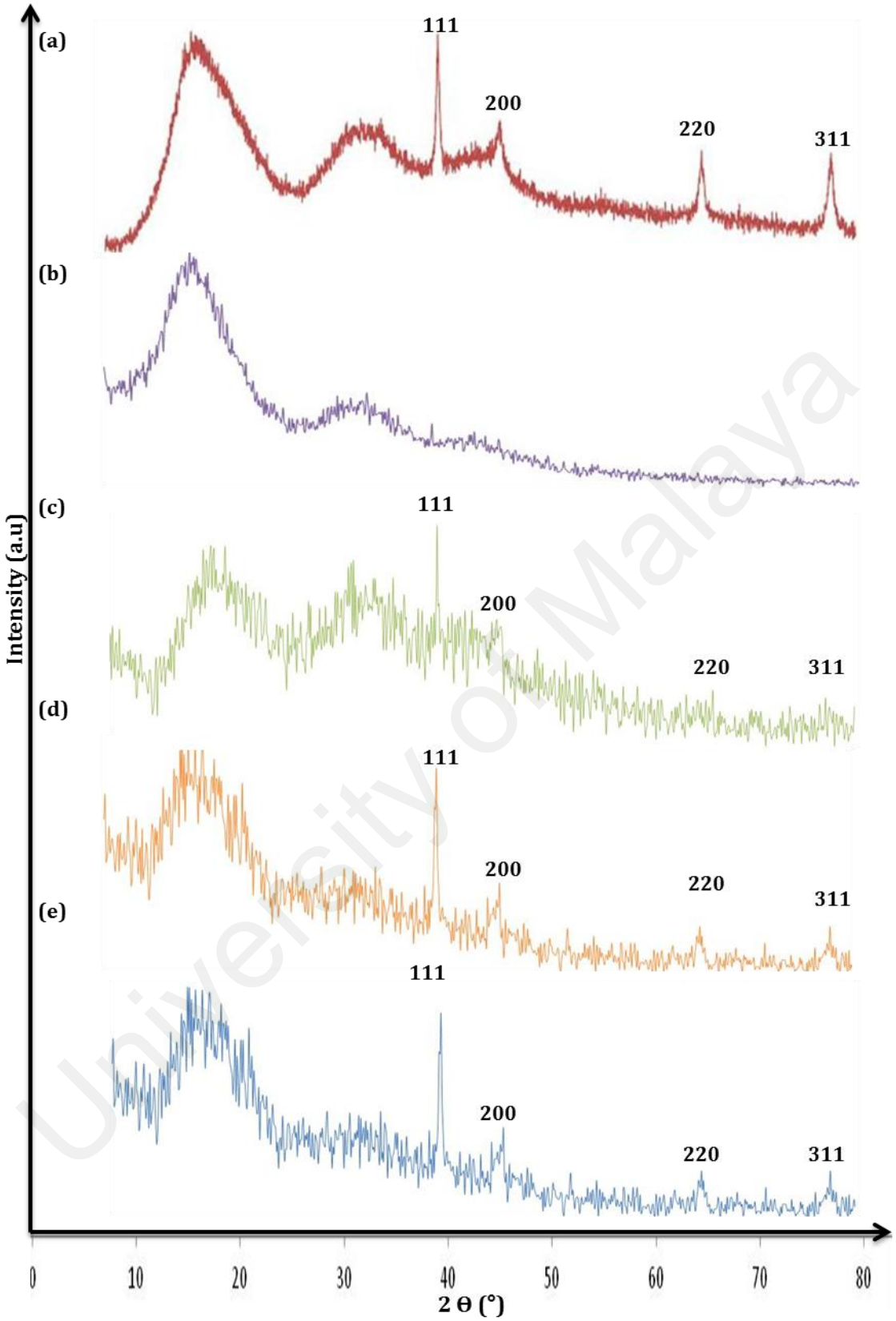

Figure 4.10: XRD patterns of (a) silver nanoparticles, (b) pure PMMA and Ag/PMMA nanocomposites at different reactant temperatures: (c) 80 (d) 100 and (e) 120 °C

4.3.2 Fourier Transform Infrared Spectroscopy (FTIR) Analysis

Figure 4.11 shows the FTIR spectra of $AgNO_3$, silver nanoparticles, DMF, PMMA. The $AgNO_3$ spectrum in Figure 4.11(a) shows an intense band at ~1300 cm^{-1}, with shoulders assigned to the symmetric C=C stretching vibration arising from the nitro group ($U_s(NO_2)$) (Fukuda *et al.*, 2003). The C=C band disappears upon mixing the solution, which is identified by the elimination of nitro group in the pure silver solution, as shown in Figure 4.11(b). The low percentage of carbonyl groups of the band at ~1690 cm^{-1} (amide-II) and ~2337 cm^{-1} (NH^{+3}) diminished significantly, denoting that the incorporation of silver nanoparticles weakened the interaction between the oxygen of the carbonyl groups and the adjacent hydrogen. The spectra also shows an intense broad band at ~3352 cm^{-1} (Figure 4.11(b)), which is assigned to the overtone of the amide-II band (Herrero & Guillen, 2002). This is possibly due to the reaction of glycol and sodium solfonate groups. The formation of the amide group is essential for stabilizing the suspension. Upon mixing the solution, the carboxylic C=O stretching band at ~1636 cm^{-1} (Figure 4.11(a)) is found to be a superposition of band centered at ~1636 cm^{-1} (Figure 4.11(b)) assigned to be amide-II band of carbonyl (Herrero & Guillen, 2002). The band at ~ 1050 cm^{-1} is identified to be wagging mode of C=C double bond from $AgNO_3$. This feature remained even after the chemical reduction process. This shows that silver nanoparticles are present in the solution.

The band of DMF spectrum is shown in Figure 4.11(c). The band at 659 cm^{-1} can be assigned to O=C-N-C torsion mode which also has a contribution from O=C-N bending motion (Sastry *et al.*, 2007). The band at 865 cm^{-1} is assigned to the N-CH_3 symmetric stretching mode (Sastry *et al.*, 2007). A week shoulder at 1061 cm^{-1} is assigned to C-H bending modes of H-C=O and methyl groups. The band at 1095 cm^{-1} is

assigned to the deformation mode of N-C-H (Sastry *et al.*, 2007). The bands at 1150 and 1256 cm^{-1} are assigned to C-H bending motion of methyl group and N-CH_3 symmetric stretching mode respectively. The highest intensity band in this region is observed at 1651 cm^{-1} which assigned to the C=O stretching mode. A broad band of the carboxylic acid group due to the O-H vibration mode is observed at 3499 cm^{-1}.

Figure 4.11(d) shows the FTIR spectrum of PMMA. Three distinct bands appeared at ~2862, ~2951 and ~2978 cm^{-1}. The first band arises from the asymmetrical (as) stretching mode in which two C-H bonds of the methyl group are extending. Meanwhile, the third one is contracting ($U_{as}CH_3$) and the second band arises from symmetrical (s) stretching ($U_{as}CH_3$) in which all three of the C=H bonds extend and contract in phase. The bands at ~1389 and 1435 cm^{-1} correspond to symmetrical bending vibration ($UsCH_3$) and the asymmetrical bending vibration ($U_{as}CH_3$) of methyl group, respectively. Ether lone peak is also present at ~1145 cm^{-1}. Strong peak appearing in the region ~1722 cm^{-1} corresponds to C=O stretching vibrations. Broader and stronger bands in the region ~1300-1000 cm^{-1} correspond to C-O stretching vibrations, which usually consists of two asymmetric coupled vibrations, i.e. C-C(=O)-O and O-C-C. A peak at ~754 cm^{-1} corresponds to out of plane C-H bending.

Figure 4.12(a-c) shows the FTIR spectra of Ag/PMMA nanocomposites for 10 percent loading of silver nanoparticles at 80, 100 and 120 °C in the solution. The spectra showed that the bonding was dominantly influenced by the PMMA and DMF solution. This is due to the electrostatic attraction between acrylate ions of PMMA and silver nanoparticles (Wang & Chen, 2006). The main bands of DMF in Ag/PMMA nanocomposites spectra are clearly seen. The similarities between DMF and Ag/PMMA nanocomposites spectra verify the vital element of DMF in Ag/PMMA nanocomposites.

It is found that the C=O (~1651 cm^{-1}) and O=C-N-C (~659 cm^{-1}) vibration modes of DMF in Ag/PMMA nanocomposites was similar to those in DMF solvent. The bands correspond to C-O-C of the methoxy group, and skeletal C-C in Ag/PMMA nanocomposites appeared at 1151 and 1257 cm^{-1}, respectively. These bands strongly affect their shape and size. A broad band of the carboxylic acid group due to the O-H (~3499 cm^{-1}) in Ag/PMMA nanocomposites becomes broader as the temperature increases. The increase in water content may be originated from the environment or product of the chemical reactions. Both bands at ~1065 and 1088 cm^{-1} in Ag/PMMA nanocomposites are assigned to the sensitive metal complexes of methyl rocking vibrations coupled with a C-N vibration mode. The Ag/PMMA nanocomposites band at ~1387 cm^{-1} is coupled in vibration, with the major contributions from CH_3 deformation and C-N stretching mode. The interaction of the PMMA segments with silver nanoparticles is demonstrated to be dependent on the regimes of the adsorption of polymer chain onto the surface.

Table 4.2: Assignment of IR bands for silver nitrate, silver nanoparticles, DMF, PMMA and Ag/PMMA nanocomposites

Materials	**Type of vibration**	**Wavenumber (cm^{-1})**
Silver Nitrate ($AgNO_3$)	C=C stretching vibration	1300
	Amide-II	1690
	NH^{3+}	2337
	Overtone Amide-II	3352
Siver Nanoparticles	C=C	1050
	C=O	1636
	Overtone Amide-II	3352

Dimethyl-formamide (DMF)	O=C-N-C torsion mode	659
	$N-CH_3$ symmetric stretching mode	865
	H-C=O and methyl groups	1061
	deformation mode of N-C-H	1095
	C-H bending motion	1150 & 1256
	C=O stretching mode	1651
	O-H vibration mode	3499
Polymethyl-methacrylate (PMMA)	C-O stretching vibrations	1000-1300
	symmetrical bending vibration CH_3	1389
	asymmetrical bending vibration CH_3	1435
	C=O stretching vibrations	1722
	stretching mode of C-H	2862
	C=H	2951
	CH_3	2978
Ag/PMMA Nanocomposites	O=C-N-C torsion mode	659
	C-N vibration mode	1065 & 1088
	C-O-C of the methoxy group	1151
	C-C	1257
	CH_3 & C-N	1387
	C=O stretching mode	1651
	O-H vibration mode	3499

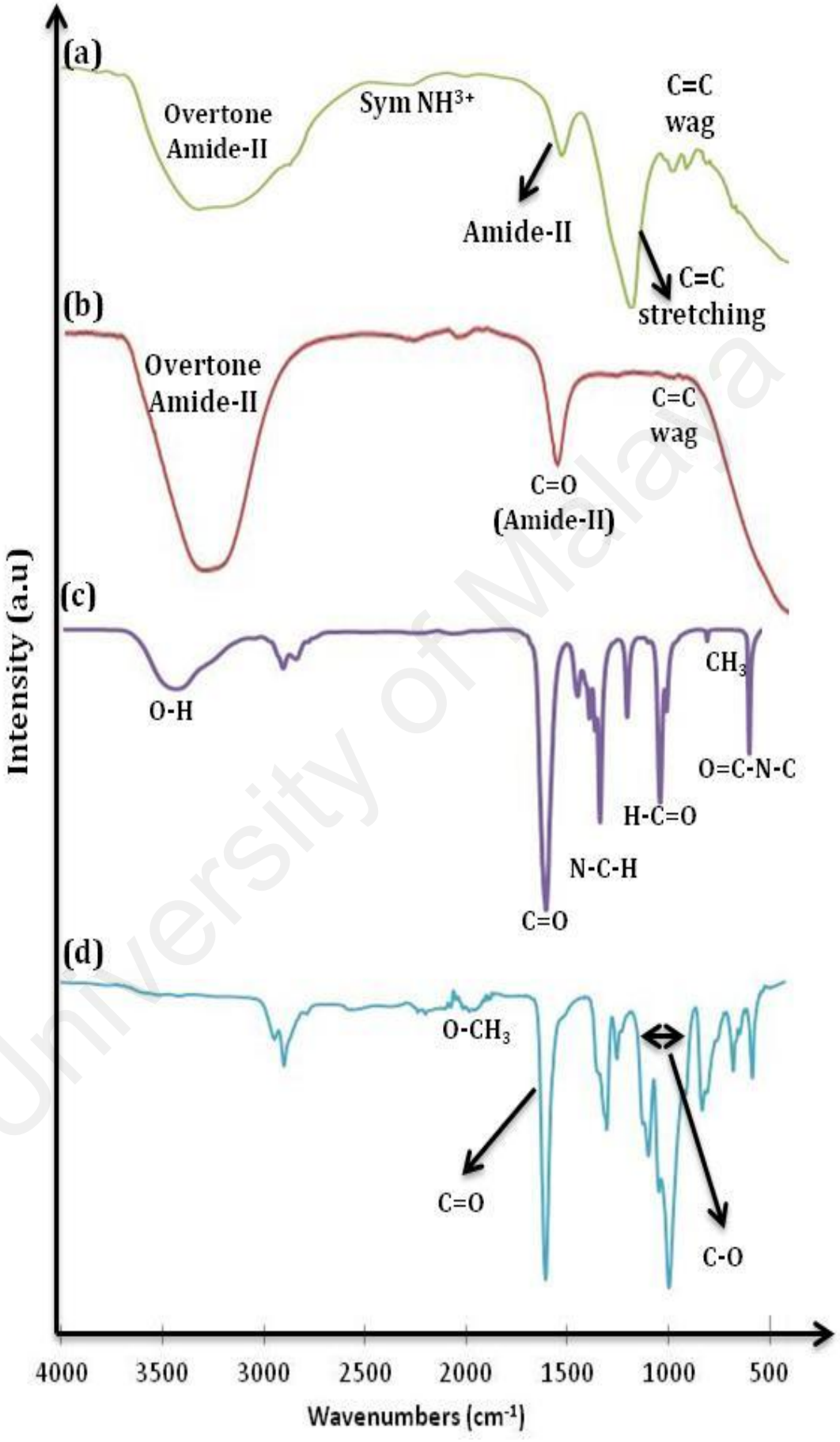

Figure 4.11: FTIR spectra for (a) $AgNO_3$, (b) silver nanoparticles, (c) DMF, (d) PMMA

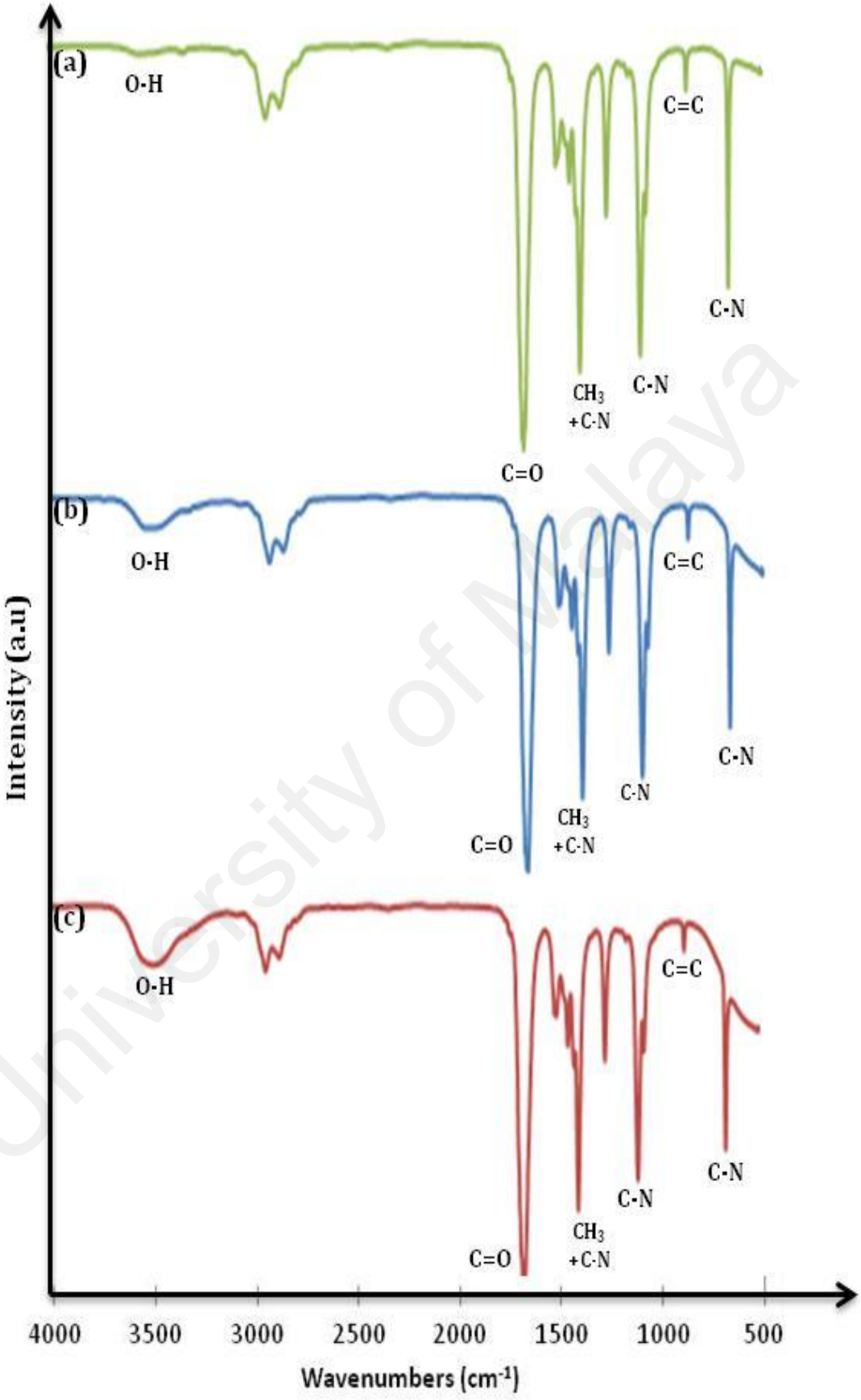

Figure 4.12: FTIR spectra for Ag/PMMA nanocomposites at (a) 80; (b) 100 and (c) 120 °C

4.3.3 Raman Spectroscopy Analysis

Figure 4.13(a-c) shows the Raman spectra of Ag/PMMA nanocomposites for different percentage loading of silver nanoparticles at 80, 100 and 120 °C. The band at ~ 240 cm^{-1} is due to the stretching vibration of Ag-N bond and two peaks at ~1409 and 1665 cm^{-1} can be attributed to symmetric and asymmetric C=O stretching vibrations, respectively (Chowdhury & Ghosh, 2004). Selective enhancement of these raman bands clearly indicates that C=O bonds of the carboxylate ions and Ag-N bond from the free amine groups are lying perpendicular to the surface of silver nanoparticles. Notably, PMMA is a raman active compound with major bands at 600 cm^{-1} for (C–C–O) and (C-COO) stretch; 811 cm^{-1} for (C–O–C) stretch; 1450 cm^{-1} for (C–H) in plane bending; and 1728 cm^{-1} for (C=O) stretch (Zhang *et al.*, 2005). Beside the observed raman bands, the band at 2957 cm^{-1} is the most prominent which is due to the C-H stretching vibration. Most of the Raman bands are identified from Willis *et al.*, (1969). The peak intensity decreases as the percentage loading of silver nanoparticles increases due to the reduction of lattice vibration. The shape and size of the Ag/PMMA nanocomposites strongly affect the vibration due to the factors like the ratio of absorption and scattering events. Particles which are relatively bigger will allow the excitation of multipoles, which are nonradioactive. As only the dipole transition leads to raman scattering, the higher-order transitions will cause a decrease in the overall efficiency of the enhancement. Particles which are relative smaller lose their electrical conductance and cannot enhance the field (Willis *et al.*, 1969).

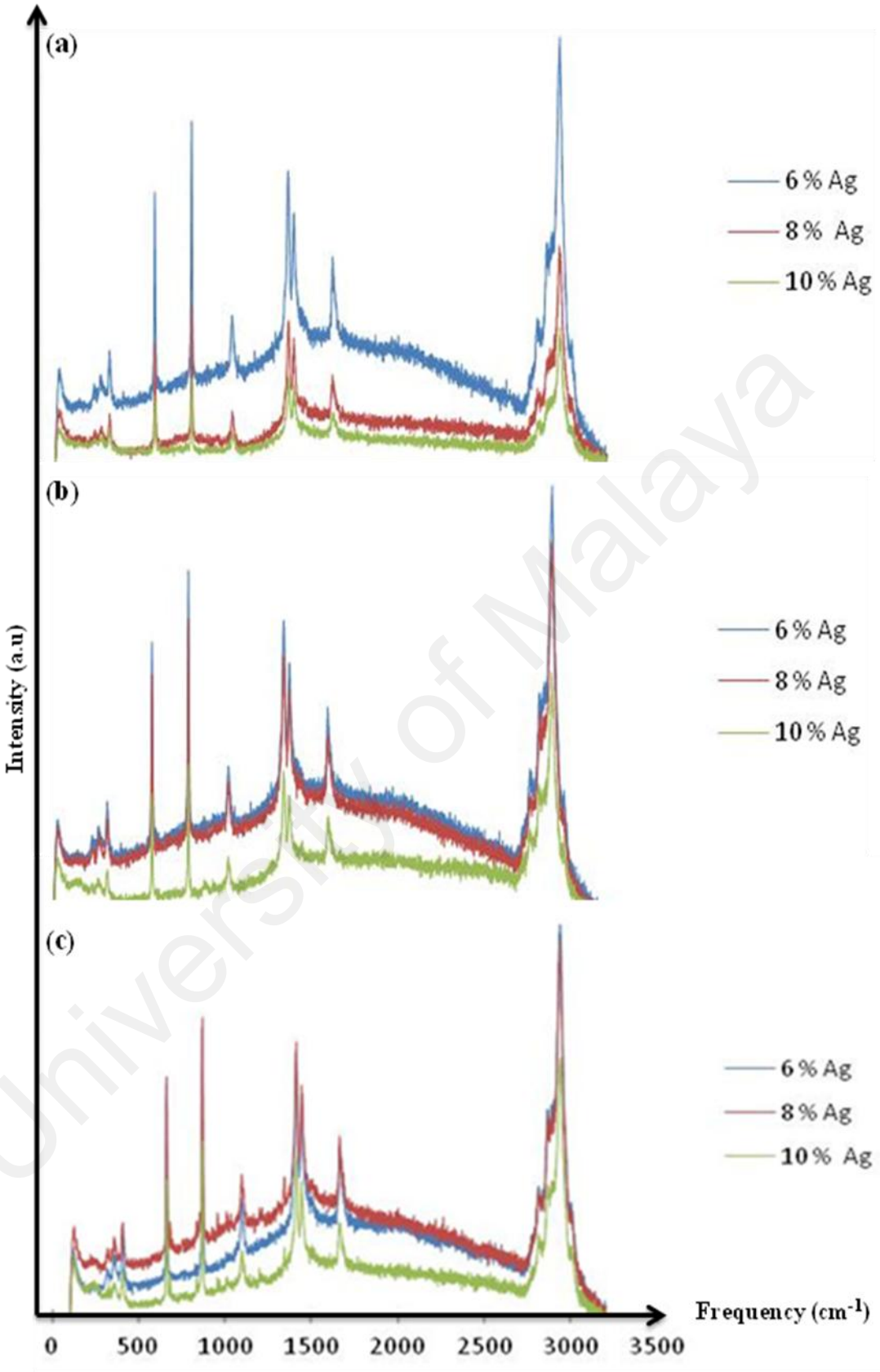

Figure 4.13: Raman spectra of the Ag/PMMA nanocomposites with various percentages loading of silver nanoparticles at (a) 80 (b) 100 and (c) 120 °C

The raman band intensity of the organic molecules (the capping agents, PMMA) which attached to the silver nanoparticles will be selectively enhanced with increasing of reactant temperature as shown in Figure 4.14. This is probably due to PMMA known to have a low activation energy for unzipping, i.e. the step wise removal of monomer units from the chain ends, a phenomenon which is commonly found when PMMA is excessively heated (Le *et al.*, 2006).

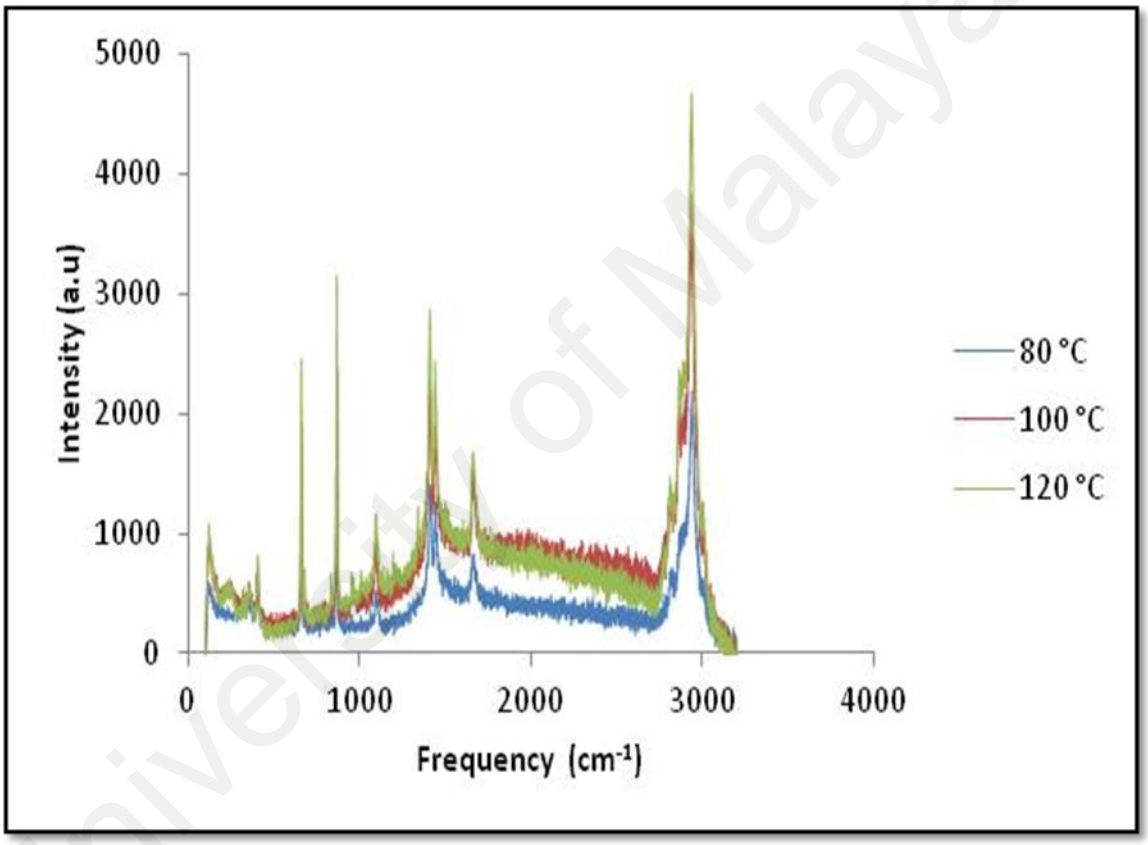

Figure 4.14: Raman spectra of the Ag/PMMA nanocomposites for 10 percent loading of silver nanoparticles at different temperature

4.4 UV-Visible (UV-Vis) spectroscopy

Figure 4.15 shows the absorption spectra of Ag/PMMA nanocomposites at 80 °C for different percentage loading of silver nanoparticles. The surface plasmon resonance (SPR) appeared at 435, 431 and 419 nm for 6, 8 and 10 percent loading of silver nanoparticles, respectively. The SPR peaks are blue shifted and their full width half maximum (FWHM) decreases as the percentage loading of silver nanoparticles increases. This indicate that the particle size decreases and become more uniform when the percentage loading of silver increases. The increase in maximum absorbance at each percentage loading of silver nanoparticles is due to the increases of particle density, which is strongly dependent on the amount of silver reduction at the surface of the medium (Chou & Ren, 2000; Khanna *et al.*, 2005; Longenberger & Mills, 1995).

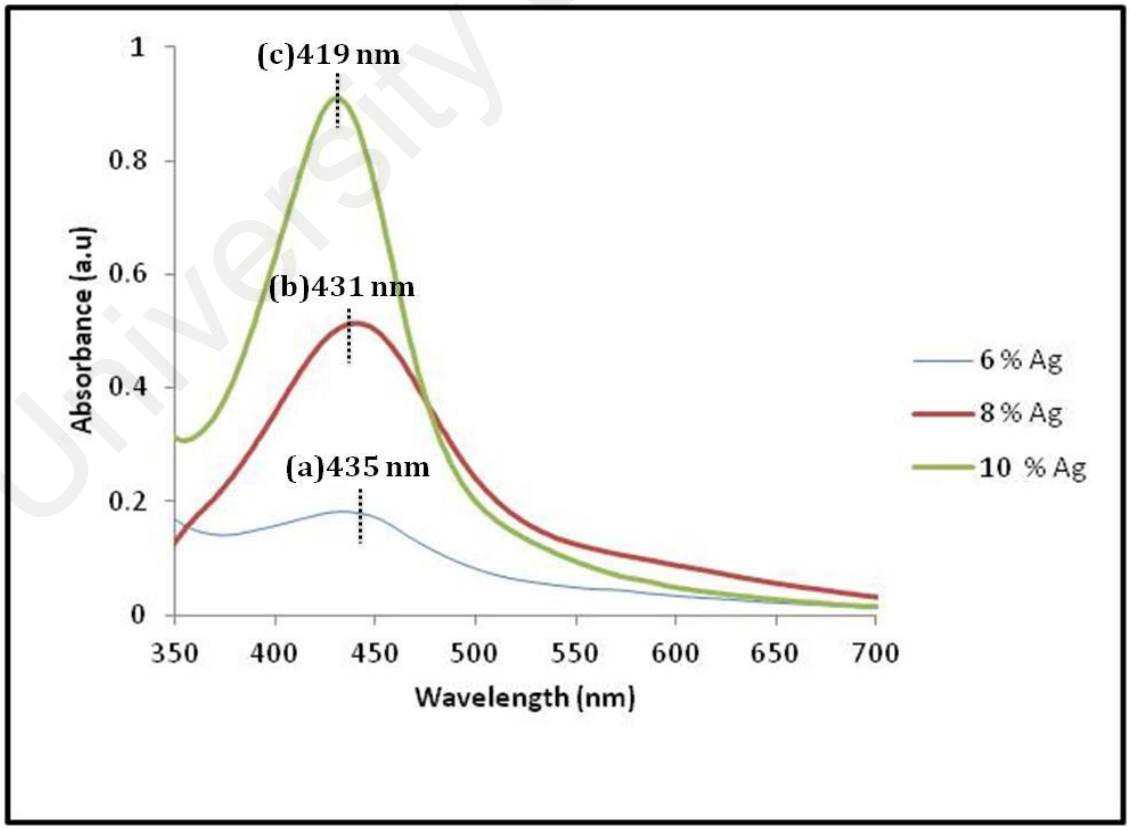

Figure 4.15: UV-Vis absorption spectra for Ag/PMMA at 80 °C with various percentage loading of silver nanoparticles

Figure 4.16 shows the absorption spectra of Ag/PMMA nanocomposites at 100 °C for different percentage loading of silver nanoparticles. The presence of SPR appeared at 441, 436 and 425 nm for 6, 8 and 10 percent loading of silver, respectively. The SPR are shifted to the smaller wavelength as the percentage loading of silver nanoparticles increases. This indicates that the size of Ag/PMMA nanocomposites become smaller at higher percentage loading of silver nanoparticles.

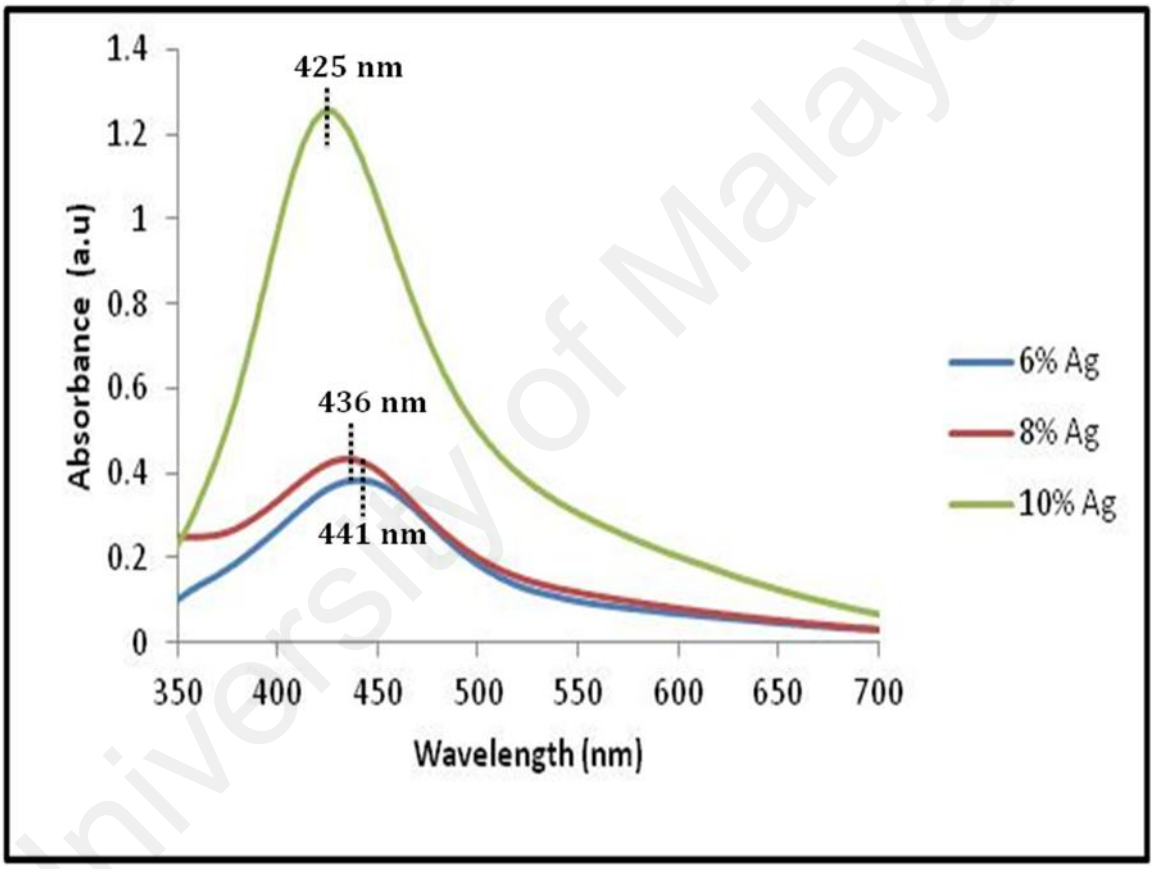

Figure 4.16: UV-Vis absorption spectra for Ag/PMMA at 100 °C with various percentage loading of silver nanoparticles

Figure 4.17 shows the absorption spectra of Ag/PMMA nanocomposites at 120 °C for various percentages loading of silver nanoparticles. The SPR peaks are blue shifted as the percentage loading of silver nanoparticles increases. This indicates the reduction of particle size as more silver nanoparticles added into the system. The

maximum absorbance is higher than Khanna and Singh (2007) and Vodnik *et al.*, (2009). The intensity of the plasma resonance in PMMA matrix absorptions decreases as temperature increase as compared with silver nanoparticles spectrum from previous studies (Khanna and Singh, 2007). This is due to the chemicals bonds between silver atoms and MMA groups lead to reduction of the free electron density (Jing *et al.*, 2009). Table 4.3 shows the SPR peaks and FWHM of all reactant temperature and percentage loading of silver nanoparticles.

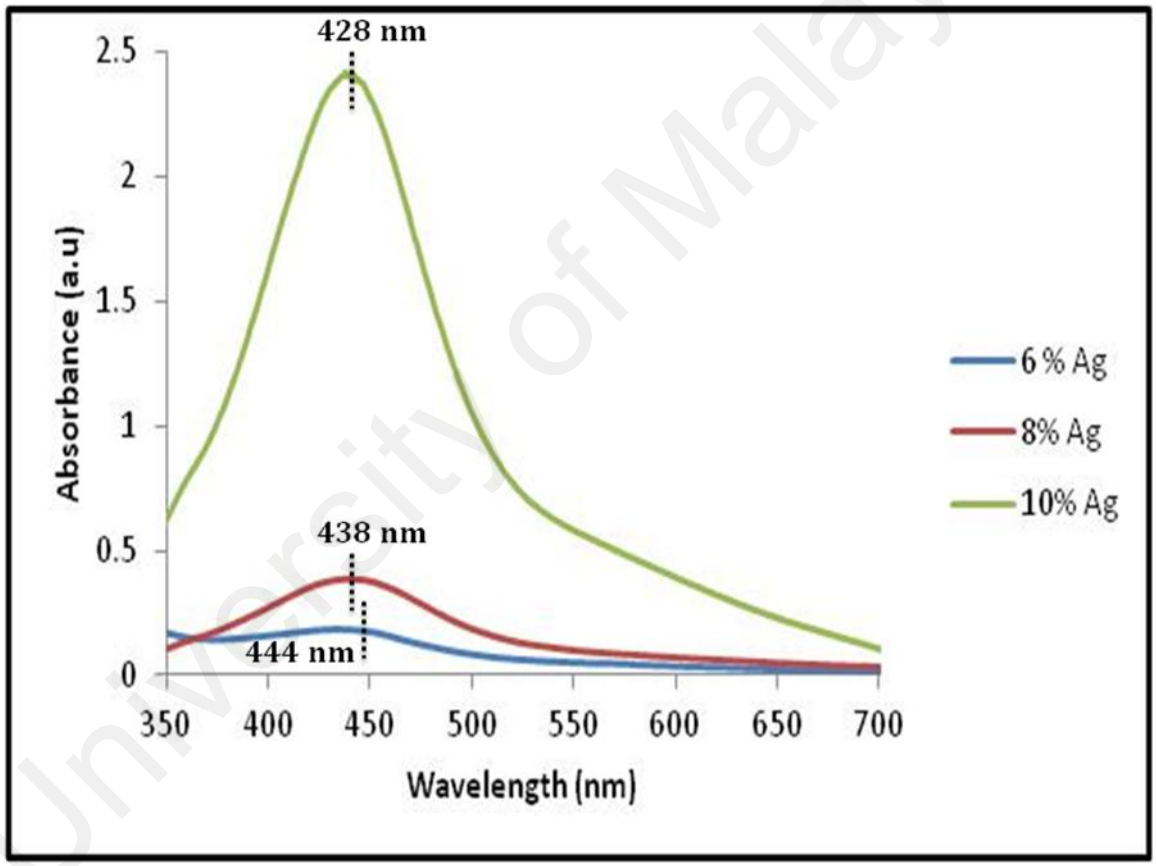

Figure 4.17: UV-Vis absorption spectra for Ag/PMMA at 120 °C with various percentage loading of silver nanoparticles

Figure 4.18 shows the absorption spectra for Ag/PMMA nanocomposites for 10 percent loading of silver nanoparticles at different reactant temperature. It shows highly broader of SPR band as temperature increases. The SPR band was red-shifted as

temperature increases. These features are associated with the agglomeration of the Ag/PMMA nanocomposites and increasing of the particles size. The observations are well accorded with the TEM results (Figures 4.2-4.4). The absorbance also provides an indication of the presence of an oxidized surface layer or absorbed substances. If neither is present, the absorption peak is narrow and located at a wavelength ranging between 390 and 450 nm. An oxidized layer is likely on the nanocomposites surfaces since there was no attempt to control the atmosphere during synthesis process (Li *et al.*, 2010). The presence of an oxidized surface layer is supported by the red-shifted in the SPR peak as well as the broadening effect as shown in Figure 4.18(Gosh, S. K & Pal, P., 2007).

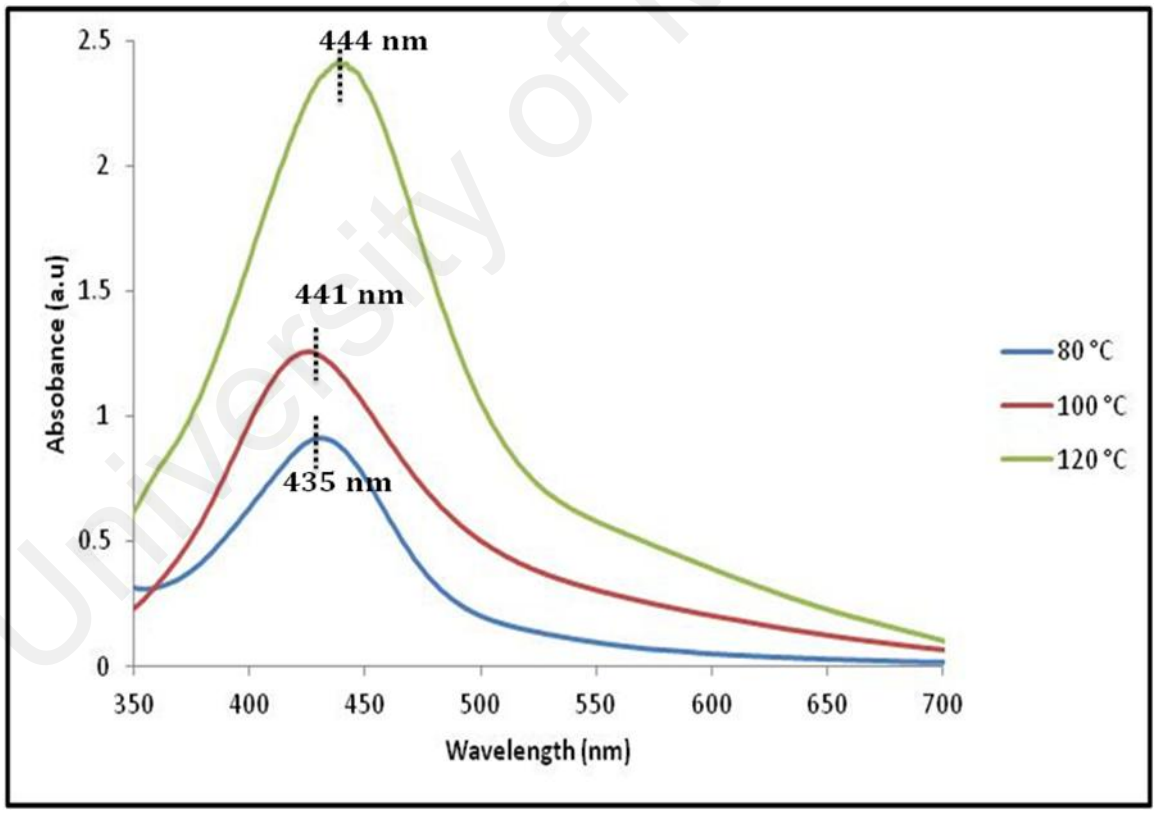

Figure 4.18: UV-Vis absorption spectra for Ag/PMMA nanocomposites at various temperatures for 10 percent loading of silver nanoparticles

Table 4.3: Optical parameters of Ag/PMMA nanocomposites synthesized by *in-situ* technique.

Reactant Temperature (°C)	Percentage loading of silver nanoparticles (%)	Figure	SPR of Ag/PMMA nanocomposites, λ_{max} (nm)	FWHM of Ag/PMMA nanocomposites, (nm)
80	6	4.15	435	93
80	8	4.15	431	89
80	10	4.15	419	73
100	6	4.16	441	150
100	8	4.16	436	139
100	10	4.16	425	97
120	6	4.17	444	158
120	8	4.17	438	154
120	10	4.17	428	103

Figures 4.19-4.21 show the transmittance spectra of Ag/PMMA nanocomposites at various temperature and different percent loading of silver nanoparticles. The plasmon resonance coincides with a sharp dip in transmittance clearly related to light absorption at optimum condition (10 percent loading of silver nanoparticles at 80 °C). The dip at $\lambda \approx 430$ nm is to be attributed to the dipolar plasmon resonance of the silver nanoparticles in mutual interaction and interacting with PMMA (Brenier, 2012). The maximum transmittance at $\lambda \approx 325$ nm corresponds to the nearly vanishing of the dielectric function of bulk silver.

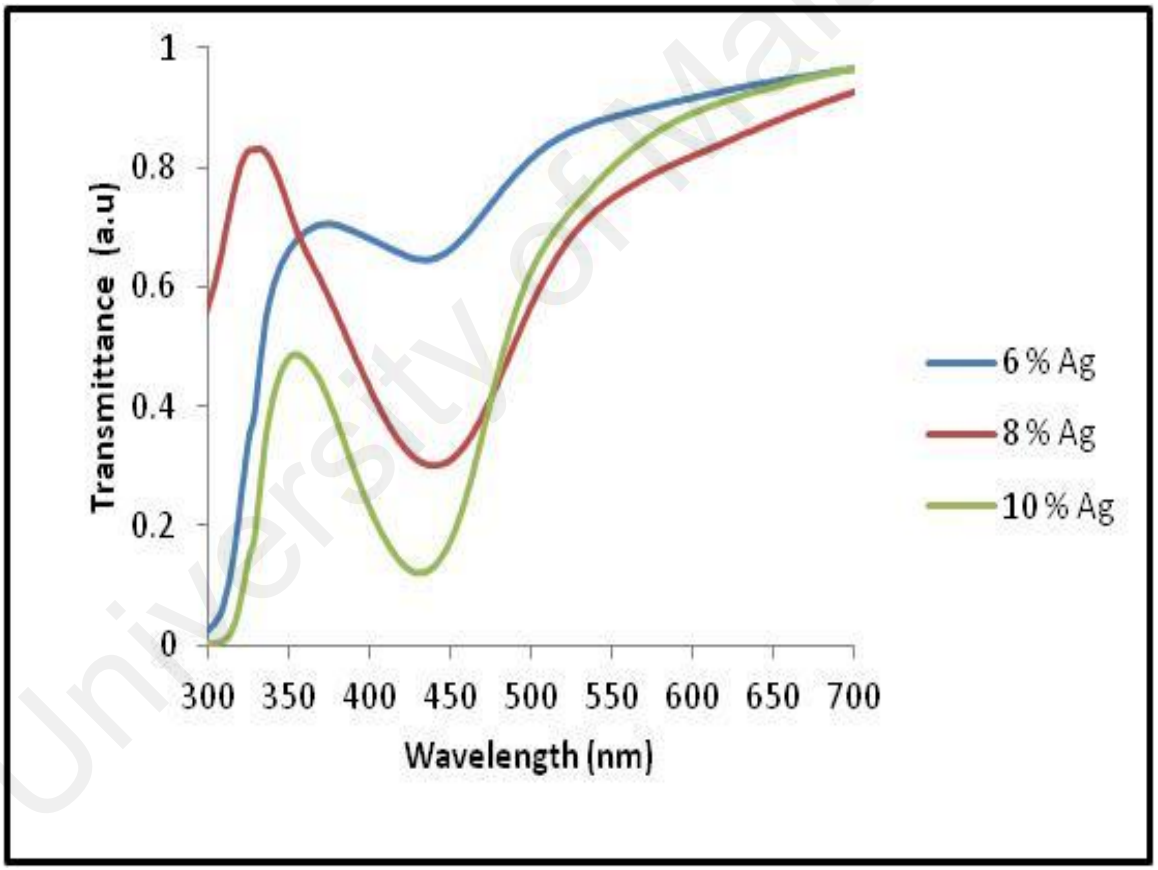

Figure 4.19: Transmittance spectra for Ag/PMMA at 80 °C with various percentage loading of silver nanoparticles

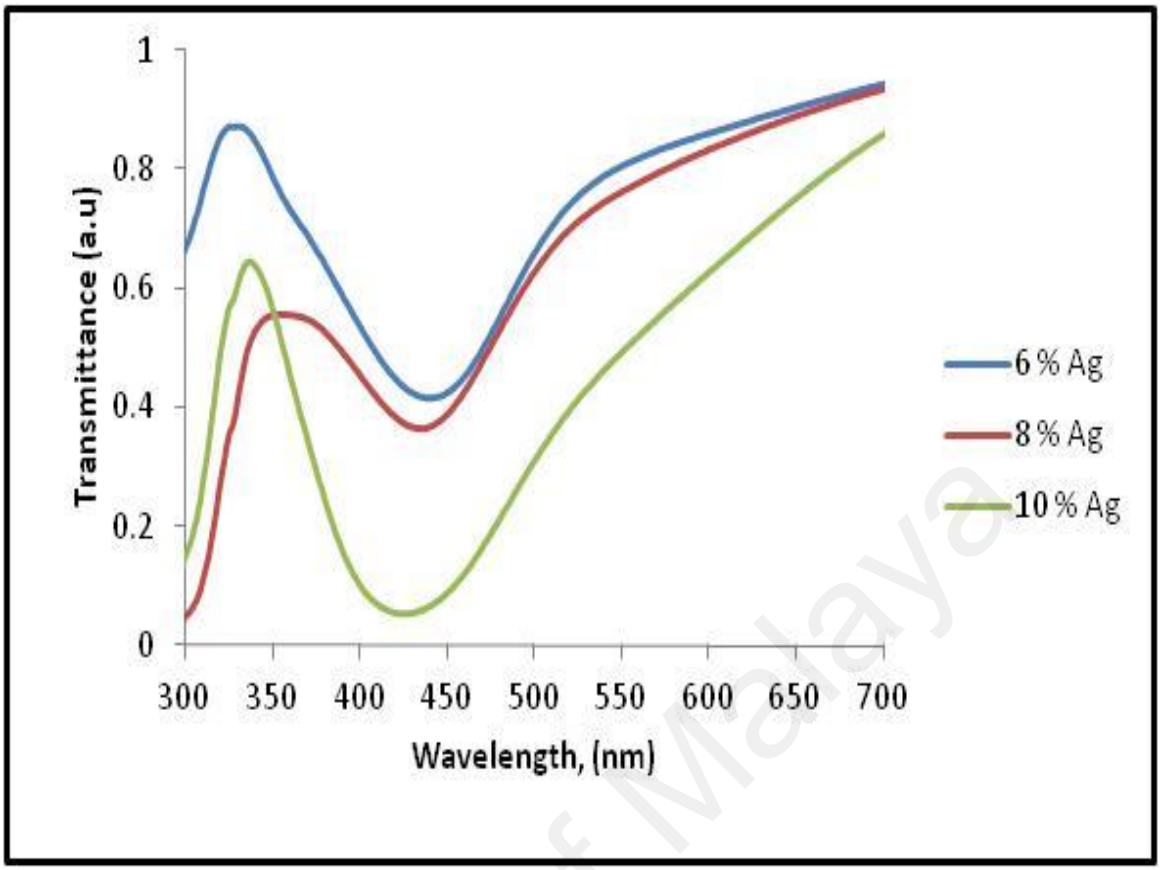

Figure 4.20: Transmittance spectra for Ag/PMMA nanocomposites at 100 °C with various percentage loading of silver nanoparticles

Figure 4.21 shows the transmittance spectra of Ag/PMMA nanocomposites at 120 °C for different percentage loading of silver nanoparticles. It shows that the transmittances decreases and the absorption edges shift slightly to a longer wavelength as the temperature increases. The red shift of the transmittances peak should be due to the quantum-size affects for silver nanoparticles capped with PMMA.

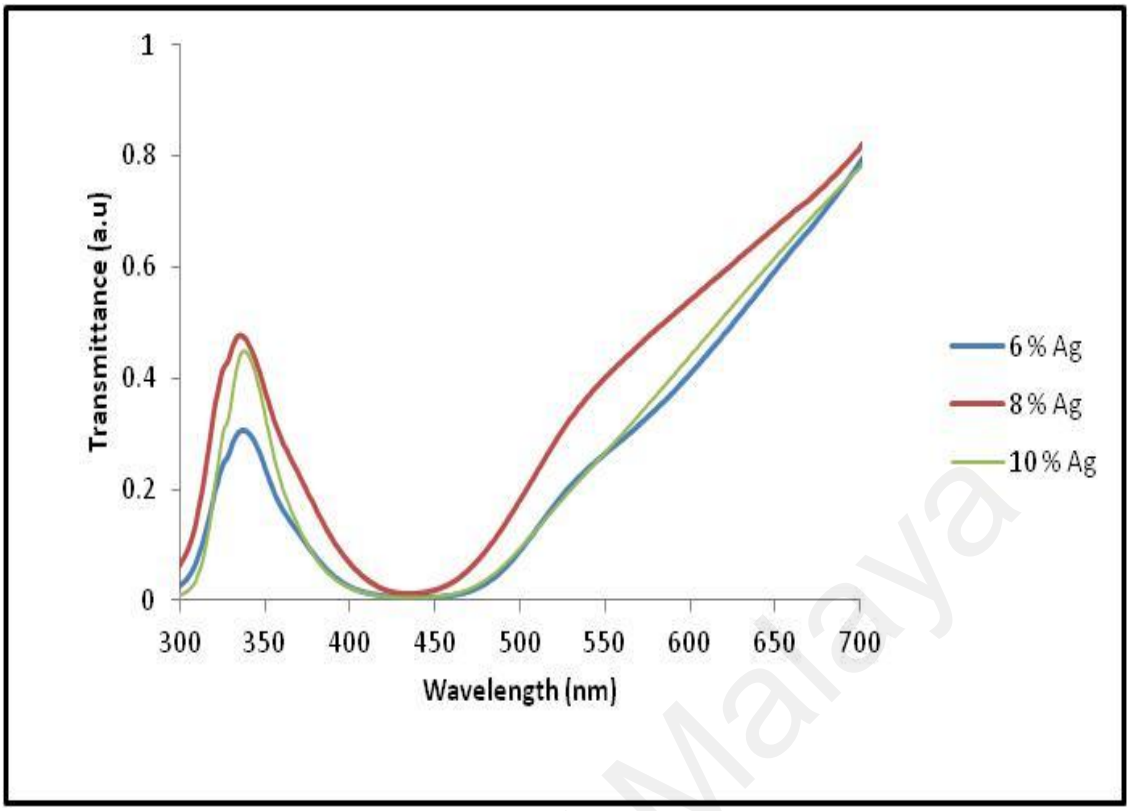

Figure 4.21: Transmittance spectra for Ag/PMMA nanocomposites at 120 °C with various percentage loading of silver nanoparticles

Figures 4.22-4.24 show the reflectance spectra of Ag/PMMA nanocomposites at 80, 100 and 120 °C for various percentages loading of silver nanoparticles. The reflectance spectra decrease with higher reactant temperature. The reflectance peaks are shifted from 435 (120 °C) to 420 nm (80 °C) and the intensity decreases by ~20 percent.

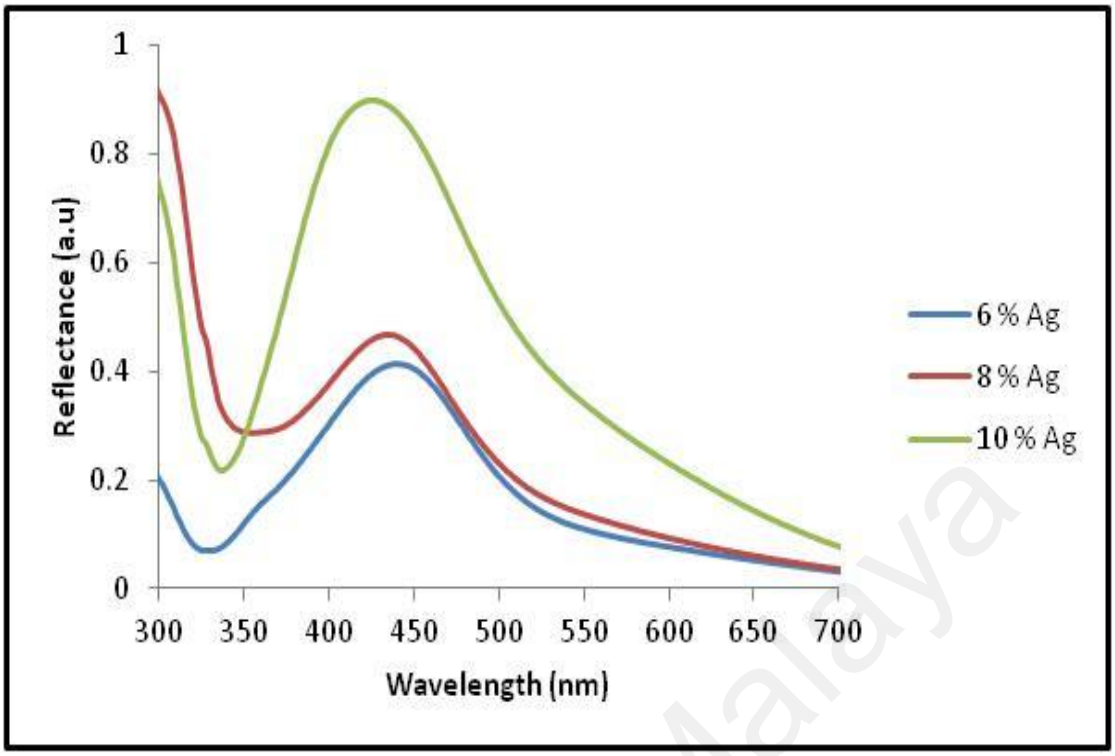

Figure 4.22: Reflectance spectra for Ag/PMMA nanocomposites at 80 °C with various percentage loading of silver nanoparticles

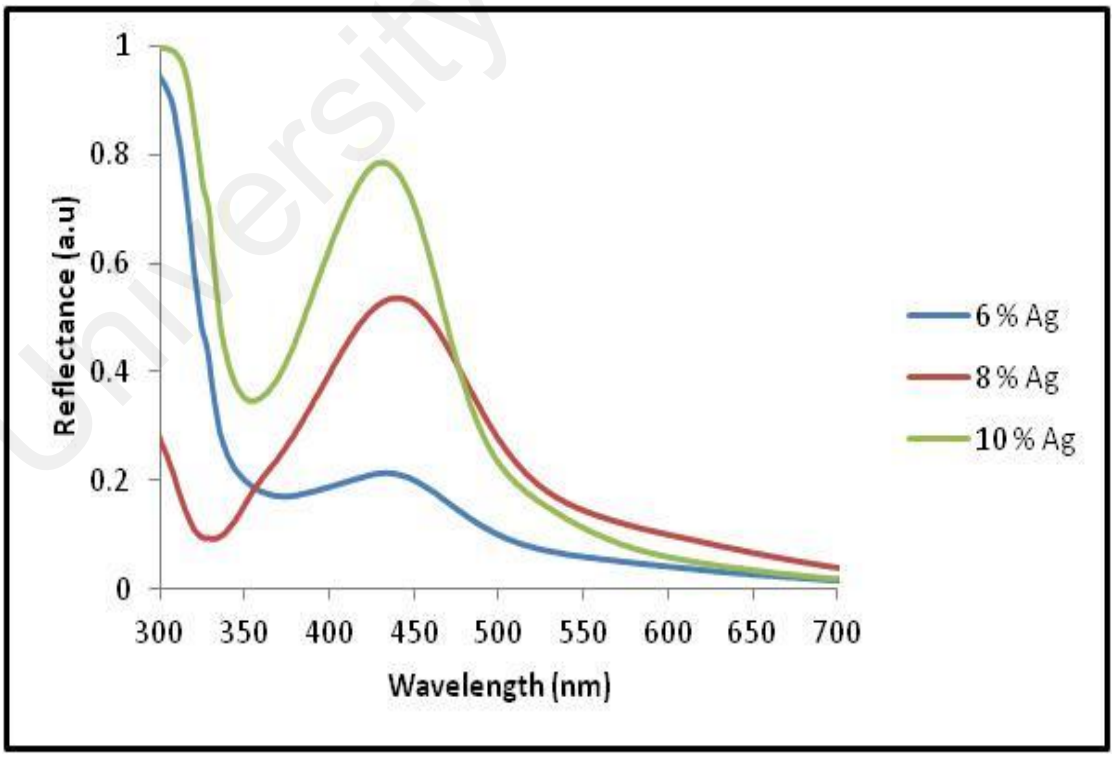

Figure 4.23: Reflectance spectra for Ag/PMMA nanocomposites at 100 °C with various percentage loading of silver nanoparticles

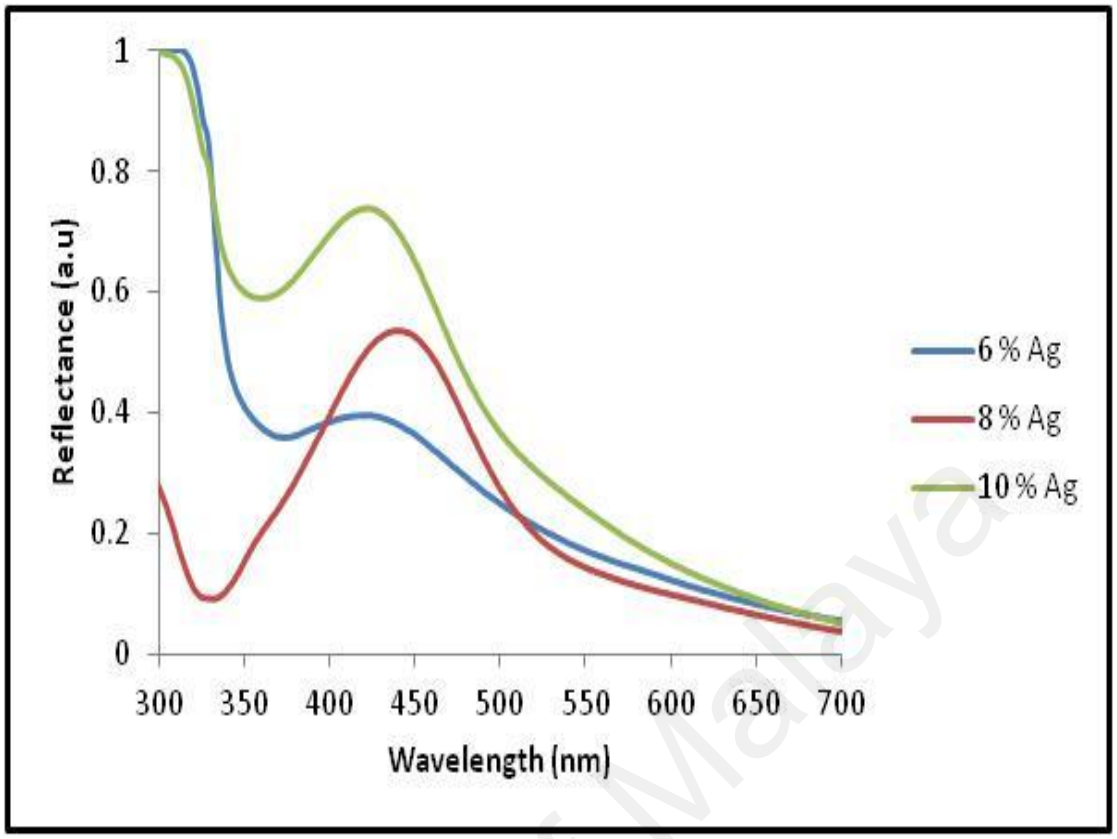

Figure 4.24: Reflectance spectra for Ag/PMMA nanocomposites at 120 °C with various percentage loading of silver nanoparticles

The refractive index, *n* of Ag/PMMA nanocomposites is calculated using Fresnel equation (Kesuma *et al.*, 2009),

$$n = \frac{1+\sqrt{R}}{1-\sqrt{R}} \tag{4.2}$$

where *R* is reflectance. Figures 4.25-4.27 show the refractive index of Ag/PMMA nanocomposites for various percentages loading of silver nanoparticles at different temperature. The reflectivity of the Ag/PMMA nanocomposites is characterized by the interference peaks which make it possible to determine the value of *n* to a certain degree of accuracy. The interference extremes at selected wavelength ranging from 400 to 500 nm. The refractive index of a material is sensitive to crystal structure (Kesuma *et al.*,

2009). The inclusion of silver nanoparticles into the media with the refractive index >1 leads to the broadening and shifting the plasmon resonance peak to longer wavelength (Sirbu *et al.*, 2008). Atoms while are easily polarize, (i.e. electron are easily displaced), give rise to a high refractive index (10 percent loading of silver nanoparticles at 80 °C), while those with tightly bound electron give rise to a low refractive index (6 percent loading of silver nanoparticles at 80 °C). The refractive index start to decrease as the wavelength increases after 470 nm.

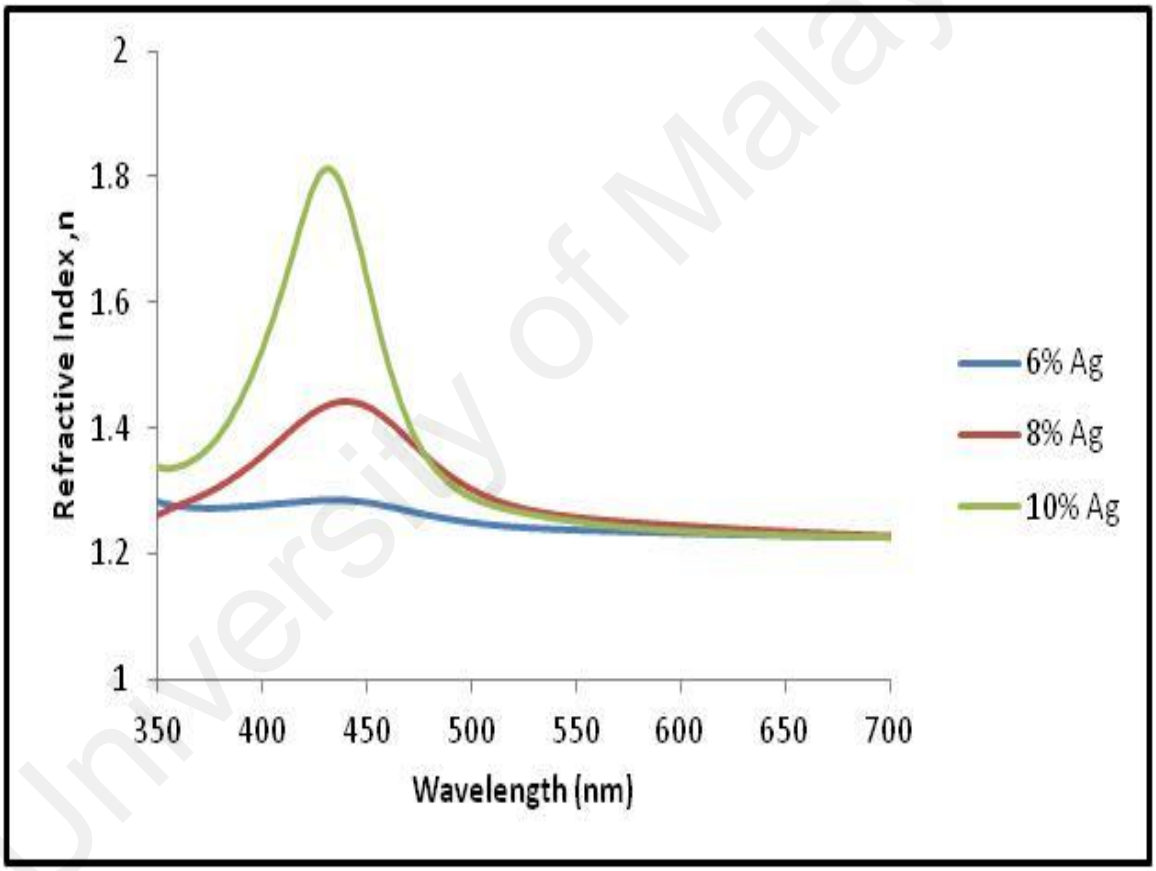

Figure 4.25: Refractive index spectra for different percentage loading of silver nanoparticles at 80 °C

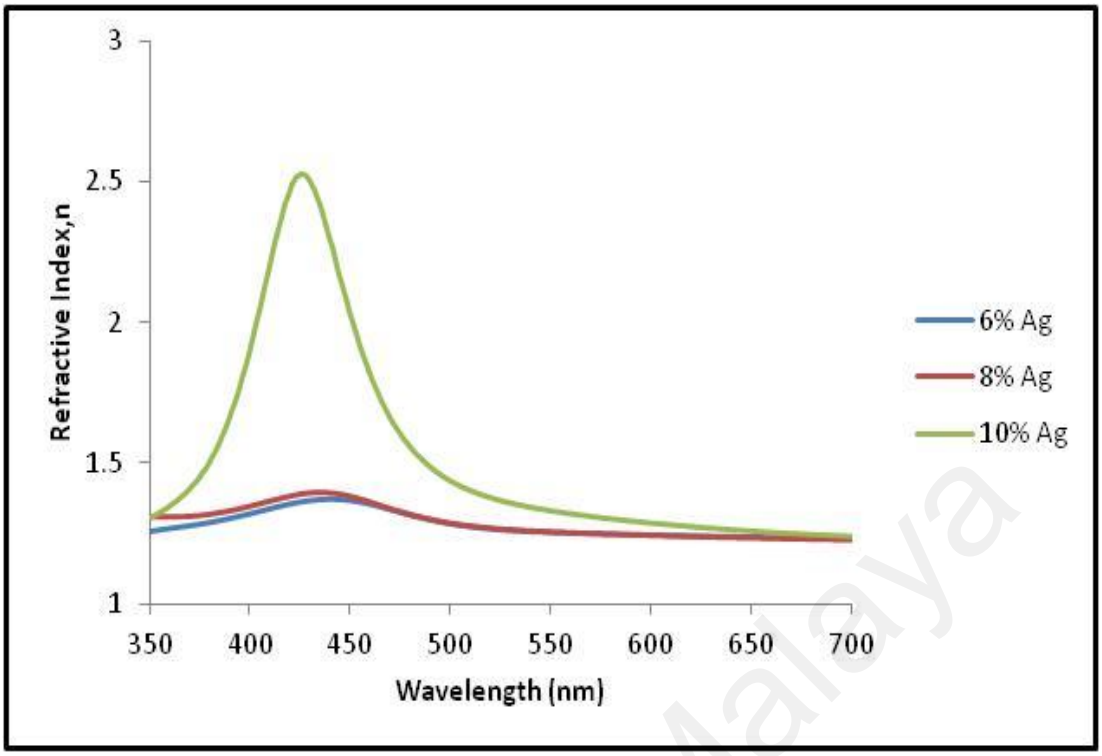

Figure 4.26: Refractive index spectra for different percentage loading of silver nanoparticles at 100 °C

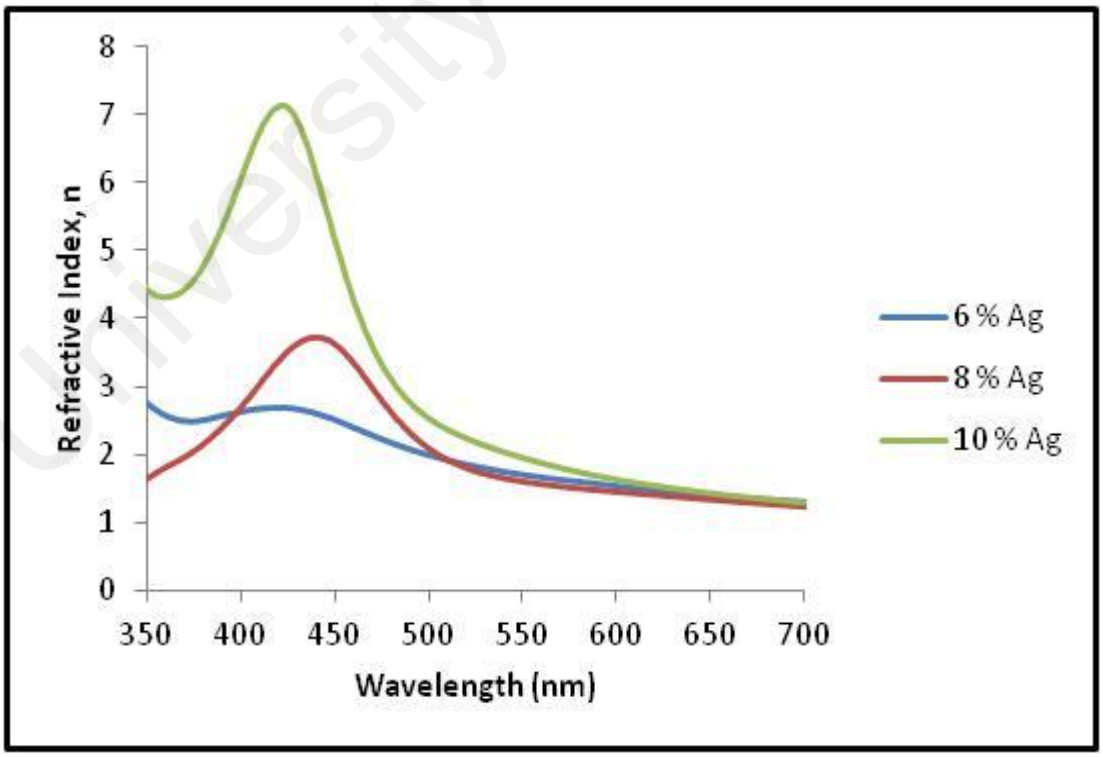

Figure 4.27: Refractive index spectra for different percentage loading of silver nanoparticles at 120 °C

4.5 Dielectric Studies

Figure 4.28 shows the real and imaginary permittivity of Ag/PMMA nanocomposites at higher frequency 1 GHz - 4.5 GHz. It is clearly observed that the dielectric constant (ε') and dielectric loss factor (ε'') are increased with the increase of the percentage loading of silver nanoparticles. The remarkable increase in dielectric constant may be due to the pilling of charges at the extended interface and/or more conducting particles (Lu *et al.*, 2006). However, the dielectric loss is relatively lower than the dielectric constant for the entire frequency. In general, the dielectric loss of the dielectric material results from distortional, dipolar, interfacial, and conduction loss (Lu *et al.*, 2006). It is related to the electronic and ionic polarization mechanism. The interfacial loss originates from the excessive polarized interface induced by the matrix and specifically the movement or rotation of the atoms or molecules in an alternating electric field. The conduction loss is attributed to the dc electrical conductivity of the materials, representing the flow of actual charge through the dielectric material.

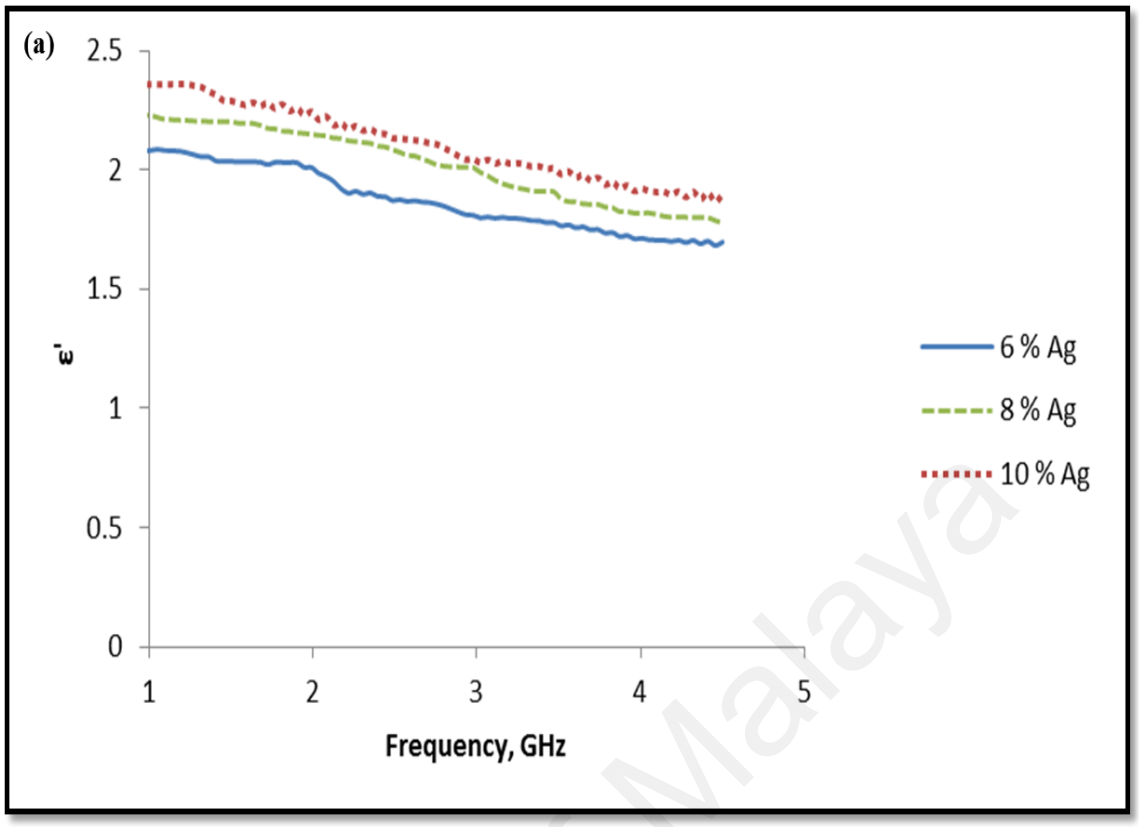

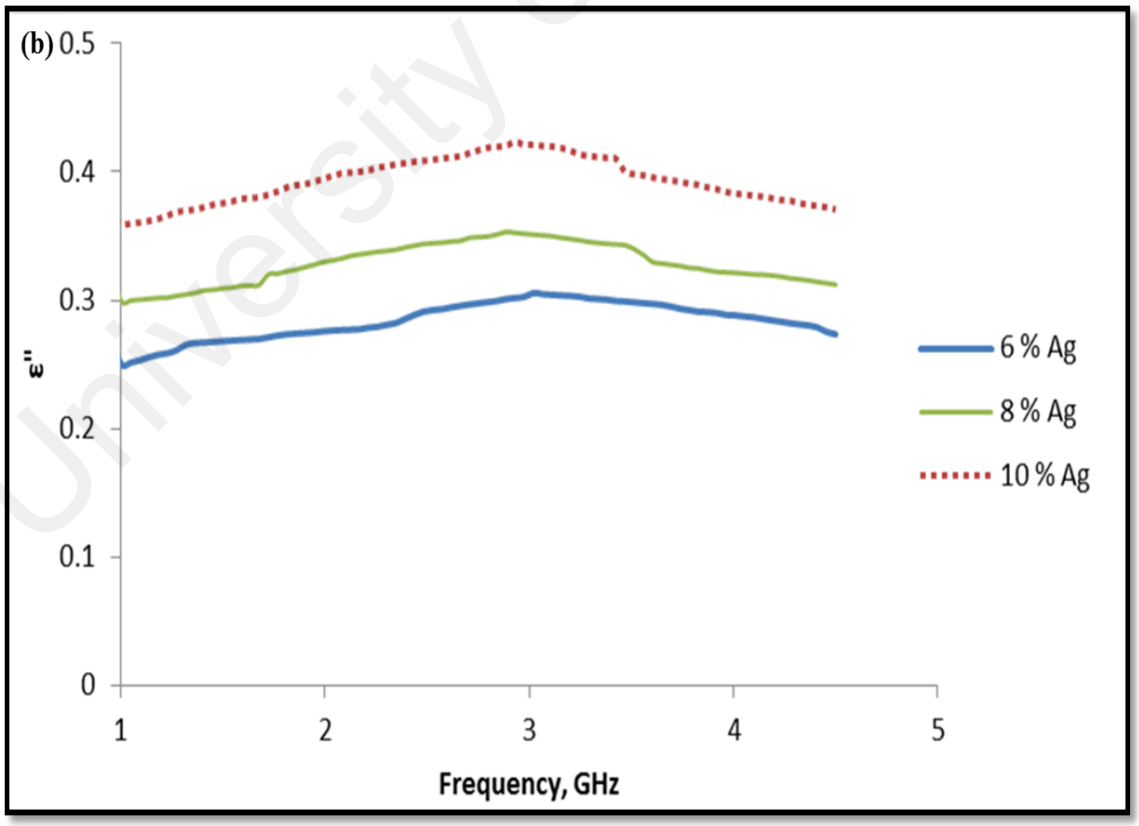

Figure 4.28: Variation in (a) dielectric constant (*ε'*) and (b) dielectric loss factor (*ε''*) of Ag/PMMA nanocomposites at 80 °C

Figure 4.28(b) shows the variation of dielectric loss factor (ε'') with frequency for different percentage loading of silver nanoparticles at 80 °C. It is clear that the dielectric loss slightly increases at the lower frequency and eventually decreases at higher frequency to the relaxation process. Similar behavior was also observed in a number of polymeric materials (El-Shahawy *et al.*, 1994; Ramya *et al.*, 2005). This is the character for polar materials, with high initial value of dialectic loss, but low value at higher frequency due to dipoles (Tareev, 1979) and the polarization effects (Ramesh *et al.*, 2002). The low frequency dispersion region is attributed to the contribution of charge accumulation at the interface. The periodic reversal of the electric field occurs faster at higher frequency. As a result no excess ions diffuse in the direction of the field. Hence, dielectric loss decreases with increasing frequency in all Ag/PMMA nanocomposites samples (Bhargav *et al.*, 2010; Mardare & Rusu, 2004). Furthermore, high value of dielectric loss for higher percentage loading of silver nanoparticles (10 percent) can be understood in terms of electrical conductivity.

Figure 4.29 shows the variation of real dielectric constant, ε' at 10 percent loading of silver nanoparticles at different temperature. The value of dielectric constant increases as the temperature increases reflecting relatively slow long-range motion and attributed to the glass transition caused by dipolar orientation (Tareev, 1979). The process might involve side group motions or conformational change in side group at higher frequency (Kader *et al.*, 1993). The similar trend of ε' was observed at different temperature. ε' is significantly increase at lower frequency and become platonic as the frequency increases. The relaxation process was occurred at higher frequency.

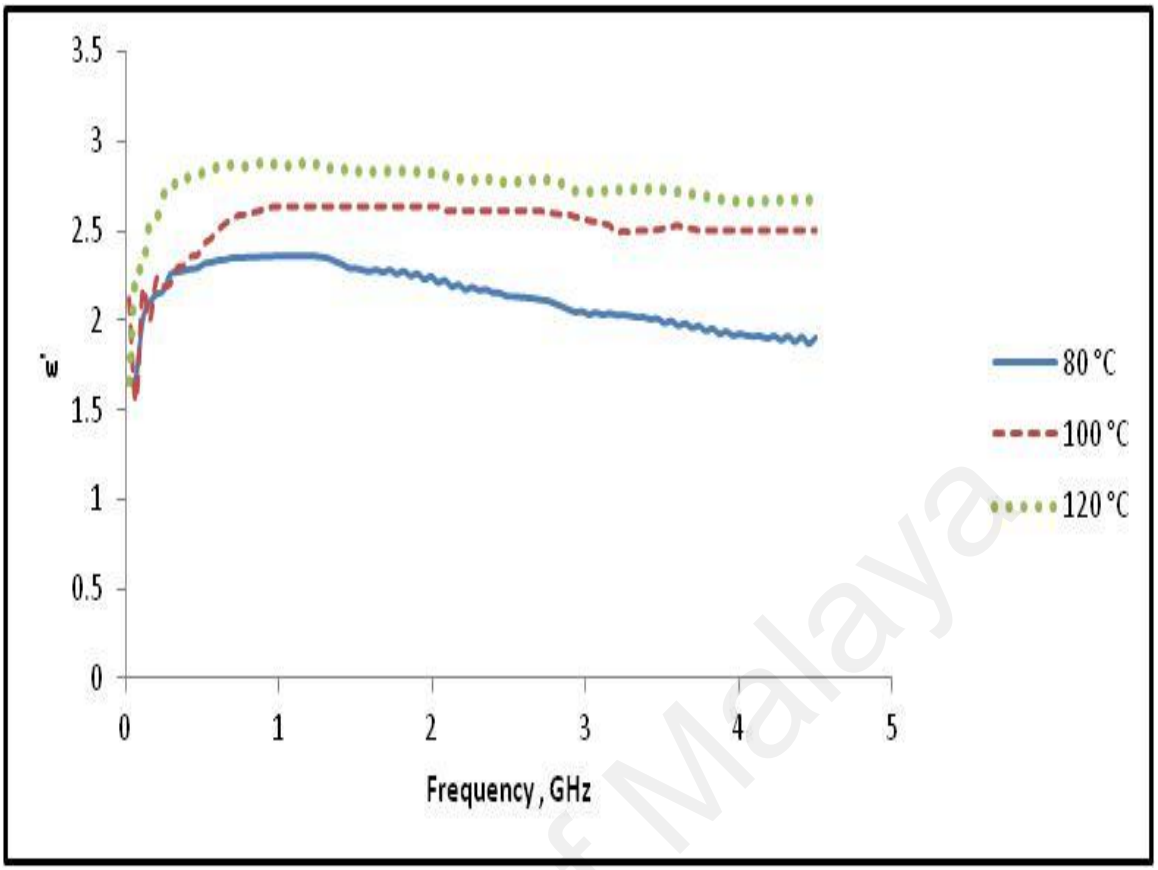

Figure 4.29: Variation in dielectric constant (ε') with frequency for different temperature at 10 percent loading of silver nanoparticles in Ag/PMMA nanocomposites

Figure 4.30 shows the variation of dielectric constant, ε' and dielectric loss factor, ε'' for lower frequency range (50 Hz – 5 MHz). Both dielectric constant and losses are decreases with the increase of frequency. This may be attributed to the tendency of dipoles in polymeric samples to orient themselves in the direction of the applied field. On the other hand, the high value of ε' and ε'' at lower frequency might be due to the particle effect and interfacial effect of the sample (Bhajantri *et al.*, 2007). The sharp decrease relaxation process also as a result of charge accumulation in different inter spaces. These process are attributed to Maxwell-Wagner-Sillars (MWS) interfacial polarization (Hedvig, 1977).

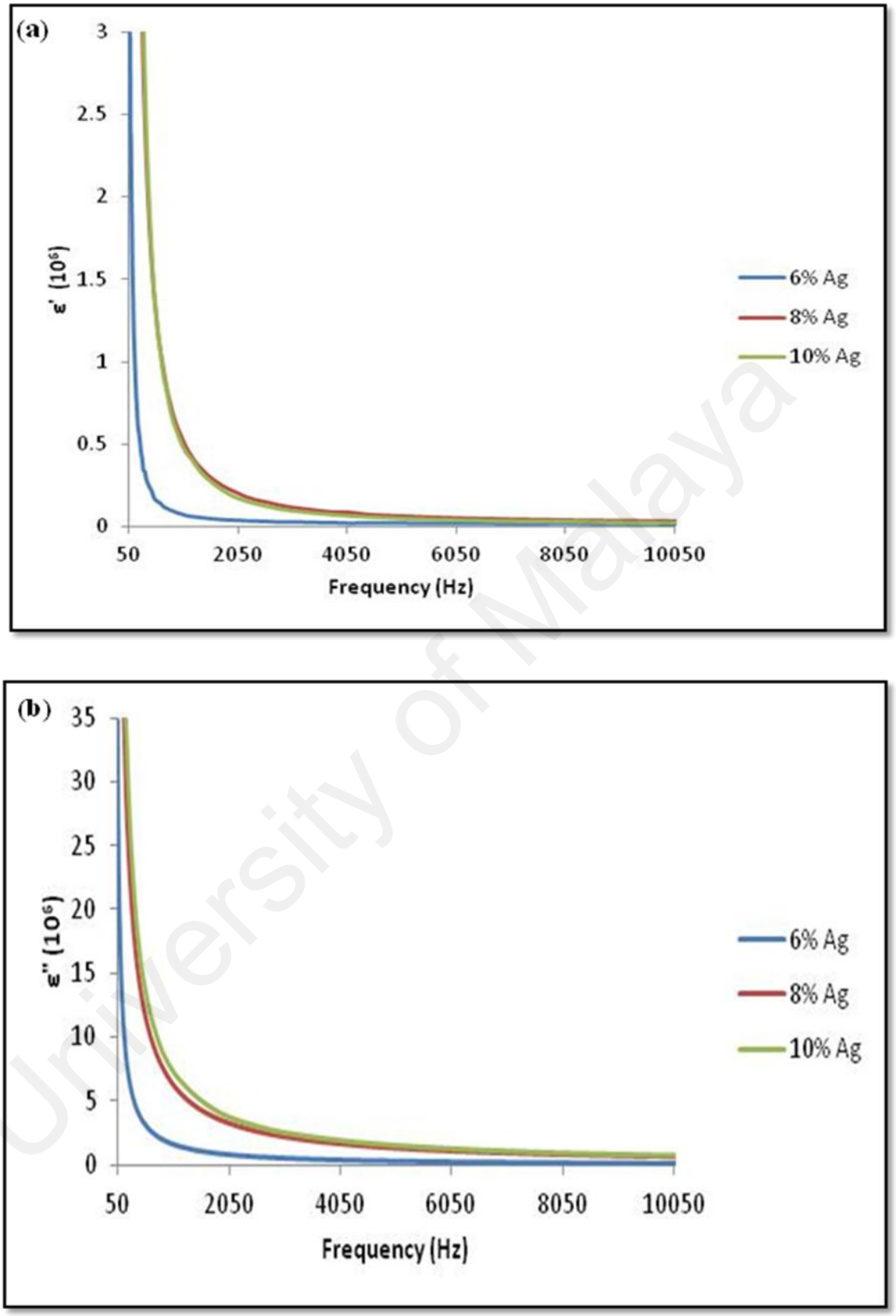

Figure 4.30: Variation in (a) dielectric constant (ε') and (b) dielectric loss (ε'') with frequency for different temperature at 10 percent loading of silver nanoparticles in Ag/PMMA nanocomposites

4.6 Thermal Studies (TGA)

Figures 4.31 – 4.33 show the TGA curves of Ag/PMMA nanocomposites at various percentages loading of silver nanoparticles for different reactant temperature. Figure 4.31 shows the TGA curves of Ag/PMMA nanocomposites at 80 °C. The first-stage decomposition started at about 223, 240 and 253 °C for 6, 8 and 10 percent loading of silver nanoparticles in PMMA. The total weight loss decreases as the percentage loading of silver nanoparticles in PMMA increases as shown in Table 4.3. It is found that Ag/PMMA nanocomposites with 6 percent loading of silver nanoparticles has lower decomposition temperature which however has gone much higher when the percentage loading of silver nanoparticles increased (10 percent loading of silver nanoparticles). Thus, it is understood that the percentage loading of silver nanoparticles enhances the thermal stability of the PMMA.

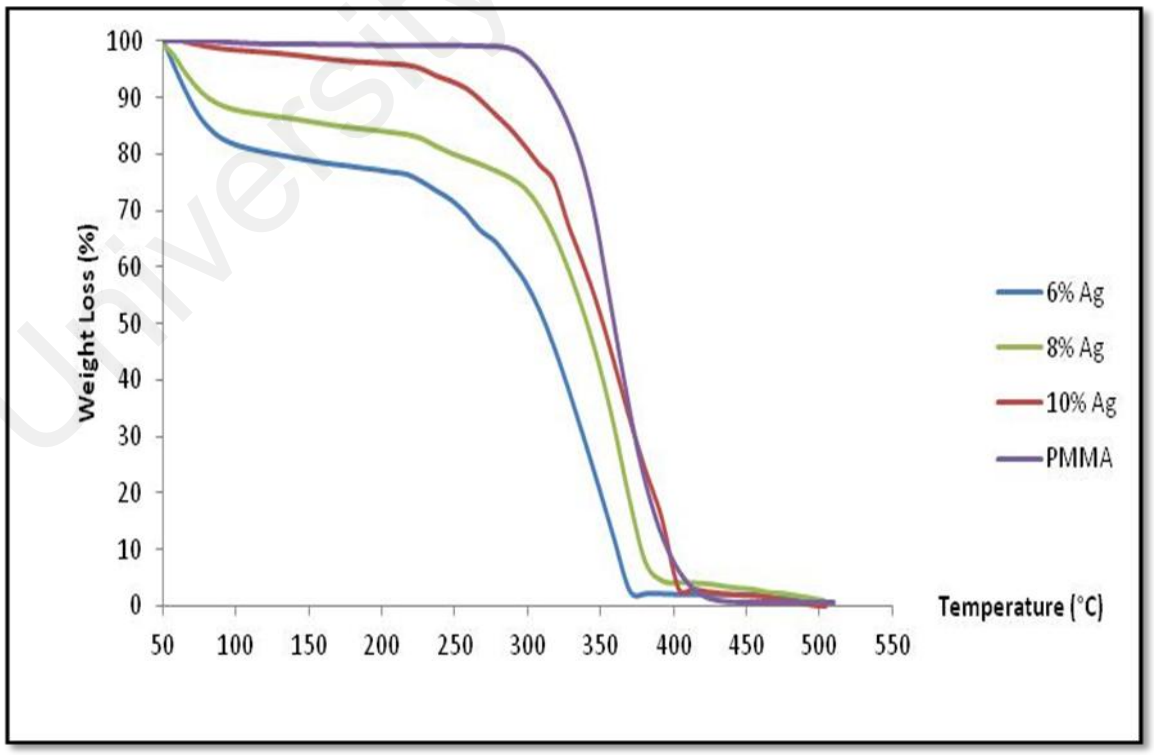

Figure 4.31: TGA curves of Ag/PMMA nanocomposites at various percentages loading of silver nanoparticles at 80 °C

Figure 4.32 shows the TGA curves of Ag/PMMA nanocomposites at 100 °C. The thermal degradation of Ag/PMMA nanocomposites occurs in two stages. The most intense peak occurred around 200 - 450 °C which depends on the percentage loading of silver nanoparticles in the PMMA and reactant temperature. The peaks were corresponds to the depolymerization initiated by random chain scission. The higher percentage loading of silver nanoparticles thus may contain some intermediate Ag^{+}/PMMA type of composites. Singh & Khanna (2007) also reported that the decomposition in PMMA alone started at about 200 ^{o}C but the loading of 2 percent silver showed first-stage decomposition started at 230 ^{o}C and the second-stage started 320 ^{o}C while continues till about 430 ^{o}C. This thermal stability can be ascribed to the fact that the presence of small amount of silver in the polymer matrix confined the motion of polymer chains and served as a nucleation site for enhanced crystallization of nanocomposites (Hsu *et al.*, 2008; Chou *et al.*, 2000).

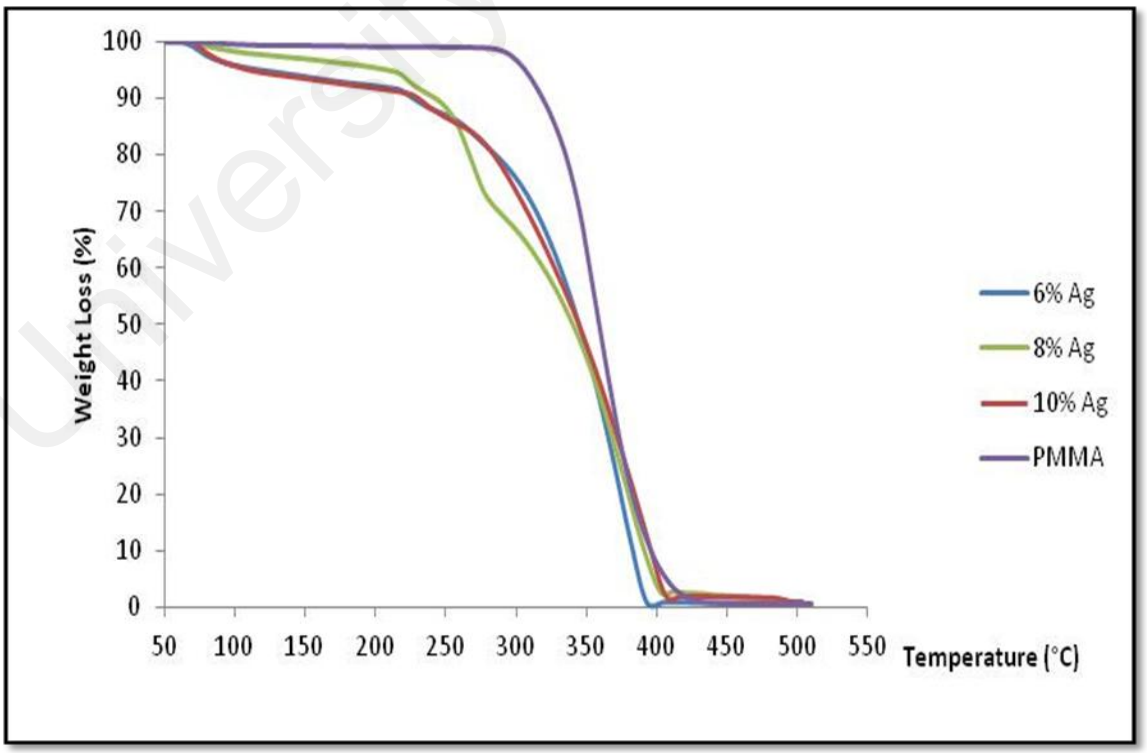

Figure 4.32: TGA curves of Ag/PMMA nanocomposites at various percentages loading of silver nanoparticles at 100 °C

Figure 4.33 shows the highest total weight lost at temperature, 120 °C. The midpoint temperature is shifted toward higher values with an increase of percentage loading of silver nanoparticles in PMMA (Vodnik *et al.*, 2009). The thermal degradation is shifted toward higher temperatures for 27 °C in the the 10 percent loading of silver nanoparticles in PMMA indicating better thermal stability compared with at 6 percent loading of silver nanoparticles. It is evident that the silver nanoparticles could efficiently improve the thermal stability of the composite in high temperature region. The total weight lost percentage increases as the temperature increase. The incorporation of silver nanoparticles shifted the decomposition toward higher temperatures. The observed behavior is most likely a consequence of the inhibiting effects of silver nanoparticles on some degradation stages of the thermo-oxidative degradation of PMMA. Table 4.4 summaries the TGA results for Ag/PMMA nanocomposites. The total weight lost of pure PMMA is much higher than that of Ag/PMMA nanocomposites. The total weight loss decreases rapidly as the percentage loading of silver nanoparticles in PMMA increases.

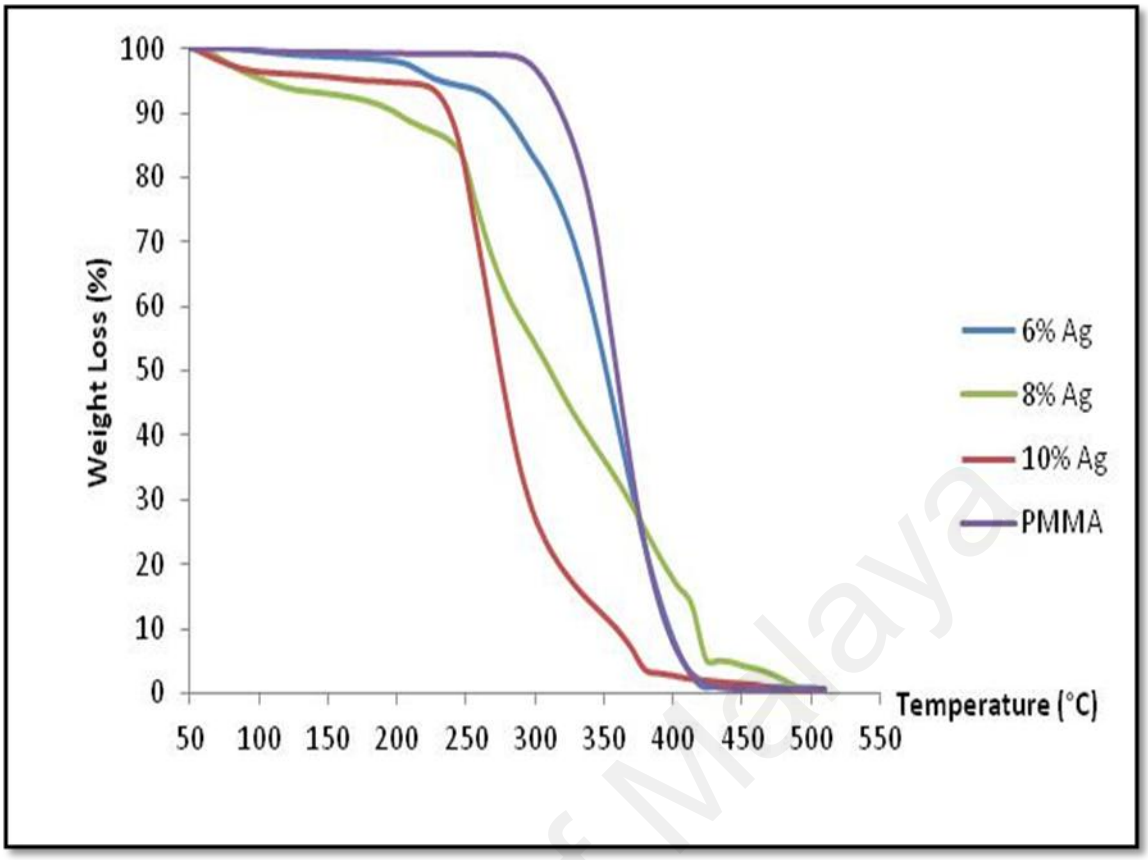

Figure 4.33: TGA curves of Ag/PMMA nanocomposites at various percentages loading of silver nanoparticles at 120 °C

Table 4.4: Thermal and mass properties of Ag/PMMA nanocomposites at various reactants temperature

Samples	Percentage loading of Silver Nanoparticles (%)	Initial Weight Lost (%)	First Decomposition Weight Lost (%)	Total Weight Lost (%)	Decomposition Temperature (°C)	Stability Temperature (°C)
Pure PMMA	-	-	-	97.6	298	430
80 °C	6	20.4	71.4	91.8	223	370
80 °C	8	3.9	76.9	80.8	240	393
80 °C	10	3.7	75.9	79.6	253	409
100 °C	6	0.9	89.7	90.5	208	392
100 °C	8	5.1	84.8	89.8	217	407
100 °C	10	1.9	75.0	76.9	228	405
120 °C	6	0.4	96.3	96.7	200	420
120 °C	8	1.8	89.3	91.1	207	430
120 °C	10	1.7	86.2	87.9	217	396

4.7 Mechanism of Silver/PMMA nanocomposites

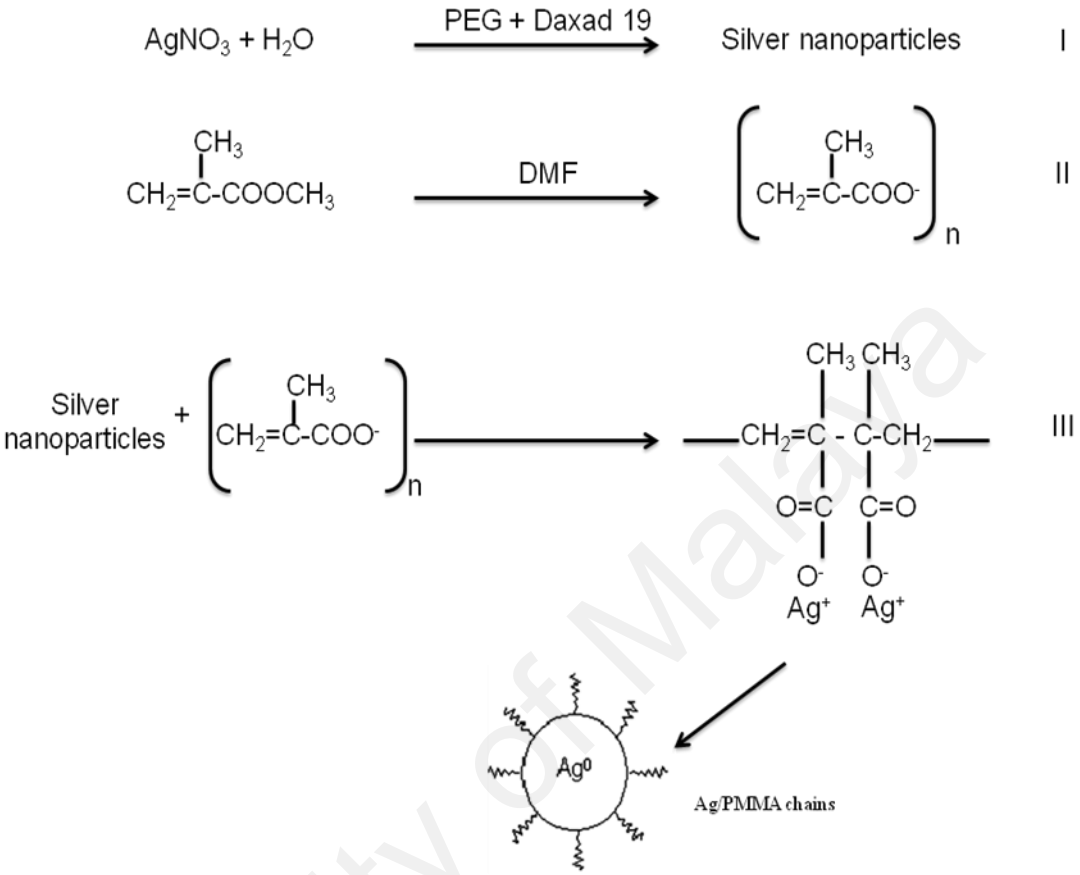

Figure 4.34: Mechanism of Ag/PMMA nanocomposites

Figure 4.34 shows the mechanism of Ag/PMMA nanocomposites. In Step I, $AgNO_3$ was dissolved in water to become Ag^+ and NO_3^-. Then the solutions turn to light brown solution after the addition of PEG and Daxad 19 as the reducing agent and stabilizer. In the Step II, heat was applied to DMF solution at 80, 100 and 120 °C with the presence of methyl methacrylate (MMA). As a result, O-CH_3 bond of methyl methacrylate (MMA) was dissociated, rendering very stable oxygen radical (Kassaee *et al.*, 2011). Silver nanoparticles were then dispersed in the MMA solution and coordinate to the oxygen atoms. This is reasonable suggestion for the acrylate in PMMA because it is reported to be well suited for chemical bonding with the metal ions (Khanna & Subbarao, 2004; Hirai, 1979). Then, the reduction of the dispersed Ag^+ ions by CH_3

gives atomic silver (Ag^{o}) which aggregate to form silver nanoparticles in PMMA. Again, the PMMA constituent prevents precipitation and further aggregation of silver nanoparticles while stabilizes and protects them through its carboxylates functional groups (Step III).

CHAPTER FIVE

CONCLUSIONS AND FUTURE WORK RECOMMENDATIONS

5.1 Conclusions

The method proposed in the present work exhibits superior performances with the smallest mean particle size. Samples subjected to higher percentage loading of silver nanoparticles at 80 °C were found to be the most effective and stable Ag/PMMA nanocomposites. The effective characteristic of Ag/PMMA nanocomposites was related to the availability of more evenly dispersed Ag/PMMA nanocomposites in the matrix, thus giving efficient optical and mechanical properties of Ag/PMMA nanocomposites. Ag/PMMA nanocomposites were prepared by *in-situ* technique. Silver nanoparticles with a moderate size distribution were obtained and were well dispersed in the PMMA matrix at a high concentration. On the other hand, an important advantage of the *in-situ* synthesis is that no additives (e.g. solvent, surface-active agent or metallic ions of reductant) are used. The advantage of the process described in this report is that it is a simple and efficient and that it consists of a one-step synthesis which produces a dispersion of silver nanoparticles in PMMA. To the best of our knowledge, this is first complete study of the use of a dispersion of silver nanoparticles at a high concentration in PMMA as a matrix. TEM and FESEM images of Ag/PMMA nanocomposites showed that an optimum size and uniform distribution of particles size at 80 °C with 10 percent loading of silver nanoparticles. The size and distribution of Ag/PMMA nanocomposites depends on the temperature, percentage loading of silver nanoparticles and the amount of PMMA used as the capping agent. DLS data shows the particle size decreases gradually with the increasing of $AgNO_3$ content and PMMA. The zeta

potential shows the maximum negative potentials occured at 80 °C for 10 percent loading of silver nanoparticles. This is the most stable condition for Ag/PMMA nanocomposites. FTIR spectra show the complexation of Ag/PMMA nanocomposites. Raman spectra show the decreases of intensity as the percentage loading of silver nanoparticles increases due to the reduction of lattice vibration. The UV-Vis absorption spectra are blue shifted with the increase of percentage loading of silver nanoparticles. On the other hand, the absorption spectra are red shifted when the temperature increases. This indicate that the increase of particle size of Ag/PMMA nanocomposites continuously to growth at higher temperature. The results for synthesis Ag/PMMA nanocomposites are in good agreement with the results of Narendra & Khanna (2007). The dielectric constant, ε' and dielectric loss factor, ε'' increase with the increase of reactant temperature and percentage loading of silver nanoparticles. ε' significantly increases at lower frequency and decreases as the frequency increases. This indicates that the dipole orientation occurred at lower frequency and become relaxed at higher frequency. It is evident that the silver nanoparticles could efficiently improve the thermal stability of the composite in high temperature region from 275 to 450 °C. Thermal analysis showed that with an increase in the percentage loading of silver nanoparticles from 6 percent to 10 percent, there is enhancement in the thermal stability of the PMMA.

5.2 Future Recommendations

In order for the results reported in this study to be implemented in real industrial applications, they must be extended and improved in further research. The attempt is to develop stabilizing agents that produce more stable silver nanoparticles that can be used as a main source in producing Ag/PMMA nanocomposites. For example, using chloroform as the stabilizer. The optimization conditions may be considered to be achieved when the key factor which controls the reaction process can be highlighted.

The effect of percentage loading of silver nanoparticles, reactant temperature, duration time and heat treatment on the growth of Ag/PMMA nanocomposites with size lesser than 24 nm and narrow particle distribution in the PMMA matrix may be further investigated via *in-situ* technique. The antibacterial studies showed that the prepared Ag/PMMA nanocomposites have antibacterial effect against E. coli, which render medical applications.

More research has to be done on the synthesized of Ag/PMMA nanocomposites based on environmentally friendly materials which are the main concern in the present world. Comprehensive studies may be implemented to estimate the best growth size of silver nanoparticles in composite matrix to get the optimum properties of nanocomposites.

REFERENCES

Abdel-Kader, M. M., El-Kabbany, F., Sayyah, S. M., Nasser, S. A., & El-Kalla, E. H. (1993). Effect of γ-radiation on the dielectric constant of poly (methyl methacrylate) modified by β-naphthol. *Journal of Materials Science Letters*, 12, 329-331.

Ahmad, A., Mukherjee, P., Senapati, S., Mandal, D., Khan, M. I., Kumar, R., & Sastry, M. (2003). Extracellular biosynthesis of silver nanoparticles using the fungus Fusarium oxysporum. *Colloids and Surfaces B: Biointerfaces*, 28, 313–318.

Ajayan, P. M., & Banhart, F. (2004). Nanotubes: Strong bundles. *Nature materials*, 3, 135.

Ajayan, P. M., James, M., & Tour, M. (2007). Nanotube Composites. *Nature*, 447, 1066.

Akamatsu, K., Takei, S., Mizuhata, M., Kajinami, A., Deki, S., Takeoka, S., Fujii, M., Hayashi, S., & Yamamoto, K. (2000). Preparation and characterization of polymer thin films containing silver and silver sulfide nanoparticles. *Thin Solid Film*, 359, 55.

Akamatsu, K., Tsuboi, N., Hatakenaka, Y., & Deki, S. (2000). In situ spectroscopic and microscopic study on dispersion of Ag nanoparticles in polymer thin films. *Journal Physics Chemistry B*, 104, 10168.

Akhavan, A., Sheikh, N., & Beteshobabrud, R. (2010). Polymethylmethacrylate/Silver Nanocomposite Prepared by γ-Ray. *Journal of Nuclear Science and Technology*, 50, 80-84.

Alan, C. J., & Albrecht, M. G. (1977). Anomalously intense Raman spectra of pyridine at a silver electrode. *Journal of American Chemical Society*, 99, 5215–5217.

Amulyavichus, A., Daugvila, A., Behm, R. J., & Brotz, P. (1998). Study of chemical composition of anostructural materials prepared by laser cutting of metals. *Fizika Metallov I Metallovedenie*, 85, 111.

An, J., Tang, B., Ning, X., Zhou, J., Xu, S., Zhao, B., Xu, W., Corredor, C., & Lombardi, J. R. (2007). Photoinduced Shape Evolution: From Triangular to Hexagonal Silver Nanoplates. *Journal Physics Chemistry C*, 111, 18055–18059.

Ash, B. J., Schadler, L. S., & Siegel, R. W. (2002). Glass transition behavior of alumina/ polymethylmethacrylate nanocomposites. *Materials Letter*, 55, 83-87.

Ash, B. J., Stone, J., Rogers, D. F., Schadler, L. S., Siegel, R. W., Benicewicz, B. C., & Apple, T. (2000). Investigation into the Thermal and Mechanical Behavior of PMMA/Alumina Nanocomposites. *Materials Research Society Symposium Proceeding*, 661.

Balberg, I., Azulay, D., Toker, D., & Millo, O. (2004). Percolation and Tunnelling in composite Materials. *International Journal of Modern Physics: B*, 18, 2091-2191.

Bazarov, V. V., Petuhhov, V. Y., Zhikharev, V. A., & Khaibullin, I. B. (1995). Conductivity of the Granular Metal Films Obtained by High Dose Ion Implantation into PMMA. *Materials Research Society Symposium Proceeding*, 388, 417.

Berciaud, S., Cognet, L., Tamarat, P., & Lounis, B. (2005). Observation of Intrinsic Size Effects in the Optical Response of Individual Gold Nanoparticles. *Nano Letter*, 5, 515.

Bhajantri, R. F., Ravindrachary, V., Harisha, A., Ranganathaiah, C., & Kumar-aswamy, G. N. (2007). Effect of barium chloride doping on PVA microstructure: positron annihilation study. *Appied Physics A*, 87, 797–805.

Bhargav, P. B., Sarada, B. A., Sharma, A. K., Rao, V. V. R. N. (2010). Electrical conduction and dielectric relaxation phenomena of PVA based polymer electrolyte films. *Journal of Macromolecular Science, Part A: Pure and Applied Chemistry*, 46, 131.

Biswas, A., Eilers, H., Hidden, R., Aktas, O. C., & Kiran, C. V. S. (2006). Large broadband visible to infrared plasmonic absorption from Ag nanoparticles with a fractal structure embedded in a Teflon AF (R) matrix. *Applied Physics Letter,* 88, 013103.

Blackborrow, J. R. & Young, D. (1979). Metal vapour synthesis. Springer-Verlag, New York.

Bradley, J. S. (1994). Clusters and Colloids (G. Schmid, Ed.). VCH, Weinheim, 477.

Brenier, R. (2012). Enhancement of Light Transmission through Silver Nanoparticles. *Journal of Physical Chemistry C*, 119, 5358-5366.

Brydoson, J. A. (1995). British Plastics and Rubber. *Plastics materials*, 6th Edition, pp. 385-391.

Callegari, A., Tonti, D., & Chergui, M. (2003). Photochemically Grown Silver Nanoparticles with Wavelength-Controlled Size and Shape. *Nano Letter*, 3, 1611.

Cao, G. Z. (2004). Nanostructures and Nanomaterials, Synthesis, Properties and Applications. Imperial College Press, London, UK.

Carotenuto, G., Nicolais, L., Mortorana, B., & Perlo, P. (2004). *Metal–Polymer Nanocomposites*. New Jersey: Wiley.

Caruso, F. (2001). Nanoengineering of Particle Surfaces. *Advanced Materials*, 13, 11–22.

Caseri, W. (2000). Nanocomposites of polymers and metals or semiconductors: Historical background and optical properties. *Macromolecule Rapid Communication*, 21,705.

Che Lah, N. A., & Johan, M. R. (2011). Facile shape control synthesis and optical properties of silver nanoparticles stabilized by Daxad 19 surfactant. *Applied Surface Science*, 257, 7494–7500.

Chen, A., Kamata, K., Nakagawa, M., Iyoda, T., Wang, H., & Li, X. (2005). Formation process of silver-polypyrrole coaxial nanocables synthesized by redox reaction between AgNO3 and pyrrole in the presence of poly(vinylpyrrolidone). *Journal Physics Chemistry B*, 109, 18283.

Chen, C. W., Chen, M. Q., Serizawa, T., & Akashi, M. (1998). In-Situ Formation of Silver Nanoparticles on Poly(N-isopropylacrylamide)-Coated Polystyrene Microspheres. *Advanced Materials,* 10, 1122.

Chen, C. W., Serizawa, T., & Akashi, M. (1999). Preparation of Platinum Colloids on Polystyrene Nanospheres and Their Catalytic Properties in Hydrogenation, *Chemistry of Materials,* 11, 1381.

Chen, S., Fan, Z., & Carroll, D. L. (2002). Silver Nanodisks: Synthesis, Characterization, and Self-Assembly. *Journal Physics Chemistry B,* 106, 10777.

Chen, Z. T., & Gao, L. (2007). A facile and novel way for the synthesis of early monodisperse silver nanoparticles. *Materials Research Bulletin*, 42, 1657–1661.

Chimentao, R., Kirm, I., Medina, F., Rodríguez, X., Cesteros, Y., Salagre, P., & Sueiras, J. (2004). Different morphologies of silver nanoparticles as catalysts for the selective oxidation of styrene in the gas phase. *Chemical Communications*, 846-847.

Choi, Y. M., Compson, C., Lin, M. C. & Liu, M. (2007), Ab initio Analysis of Sulfur Tolerance of Ni, Cu, and Ni—Cu Alloys for Solid Oxide Fuel Cells. *Journal of Alloys and Compounds, 427, 25-29.*

Chou, K. S., & Ren, C. H. (2000). Synthesis of nanosized silver particles by chemical reduction method. *Materials Chemistry and Physics,* 64, 241-246.

Chowdhury, J., & Ghosh, M. (2004). Concentration-dependent surface-enhanced Raman scattering of 2-benzoylpyridine adsorbed on colloidal silver particles. *Journal Colloid Interface Sciences,* 277, 1, 121.

Creighton, J. A., Blatchford, C. G., & Albrecht, M. G. (1979). Plasma resonance enhancement of Raman scattering by pyridine adsorbed on silver or gold sol particles of size comparable to the excitation wavelength, *Journal of the Chemical Society, Faraday Transaction 2: Molecular and Transaction Physics*, 75, 790–798.

Dagani, R. (1999). Putting the nano finger on atoms. *Chemical and Engineering News*, 77, 54.

Deng, Y., Sun, Y., Wang, P., Zhang, D., Ming, H., & Zhang, Q. (2008). In situ synthesis and nonlinear optical properties of Ag nanocomposite polymer films. *Physica E: Low-dimensional Systems and Nanostructures*, 40, 911-914.

Deng, Y., Wang, P., Sun, Y. Y., Ming, H., Zhang, Qi, J., Jiao, Y., & Sun, X, Q., (2006). Nonlinear optical properties of Ag/PMMA nanocomposites polymer film. *IEEE Conference Publication,* 373-376.

Dirix, Y., Bastiaansen, C., Caseri, W., & Smith P. (1999). Preparation, structure and properties of uniaxially oriented polyethylene-silver nanocomposites. *Journal of Materials Sciences, 34*, 3859-3866.

Dougherty, G. M., Rose, K. A., Tok, J. B. H., Pannu, S. S., Chuang, F. Y. S., Sha, M. Y., Chakarova, G., & Penn, S. G. (2007). The zeta potential of surface functionalized metallic nanorod particles in aqueous solution. *Electrophoresis*, 29, 1131-1139.

Edelstein, A. S., Murday, J. S., & B.B. Rath, B. B. (1997). Challenges in nanomaterials design. *Progress in Materials Sciences*, 42, 5–21.

Eickmans, J., Leenders, L., Lamotte, J., Dierksen, K., & Jacobsen, W. (1997). Dry Phototool in the Production of Printed Circuit Boards. *Circuit World*, 22, 26.

El-Sayed, M. A. (2001). Some interesting properties of metals confined in time and nanometer space of different shapes. *Accounts of Materials Research*, 34, 257.

El-Shahawy, M. A. & Elkholy, M. M. (1994). Dielectric-Properties Of Cobalt-Doped Poly(Vinyl Alcohol). *European Polymer Journal*, 30, 259-263.

Erschov, B.G., & Henglein, A. (1998). A. Reduction of Ag^+ on polyacrylate chains in aqueous solution. *Journal Physics Chemistry B*, 102, 10667.

Ershov B. G., Janata, E., Henglein, A., & Fojtik, A. (1993). Silver atoms and clusters in aqueous solution: absorption spectra and the particle growth in the absence of stabilizing Ag^+ ions. *Journal Physics Chemistry*, 97, 4589–4594.

Ershov, B. G., & Henglein, A. (1998). Reduction of Ag^+ on polyacrylate chains in aqueous solution. *Journal of Physical Chemistry B*, 102, 10663-10666.

Firth, A. V., Haggata, S. W., Khanna, P. K., Williams, S. J., Allen, J. W., Magennis, S. W., Samuel, I. D. W., & Cole-Hamilton, D. J. (2004). Production and luminescent properties of CdSe and CdS nanoparticle-polymer composites. *Journal of Luminescence*, 109, 163-172.

Frangala, M. E., Compagnini, G., Malandrino, G., Soinella, C., &Puglisi, O. (1999). Silver nanoparticles dispersed in polyimide thin film matrix. *The European Physical Journal D*, 9, 631.

Fukuda, S., Kawamoto, S., & Gotoh Y. (2003). Degradation of Ag and Ag-alloy mirrors sputtered on poly(ethylene terephthalate) substrates under visible light irradiation, *Thin Solid Films*, 442,1–2,117–120.

Fuyuki, T., & Matsunmi, H. (1986). Electronic Properties of the Interface between Si and TiO2 Deposited at Very Low Temperatures. *Journal Applied. Physics*, 25, 1288–1291.

Gaffet, E., Tachikart, M., Kedim, O. E. I., & Rahouadj, R. (1996). Nanostructural materials formation by mechanical alloying: Morphologic analysis based on transmission and scanning electron microscopic observations. *Materials Characterization*, 36, 185.

Gangopadhyay, R., & Amitabha, D. (2000). Conducting polymer nanocomposites: a brief overview. *Chemistry Materials*, 12, 608.

Garcia Cerda, L. A., Romo Mendova, L.E., & Quevedo-Lopez, M. A. (2009). Synthesis and characterization of NiO nanoparticles and their PMMA nanocomposites obtained by in situ bulk polymerization, *Journal Materials Sciences*, 44, 4553.

Ghosh, K., & Maiti, S. N. (1996). Mechanical properties of silver-powder-filled polypropylene composites. *Journal Applied Polymer Science*, 60, 323.

Gleick, J. (1992). The Life and Times of Richard Feynmann. New York: Panteon.

Gleiter, H. (1989). Nanocrystalline materials. *Progress Materials Sciences*, 33, 223.

Gleiter, H. (2000). Nanostructured materials: basic concepts and microstructure. *Acta Materials*, 48, 1–29.

Godovsky, D. Y. (2000). Applications of Polymer-Nanocomposites. *Advances in Polymer science*, 153,165-205.

Gosh, S. K & Pal, P. (2007). Interparticle Coupling Effect on the Surface Plasmon Resonance of Gold Nanoparticles: From Theory to Applications. *Chemical Reviews,* 107, 4797−4862

Gotoh, Y., Igarashi, R., Ohkoshi, Y., Nagura, M., Akamatsu, K., & Deki, S. (2000). Preparation and structure of copper nanoparticle/poly(acrylicacid) composite films. *Journal Materials Chemistry,* 10, 2548.

Graf, C., Vossen, D. L. J., Imhof, A., & Blaaderen, A. V. (2003). A General Method to Coat Colloidal Particles with Silica. *Langmuir*, 19, 6693.

Gutierrez, M., & Henglein, A. (1993). Formation of colloidal silver by "pushpull" reduction of silver (1^{+}). *Journal Physics Chemistry*, 97, 11368.

Guzman, M. G., Dille, J., & Godet, S. (2008). Synthesis of silver nanoparticles by chemical reduction method and their antibacterial activity. *World Academy of Science, Engineering and Technology*, 43, 357–364.

Hahn H. (1997). Unique Features and Properties of Nanostructured Materials. *Nanostructured Materials*, 9, 3.

Hamilton, J. F., & Baetzold, R. C. (1979). Catalysis by small metal clusters. *Science*, 205, 1213.

Hao, E., Kelly, K. L., Hupp, J. T., & Schats, G. C. (2002). Synthesis of Silver Nanodisks Using Polystyrene Mesospheres as Templates. *Journal of American Chemical Society*, 124, 15182.

Hatchett, D. W., Josowicz, M., Janata, J., & Baer, D. R. (1999). Electrochemical formation of Au clusters in polyaniline. *Chemistry Materials*, 11, 2989.

He, B., Li, Y., Feng, X. and Zhang, G. (2004). Inorganic/Organic Salts as Heterogeneous Basic Catalysts for Cyanosilylation of Carbonyl Compounds. ChemInform, 35: no. doi: 10.1002/chin.200452073.

He, S., Yao, J., Jiang, P., Shi, D., Zhang, H., Xie, S., Pang, S., & Gao, H. (2001). Formation of silver nanoparticles and self-assembled two-dimensional ordered superlattice. *Langmuir*, 17, 1571.

Hedvig, P. (1977). Dielectric Spectroscopy in Polymers. Bristol: Adam Hilger.

Heilmann, A., Quinten, M., & Werner, J. (1998). Optical response of thin plasma-polymer films with non-spherical silver nanoparticles. *The European Physical Journal B*, 3, 455.

Henglein, A. (1989). Small-particle research: physicochemical properties of extremely small colloidal metal and semiconductor particles. *Chemical Reviews,* 89, 1861-1864.

Herrero, J., & Guillén, C. (2002). Transparent films on polymers for photovoltaic applications, *Vacuum*, 67, 3–4, 611–616.

Hirai, H. (1979). Formation and Catalytic Functionality of Synthetic Polymer-Noble Metal Colloid. *Journal of Macromolecular Science: Part A – Chemistry*, 13, 633.

Hsu, S. L., & Wu, R. T. (2008). Preparation of highly concentrated and stable suspensions of silver nanoparticles by an organic base catalyzed reduction reaction, *Materials Research Bulletin*, 43, 1276–1281.

Hu, M. Z., & Easterly, C. E. (2009). A novel thermal electrochemical synthesis method for production of stable colloids of "naked" metal (Ag) nanocrystals. *Materials Science Engineering C*, 29, 726–736.

Huang, C. J., Yen, C. C., Chang, T. C. (1991). Studies on the Preapration and Properties of Conductive Polymer. *Journal Applied Polymer Science*, 42, 2237.

Hutter, E., & Fendler, J. H. (2004). Exploitation of localized Surface Plasmon Resonance. *Advance Materials*, 1685, 16.

Jackson, J. B., & Halas, N.J. (2001). Surface-enhanced Raman scattering on tunable plasmonic nanoparticle substrates. *Journal Physics Chemistry B*, 105, 2743.

Jellinek, H. H. T. (1955). Degradation of Vinyl Polymers. New York: Academic Press.

Jenkins, R., & Snyder, R. L. (1996). Introduction to X-Ray Powder Diffractometry. New York: Wiley.

Jian, Z., Xian, Z., & Yong, Chang, W. (2005). Electrochemical synthesis and fluorescence spectrum properties of silver nanospheres. *Microelectronic Engineering*, 77, 58–62.

Jiang, H., Moon, K. S. & Wong, C. P. (2005). Synthesis of Ag-Cu alloy nanoparticles for lead-free interconnects materials. *Advanced Packaging Materials: Processes, Properties and Interfaces* (pp. 173-177).

Jin, R. C., Cao, Y. W., Mirkin, C. A., Kelly, K. L., Schatz, G. C., & Zheng, J. G. (2001). Photoinduced conversion of silver nanospheres to nanoprisms. *Science*, 294, 1901-1903.

Jung, Y. S. (2004). Study on texture evolution and properties of silver thin films prepared by sputtering deposition. *Applied Surface Science*, 221, 281-287.

Kamat, P. V. (2002). Photophysical, Photochemical and Photocatalytic Aspects of Metal Nanoparticles. *Journal Physic Chemistry B*, 106, 7729.

Kamat, P. V., Flumiani, M., & Hartland, G.V. (1998). Picosecond dynamics of silver nanoclusters. *Journal of Physical Chemistry B*, 102, 3123–3128.

Kashiwagi, T., Hirata, T., & Brown, J. E. (1985). Thermal and oxidative degradation of poly(methyl methacrylate) molecular weight. *Macromolecules*, 18,131.

Kassaee, M. Z., Mohammadkhani, M., Akhavan, A., & Mohammadi, R. (2011). In situ formation of silver nanoparticles in PMMA via reduction of silver ions by butylated hydroxytoluene. *Structural Chemistry*, 22, 11-15.

Kesuma, H. H., Sidin, M. K., & Ibrahim, Z. (2009). Optical Properties of Ti:Al2O3 Single Crystal. *Journal Fizik UTM*, 4, 42-49.

Khanna, P. K., & Singh, N. (2007). *In-situ* synthesis of silver nano-particles in polymethimethacrylate. *Materials Chemistry and Physics*, 104, 367.

Khanna, P. K., & Subbarao, V. V. V. S. (2004). Synthesis of fine CdS powder from direct in-situ reduction of sulphur and cadmium salts in aqueous N, N′-dimethylformamide. *Materials Letters*, 58, 2801-2804.

Khanna, P. K., Singh, N., Charan, S., Subbarao, V. V. V .S., Gokhale, R. & Mulik, U. P. (2005). Synthesis and characterization of Ag/PVA nanocomposite by chemical reduction method. *Journal Materials Chemistry Physics*, 93,117-121.

Khaydarov, R. A., Khaydarov, R. R., Gapurova, O., Estrin, Y., & Scheper, T. (2009). Electrochemical method for the synthesis of silver nanoparticles. *Journal of Nanoparticles Research*, 11, 1193–1200.

Khomutov, G., & Gubin, S. (2002). Interfacial synthesis of noble metal nanoparticles. *Materials Science Engineering C*, 22, 141.

Kickelbick, G. (2003). Concepts for the Incorporation of Inorganic Building Blocks into Organic Polymers on a Nanaoscale. *Progress in Polymer Science*, 28, 83-114.

Kim, D., Jeong, S., & Moon. (2006). Synthesis of silver nanoparticles using the polyol process and the influence of precursor injection. *Nanotechnology*, 17, 4019.

Kim, H. S., Ryu, J. H., Jose, B., Lee, B. G., Ahn, B. S., & Kang, Y. S. (2001). Formation of Silver Nanoparticles Induced by Poly(2,6-dimethyl-1,4-phenylene oxide). *Langmuir*, 17, 5817–5820.

Klabunde, K. J. & Trivino, G. C. C. (1994). Active Metals. Weinheim: VCH.

Klabunde, K. J. (1980). Free atoms and particles. New York: Academic Press.

Klabunde, K. J., Li, Y. X., & Tan, B. J. (1991). Solvated metal atom dispersed catalysts. *Chemistry of materials*, 3, 30-39.

Kossyrev, P. A., Yin, A., Cloutier,S. G., Cardimona, D. A., Huang, D., Alsing, P. M., & Xu, J. M. (2005). Electric field tuning of plasmonic response of nanodot array in liquid crystal matrix. *Nano Letter*, 5, 1978.

Kumar, R.V., Mastai, Y., Diamint, Y., & Gedenken, A. (2001). Sonochemical synthesis of amorphous Cu and nanocrystalline Cu_2O embedded in a polyaniline matrix. *Journal Materials Chemistry*, 165, 127.

Kumar. R. V., Elgamiel, R., Diamant, Y., & Gedanken, A. (2001). Sonochemical synthesis and characterization of nancrystalline copper oxide embedded in polyvinyl alcohol and its effect on control crystal growth of copper oxide. *Langmuir*, 17, 1406.

Kunza, M. S., Shull, K. R., & Kellock, A. (1993). Colloidal Gold Dispersions in Polymeric Matrices. *Journal Colloid Interface Science*, 156, 240.

Le, K. P., Lehman, R. L., Mann, A. B., & Idol, J. D. (2006). Raman Characterization in Blends of Poly(L-lactide) and Poly(methyl methacrylate), *Journal Biomaterials Science Polymer*, 17, 121.

Lee, K. J., Lee, Y., Shim, I., Jun, B. H., Cho, H. J., & Joung, J. (2007). Large-scale synthesis of polymer-stabilized silver nanoparticles. *Solid State Phenomena*, 124, 1189–1192.

Lee, P. C., & Meisel, D. (1982). Adsorption and Surface Enhanced Raman of Dyes on Silver and Gold Sols. *Journal Physics Chemistry*, 86, 3391.

Li, X., Lenhart, J. J., & Walker, H. W. (2010). Dissolution-Accompanied Aggregation Kinetics of Silver Nanoparticles. *Langmuir*, 26, 16690-16698.

Lim, M. H., & Ast, D. G. (2001). Free-Standing Thin Films Containing Hexagonally Organized Silver Nanocrystals in a Polymer Matrix. *Advance Materials*, 13, 718.

Lim, P. Y., Liu, R. S., She, P. L., Hung, C. F., & Shih, H. C. (2006). Synthesis of Ag nanospheres particles in ethylene glycol by electrochemical-assisted polyol process. *Chemical Physical Letters*, 420, 304-308.

Liu, H., Ge, X., Ni, Y., Ye. Q., Zhang, Z. (2001). Synthesis and characterization of polyacrylonitrile–silver nanocomposites by γ-irradiation Radiat. *Physics Chemistry*, 61, 89.

Liu, S., Huang, W., Chen, S., Avivi, S., & Gedanken, A. (2001). Synthesis of X-ray amorphous silver nanoparticles by the pulse sonoelectrochemical method. *Journal Non-Crystalline Solids*, 283, 231–236.

Longenberger, L., & Mills, G. (1995). Formation of Metal Particles in Aqueous Solutions by Reactions of Metal Complexes with Polymers. Journal *Physical Chemistry*, 99, 475–478.

Lu, J., Moon, K., Xu, J., & C. P. Wong. (2006). Synthesis and dielectric properties of novel high-K polymer composites containing in-situ formed silver nanoparticles for embedded capacitor applications. *Journal Materials Chemistry*, 16, 1543-1548.

Luechinger, N. A., Booth, N., Heness. G., Bandyopadhyay, S., Grass, R. N., & Stark, W. J. (2008). Surfactant free melt-processable metal/polymer hybrid materials: Use of graphene as a dispersing agent. *Advance Materials*, 20, 3044–3049.

Lundahl, P., Stokes, R., Smith, E., Martin, R., & Graham, D. (2008). Synthesis and characterisation of monodispersed silver nanoparticles with controlled size ranges. *Micro Nano Letter*, 3, 62–65.

Luo, C. C., Zhang, Y. H., Zeng, X. W., Zeng, Y. W., & Wang, Y. G. (2005).The role of poly(ethylene glycol) in the formation of silver nanoparticles. *Journal Colloid Interface Scence*, 288, 444–448.

Luo, L.-B., S.-H. Yu, H.-S. Qian T. & Zhou, T. (2005). Large-scale fabrication of flexible silver/cross-linked poly(vinyl alcohol) coaxial nanocables by a facile solution approach. *Journal of American Chemical Society*, 127, 2822.

Maillard, M., Giorgio, S., & Pileni, M. P. (2002). Silver Nanodisks. *Advance Materials*, 14, 1084–1086.

Mandal, S., Gole, A., Lala, N., Gonnade, R., Ganvir, V., & Sastry, M. (2001). Studies on the reversible aggregation of cysteine-capped colloidal silver particles interconnected via hydrogen bonds. *Langmuir*, 17, 6262.

Manikam, V. R., Cheong. K. Y., & Razak, K. A. (2011). Chemical reduction methods for synthesizing Ag and Al nanoparticles and their respective nanoalloys. *Materails Science and Engineering: B*, 176, 187-203.

Manna, A., Imae, T., Iida, M., & Hisamatsu, N. (2001). Formation of Silver Nanoparticles from a N-Hexadecylethylenediamine Silver Nitrate Complex. *Langmuir*, 17, 6000.

Mansfield, E., Kar, A., Quinn, T. P., & Hooker, S. A. (2010). Quartz Crystal Microbalances for Microscale Thermogravimetric Analysis. *Analytical Chemistry*, 82, 9977–9982.

Mardare, D., & Rusu, G. I. (2004). Comparison of the dielectric properties for doped and undoped tio2 thin films. *J. Optoelectron. Advance Materials*, 6, 333-336.

Mark, H. F. (1985) Encyclopedia of polymer science and technology (3rd ed.), New York: Wiley.

Marutani, E., Yamamoto, S., Ninjbagar, T., Tsujii, Y., Fukuda, T., & Takano, M. (2004). Surface-initiated atom transfer radical polymerization of methyl methacrylate on magnetite nanoparticles. *Polymer*, 45, 2231.

Mbhele, Z. M., Sakmane, M. G., Van Sittert, C. G. C. E., Nedeljkovic, J. M., Djokovic, V., Luyt, A. S. (2003). Fabrication and characterization of silver-polyvinyl alcohol nanocomposites. *Chemistry of Materials*, 15, 5019.

McFarland, D. A., & Van Duyne, R. P. (2003). Single Silver Nanoparticles as Real-Time Optical Sensors with Zeptomole Sensitivity. *Nano Letter*, 3, 1057.

McNeill, I. C. (1968). A study of a thermal degradation of methyl methacrylate polymers and copolymers by thermal volatilization analysis. *European Polymer Journal*, 4, 21-30.

Métraux, G. S., Cao, Y.C., Jin. R., & Mirkin, C.A. (2003). Triangular Nanoframes Made of Gold and Silver. *Nano Letter*, 3(4), 519.

Mirkin, C. A., Letsinger, R. L., Mucic, R. C., & Storhoff, J. J. (1996). A DNA-based method for rationally assembling nanoparticles into macroscopic materials. *Nature*, 382, 607.

Mitzi, D. B. (2001). Thin-film deposition of organic-inorganic hybrid materials. *Chemistry of Materials*, 13, 3283.

Monti, L. A., Fourkas, J. T., & Nesbitt, D. J. (2004). Diffraction-Limited Photogeneration and Characterization of Silver Nanoparticles. *Journal Physics Chemistry B*, 108, 1604-1612.

Mullick, K., Witcomb, M. J., & Scurrell, M. S. (2004). Polymer stabilized silver nanoparticles: a photochemical synthesis route. *Journal of Materials Science*, 39, 4459.

Mulvaney, P. (1996). Surface Plasmon Spectroscopy of Nanosized Metal Particles. *Langmuir*, 12, 788.

Nair, A. S., & Pradeep, T. Y. (2003). Halocarbon mineralization and catalytic destruction by metal nanoparticles. *Current Science*, 84, 1560.

Navaladian, Natalia, A., Barmatov, E. B., Dmitry, Pebalk, A., Marina, V., Domi'nguez-Espinosa, B. G., Diaz-Calleja, R., Pissis, P. (2007). *Journal Physics Chemistry C*, 111, 8451.

Nickel, U., Castell, A. Z., Poppl, K., & Schneider, S. (2000). A Silver colloid produced by reduction with hydrazine as support for highly sensitive surface-enhanced Raman spectroscopy. *Langmuir*, 16, 9087.

Oliveira, M. M., Salvador, M. A., Coelho, P. J., & Carvalho, L. M. (2005). New Benzopyranocarbazoles: Synthesis and Photochromic Behavior. *Tetrahedron*, 61, 1681-1691.

Pandey, A., Singh, A. K., Maurya, S. K., Rai, R., & Shukla, H. S. (2008). Nanoscience and Their Biological Importance: Human Health And Disease. *Digest Journal of Nanomaterials and Biostructures*, 3, 141 – 146.

Park, S. J., Lim, S. T., Cho, M. S., Kim, H. M., & Choi, H. J. (2005). Electrical properties of multi-Walled Carbon Nanotubes/ poly (methyl methacrylate) nanocomposites. *Current Applied Physics*, 5, 302-304.

Pastoriza-Santos, I., & Liz-Marzan, L. M. (1999). Formation and stabilization of silver nanoparticles through reduction by N,N-dimethylformamide. *Langmuir*, 15, 948-951.

Pastoriza-Santos, I., & Liz-Marzán, L. M. (2002). Formation of PVP-Protected Metal Nanoparticles in DMF. *Langmuir*, 18, 2888-2894.

Peterson, J.D., Vyazovkin, S., & Wight, C.A. (1999). Kinetic Study of Stabilizing Effect of Oxygen on Thermal Degradation of Poly(methyl methacrylate). *Journal of Physical Chemistry B*, 103, 8087-8092.

Phong, N. T. P., Minh, N. H., Thanh, N. V. K., & Chien, D. M. (2009). Green synthesis of silver nanoparticles and silver colloidal solutions. *Journal Physics: Conf. Ser.*, 187, 012078.

Popa, M., Pradell, T., Crespo, D., & Calderon-Moreno, J. M. (2007). Stable silver colloidal dispersions using short chain polyethylene glycol. *Colloids Surface A*, 303, 184–190.

Porel, S., Singh, S., Harsha, S. S., Rao, D. N., & Radhakrishnan, T. P. (2005). Nanoparticle-Embedded Polymer: In Situ Synthesis, Free-Standing Films with Highly Monodisperse Silver Nanoparticles and Optical Limiting. *Chemistry Materials*, 17, 9.

Qian, X. F., Yin, J., Huang, J, C., Yang, Y. F., Guo, X. X., & Zhu, Z. K. (2001). The preparation and characterization of PVA/Ag2S nanocomposite. *Materials Chemistry Physics*, 68, 95-7.

Quaroni, L., & Chumanov, G. (1999). Preparation of polymer-coated functionalized silver nanoparticles. *Journal of American Chemistry Society*, 121, 10642.

Ramesh, S., Yahana, A. H., & Aroof, A. K. (2002). Dielectric behaviour of PVC-based polymer electrolytes. *Solid State Ionics*, 152–153, 291.

Ramya, C. S., Savitha, T., Selvasekharapandian, S. & Hiran, Kumar, G. (2005). Transport mechanism of Cu-ion conducting PVA based solid-polymer electrolyte. *Ionics*, 11, 436.

Ramya, C. S., Selvasekarapandian, S., Hirankumar, G., Savitha, T., & Angelo, P. C. (2008). Investigation on dielectric relaxations of PVP–NH_4SCN polymer electrolyte *Journal of Non-Crystalline Solids*, 354, 1494-1502.

Rane, S. B., Khanna, P. K., Seth, T., Phatak, G. J., Amalnerkar, D. P., & Das, B. K. (2003). Firing and processing effects on microstructure of fritted silver thick film electrode materials for solar cells. *Materials Chemistry and Physics*, 82, 237-245.

Rao, C. R. K., & Trivedi, D. C. (2005). Synthesis and characterization of fatty acids passivated silver nanoparticles-their interaction with PPy. *Synthetic Metals*, 155, 324–327.

Rao, C. R. K., & Trivedi, D. C. (2006).Biphasic synthesis of fatty acids stabilized silver nanoparticles: Role of experimental conditions on particle size. *Materials Chemistry and Physics*, 99, 354–360.

Reddy, V. R., Currao, A., & Calzaferri, G. (2007). Gold Colloid Modified Silver Chloride Photocatalyst For Water Oxidation To O_2. *Journal Physics, Conf. Ser.*, 61,960.

Rele, M., Kapoor, S., Sharma, G., & Mukherjee, T. (2004). Reduction and aggregation of silver and thallium ions in viscous media, *Physics Chemistry*, 6, 590-595.

Revina, A., & Egorova, E. (2000). Synthesis of metallic nanoparticles in reverse micelles in the presence of quercetin. *Colloids and Surfaces A: Physicochemical and Engineering Aspects*, 168, 87.

Rivas, L., Sanchez-Cortes, S., Garcia-Ramos, J. V., & Morcillo, G. (2001). Growth of silver colloidal particles obtained by citrate reduction to increase the Raman enhancement factor. *Langmuir*, 17,574.

Rosi, N. L., & Mirkin, C.A. (2005). Nanostructures in Biodiagnostics. *Chemical Review.* 105, 1547.

Rotello, V. M. (2004). Nanoparticles: *Building Blocks for Nanotechnology, Kluwer Academic.* New York: Plenum Publishers.

Salkar, R. A., Jeevanandam, P., Aruna, T., Koltypin, Y., & Gedanken. A. (1999). The sonochemical preparation of amorphous silver nanoparticles. *Journal of Materials Chemistry*, 9, 1333–1335.

Sastry, M., Rai, A., Chaudry, M., Ahmad, A., & Bharghava, S. (2007). *Materials Research Bulletin*, 42, 1212.

Schirtcliffe, N., Nickel, U., & Schneider, S. (1999). Reproducible preparation of silver sols with small particle size using borohydride reduction: for use as nuclei for preparation of larger particles. *Journal Colloid Interface Science*, 211,122.

Schmid, G., Decker, M., Ernst, H., & Fuchs, H. (2003). Small Dimensions and Material Properties. Europaische Akademie's.

Schneider, S., Halbig, P., Grau, H., & Nickel, U. (1994). Reproducible preparation of silver sols with uniform particle size for application in surface-enhanced Raman spectroscopy. *Photochemistry and Photobiology*, 60, 605. doi: 10.1111/j.1751-1097.1994.tb05156.x.

Shankar, S. S., Ahmad, A., & Sastry, M. (2003). Geranium leaf assisted biosynthesis of silver nanoparticles. *Biotechnology Progress*, 19**,** 1627-1635.

Shkilnyy, A., Souce, M., Dubios, P., Warmont, F., Saboungi, M. L., & Chourpa, I. (2009). Poly(ethylene glycol)-stabilized silver nanoparticles for bioanalytical application of SERS spectroscopy. *Analyst*, 134, 1868–1872.

Siegel, R.W. (1991). Cluster-Assembled Nanophase Materials. *Annual Review of Materials Science*, 21, 559.

Sileikaite, A., Prosycevas, I., Puiso, J., Juraitis, A., & Guobiene, A. (2006). Analysis of Silver Nanoparticles Produced by Chemical Reduction of Silver Salt Solution. *Materials Science*, 12, 287–291.

Silvert, P. Y., & Tekaia-Elhsissen, K. (1995). Synthesis of monodisperse submicronic gold particles by the polyol process. *Solid State Ionics*, 82, 53-60.

Singh, N., & Khanna, P. K. (2007). *In situ* synthesis of silver nanoparticles in polymethylmethacrylate, *Materials Chemistry and Physic*, 104, 367-372.

Sirbu, L., Sergentu, V., Ursaki, V., Tiginyanu, I., Piredda, G., & Boyd, R.W. (2008). Surface Plasmon Resonance in Ag nanoparticles deposited inside porous GaP templetes. Semiconductor Conference (pp. 113-116).

Somorjai, G. A. (1978). Active sites for hydrocarbon catalysis on metal surfaces. *Pure and Applied Chemistry*, 50, 963.

Sondi, I., Goia, D. V., & Matijevi, E. (2003). Preparation of highly concentrated stable dispersions of uniform silver nanoparticles. *Journal of Colloid and Interface Science*, 260, 75-81.

Sondi, I., Siiman, O., & Matijevi, E. (2004). Synthesis of CdSe Nanoparticles in the Presence of Aminodextran as Stabilizing and Capping Agent. Journal Colloid Interface Science, 275, 503-507.

Starowicz, M., Stypuła, B., & Banas, J. (2006). Electrochemical synthesis of silver nanoparticles. *Electrochemical Communication,* 8, 227–230.

Stepanov, A. L., Abdullin, S. N., Petukhov, V. Y., Osin, Y. N., Khaibullin, R. I., & Khaibullin, I. B. (2000). Formation of metal-polymer composites by ion implantation. *Philosophical Magazine B,* 80, 23.

Stepanov, A. L., Popok, V. N., Khaibullin, I. B., & Kreibig, U. (2002). Optical properties of polymethylmethacrilate with implanted silver nanoparticles. *Nuclear Instruments and Methods in Physics Research B,* 191, 473.

Storhoff, J. J., Elghanian, R., Mucic, R. C., Mirkin, C. A., & Letsinger, R. L. (1998). One-Pot Colorimetric Differentiation of Polynucleotides with Single Base Imperfections Using Gold Nanoparticle Probes. *Journal of American Chemical Society*, 120, 1959.

Suber, L., Sondi, I., Matijevi, E., & Goia, D. V. (2005). Preparation and the mechanisms of formation of silver particles of different morphologies in homogeneous solutions. *Journal Colloid Interface Science*, 288, 489–495.

Sudrik, S. G., Chaki, N. K., Chavan, V. B., Chavan, S. P., Chavan, S. P., Sonawane, H. R. & Vijayamohanan, K. (2006). Silver Nanocluster Redox-Couple-Promoted Nonclassical Electron Transfer: An Efficient Electrochemical Wolff Rearrangement of α-Diazoketones. *Chemistry,* 12, 859–864.

Sun, S., Tsubaki, N., & Fujimoto, K. (2000). Promotional Effect of Noble Metal to Co-based Fischer-Tropsch Catalysts Prepared from Mixed Cobalt Salts. *Chemicals Letters*, 29, 176.

Sun, Y., & Xia, Y. (2002). Shape-Controlled Synthesis of Gold and Silver Nanoparticles. *Science,* 298, 2176-2179.

Sun, Y., & Xia, Y. (2003). Triangular Nanoplates of Silver: Synthesis, Characterization, and Use as Sacrificial Templates for Generating Triangular Nanorings of Gold. *Advances Materials*, 15, 695–699.

Takele, H., Greve, H., Pochstein, C., Zaporojtchenko, V., & Faupel, F. (2006). Plasmonic properties of Ag nanoclusters in various polymer matrices. *Nanotechnology*, 17, 3499.

Tan, Y., Li Y., & Zhu, D. (2003). Preparation of silver nanocrystals in the presence of aniline. *Journal Colloid Interface Science*, 258, 244–251.

Tareev, B. (1979). Physics of Dielectric Materials, Moscow: MIR Publications.

Taton, T. A., Mirkin, C. A., & Letsinger, R. L. (2000). Scanometric DNA Array Detection with Nanoparticle Probes. *Science*, 89, 1757.

Tessier, P. M., Velev, O. D., Kalambur, A. T., Rabolt, J. F., Lenhoff, A. M., & Kaler, E. W. (2000). Assembly of gold nanostructured films templated by colloidal crystals and use insurface-enhanced Raman spectroscopy. *Journal of American Chemical Society,* 122, 9554.

Thomas, S., Saritha, K., Nair, E., Jamal, M. A., Harthi, S. H. Varma, M. R., & Anantharam, M. R. (2008). Size-dependent surface plasmon resonance in silver silica nanocomposites, *Nanotechnology*, 19, 7.

Tolaymat, T. M., El Badawy, A. M., Genaidy, A., Scheckel, K. G., Luxton, T. P., & Suidan, M. (2010). An evidence-based environmental perspective of manufactured silver nanoparticle in syntheses and applications: a systematic review and critical appraisal of peer-reviewed scientific papers. *Science Total Environment*, 408, 999–1006.

Tukhvatullin, F. H., Pogorelov, V. E., Tashkenbaev, U. N., Jumaboev, A., Hushvaktov, H., Seit-Enon, M., & Osmanov, S. A. (2003). Intermolecular interaction in liquid dimethylformamide and its manifestation in Raman spectra. *Journal Raman Spectroscopy*, 34, 813-818.

Tuval, T., & Gedanken, A.. (2007). A microwave-assisted polyol method for the deposition of silver nanoparticles on silica spheres. *Nanotechnology*, 18, 255601.

Vilchis-Nestor, A., Sánchez-Mendieta, V., Camacho-López, M., Gómez-Espinosa, R., Camacho-López, M., & Arenas-Alatorre, J. (2008). Solventless synthesis and optical properties of Au and Ag nanoparticles using Camellia sinensis extract. *Materials Letter*, 62, 3103.

Vodick, V. V., Bozaniac, D. K., Dzunuzonic, E., Vukovic, J., & Nedeljkovic, J. M. (2009). Synthesis and characterization of silver-poly(methylmethacrylate) nanocomposites. *Journal of European Polymer*, 18, 8.

Vossmeyer, T., Guse, B., Besnard, I., Bauer, R, E., Mullen, K,, & Yasuda, A. (2002). Gold Nanoparticle/Polyphenylene Dendrimer Composite Films: Preparation and Vapor-Sensing Properties. *Advanced Materials*, 14, 238.

Wang, D., An, J., Luo, Q., Li, X., & Li, M. (2008). A convenient approach to synthesize stable silver nanoparticles and silver/polystyrene nanocomposite particles. *Journal of Applied Polymer Science*, 110, 3038–3046.

Wang, L., & Chen, D. (2004). ‘‘One-pot’’ Fabrication of Ag/PMMA ‘‘shell/core’’ Nanocomposites by Chemical Reduction Method. *Chemistry Letter*, 33, 1010.

Willis, H, A., Zichy, V. J. I., & Hendra, P. J. (1969). Laser-Raman and infra-red spectra of poly(methyl methacrylate). *Polymer*, 10, 737–746.

Wolfgang, S. (2007). Sample preparation in Light Scattering from Polymer Solutions and Nanoparticles Dispersions. Berlin: Springer.

Yang, J., Hasell, T., Wang, W., & Howdle, S.M., (2008). A Novel Synthetic Route to Metal-polymer Nanocomposites by In Situ Suspension and Bulk Polymerization. *Journal of European Polymer*, 44, 1331.

Yeo, S., Lee, H., & Jeong, S. (2003). Preparation of nanocomposite fibers for permanent antibacterial effect. *Journal of Material Science*, 38, 2143.

Yeum, J. H., & Deng, Y. (2005). Synthesis of high molecular weight poly(methyl methacrylate) microspheres by suspension polymerization in the presence of silver nanoparticles. *Colloid Polymer Science*, 283, 1172.

Yin, Y., Lu, Y., Sun, Y., & Xia, Y. (2002). Silver Nanowires Can Be Directly Coated with Amorphous Silica to Generate Well-Controlled Coaxial Nanocables of Silver/Silica. *Nano Letter*, 2(4), 427.

Yon, J. M., & Jamie, R. L. (2008). Manufactured nanoparticles: an overview of their chemistry, interactions and potential environmental implications. *Science Total Enviroment*, 400, 396–414.

Yoosaf, K., Ipe, B. I., Suresh, C. H., & Thomas, K. G. (2007). In Situ Synthesis of Metal Nanoparticles and Selective Naked-Eye Detection of Lead Ions from Aqueous Media. *Journal of Physics Chemistry C*, 111, 12839.

Zeng, R., Rong, M. Z., Zhang, M. Q., Liang, H. C., & Zeng, H. M. (2002). Laser ablation of polymer-based silver nanocomposites. *Applied Surface Science*, 187, 239.

Zhang, D., Qi, L., Ma, J., & Cheng, N. (2001). Formation of Silver Nanowires in Aqueous Solutions of a Double-Hydrophilic Block Copolymer. *Chemistry Materials*, 13, 2753.

Zhang, L., Zhang, C., & Li, G. M (2007) Synthesis and properties of copolymer microemulsions of siloxane and acrylate with a high solid content, *Journal of Applied Polymer Science*, 104, 851–857.

Zhang, S. W., Zhou, S. X., Weng, Y. M., & Wu, L. M. (2005). Synthesis of SiO_2 / Polystyrene Nanocomposite Particles via Miniemulsion polymerization, *Langmuir*, 21, 2124.

Zhang, Z., & Han, M. (2003). One-step preparation of size-selected and well-dispersed silver nanocrystals in polyacrylonitrile by simultaneous reduction and polymerization. *Journal of Materials Chemistry*, 13, 641-643.

Zheng, J., Stevenson, M. S., Hikida, R. S., & Van Patten, O. G. (2002). Influence of pH on dendrimer-protected nanoparticles. *Journal of Physics Chemistry B*, 106, 1252.

Zheng, M., Gu, M., Jin, Y., & Jin, G. (2001). Optical properties of silver-dispersed PVP thin film. *Materials Research Bulletin*, 36, 853.

Zhou, Y., Yu, S. H., Cui, X. P., Wang, C. Y., & Chen, Z. Y. (1999). Formation of silver nanowires by a novel solid-liquid phase arc discharge method. *Chemistry Materials*, 11, 545.

Zhou, Y., Yu, S. H., Wang, C. Y., Li, X. G., Zhu, Y. R., & Chen, Z. Y. (1999). A novel ultraviolet irradiation photo-reduction technique for preparation of single crystal Ag nanorods and Ag dendrites. *Advanced Materials*, 11, 850.

Zhu, Y., Qian, Y., & Zhang, M. (1997). Ɣ-Radiation synthesis and characterization of polyacrylamide-silver nanocomposites. *Chemistry Communications*, 12, 1081.

Internet References

http://en.wikipedia.org/wiki/Dimethylfor